UNIVERSITATEA NAȚIONALĂ DE ȘTIINȚĂ ȘI TEHNOLOGIE
POLITEHNICA DIN BUCUREŞTI
ŞCOALA DOCTORALĂ DE INGINERIE ELECTRICĂ

DEPARTAMENTUL DE ELECTROTEHNICĂ

ABSTRACT OF THE DOCTORAL THESIS

Contribuții privind îmbunătățirea performanțelor în reducerea riscului de accidente în instalațiile electrice de joasă tensiune

Contributions to improving performance in reducing the risk of accidents in low voltage electrical installations

Scientific Supervisor:

Prof. Dr. Eng. Mihai IORDACHE

Doctoral Candidate:

Eng. Adrian Florian GEORGESCU

BUCHAREST
2026

ACKNOWLEDGEMENTS

First and foremost, I would like to express my deep appreciation and sincere gratitude to Prof. Dr. Eng. Mihai IORDACHE, whose constant support was essential in the completion of this thesis. Through his guidance, motivation and understanding, he continuously encouraged me to achieve my objective. The recommendations and advice he provided throughout this stage of study and research contributed significantly to the timely completion of this work.

I would also like to express my warmest thanks to Prof. Dr. Eng. Marilena STĂNCULESCU, Assoc. Prof. Dr. Eng. Dragoș NICULAE, Assist. Prof. Dr. Eng. Georgiana ZAINEA, and Dr. Eng. Maria Lavinia BOBARU, who supported me in discovering the complexity and beauty of this research topic. The trust they placed in me, together with their constant guidance and encouragement, has been particularly valuable throughout my academic journey.

I also extend my gratitude to the members of the Doctoral School within the Faculty of Electrical Engineering of the National University of Science and Technology POLITEHNICA Bucharest, for the support provided at various stages in the development of this work. I deeply appreciate the understanding, support and advice received throughout my doctoral studies.

Finally, but with equal consideration, I am grateful to my family for their unconditional support, patience and understanding, which were fundamental in achieving this objective.

Cuprins

Chapter 1 6

Introduction 6

1.1 Purpose of the Doctoral Thesis 6

1.2 Content of the Doctoral Thesis 6

Chapter 2 8

Current State of Research and Regulations in the Field of Low-Voltage Electrical Installations 8

Chapter 3 11

Risk Analysis and Determining Factors in Low-Voltage Electrical Installations 11

Chapter 4 14

Power Supply Schemes and Systems in Medical Infrastructures 14

Partial Conclusions 18

Chapter 5 18

Criteria and Policies for the Modernisation of Low-Voltage Electrical Installations 18

Conclusions 22

Chapter 6 22

Thermal Monitoring System for Electrical Panels 22

Conclusions 28

Chapter 7 28

Impedance Matching in Signal Transmission Lines 28

Chapter 8 35

Generation of Parameters for Quadripoles and Analogue Filters 35

Chapter 9 52

Analysis of the Induction Motor in Periodic Sinusoidal Regime, Taking into Account the Magnetisation Characteristic and the Variation of Rotor Resistance with Slip 52

Chapter 10 62

General Conclusions and Future Research Directions 62

10.1. List of Published Works 63

10.2. Scientific and Applied Impact 64

References 64

Lista tabelelor

TABELUL 2.1. MAIN REGULATIONS IN THE FIELD OF ELECTRICAL INSTALLATIONS [24]–[29]. 10
TABELUL 3.1. CLASSIFICATION OF TYPES OF RISKS IN LOW-VOLTAGE INSTALLATIONS. 11
TABELUL 3.2. INSULATION AGEING WITH INCREASING TEMPERATURE. 13
TABELUL 3.3. RISK LEVEL ASSOCIATED WITH TEMPERATURE INCREASE. 13
TABLE 4.2. CORRELATION BETWEEN THE TYPE OF POWER SUPPLY SCHEME AND THE ESTIMATED RISK LEVEL. 17
TABLE 5.1. INDICATIVE SERVICE LIFE OF ELECTRICAL INSTALLATION COMPONENTS. 19
TABLE 6.2. EMPERATURE THRESHOLDS FOR THE MONITORING SYSTEM. 25

Lista figurilor

FIG. 2.1. LIST OF INCIDENTS OCCURRING IN HOSPITAL UNITS.. 8
FIG. 2.2. EXAMPLES OF ELECTRICAL PANELS IN HOSPITALS BEFORE AND AFTER MODERNISATION. 9
FIG. 2.3. EXAMPLES OF UNDERSIZED CABLES AND ELECTRICAL PANELS WITH DAMAGED CONNECTIONS. 9
FIG. 3.1. VISUAL EXAMPLES OF DEFICIENCIES: OXIDISED CONNECTIONS, OVERHEATED CABLES, IMPROVISED SOLUTIONS. 12
FIG. 4.1. GENERAL POWER SUPPLY SCHEME OF A HOSPITAL: MAIN SOURCE AND GENERATOR SET. 16
FIG. 4.2. EXAMPLE OF A MEDICAL IT SCHEME FOR AN OPERATING ROOM (SCHNEIDER ELECTRIC). 17
FIG. 5.1. VISUAL COMPARISON BETWEEN AN OLD ELECTRICAL PANEL AND A MODERN ONE EQUIPPED WITH RESIDUAL CURRENT PROTECTION AND SENSORS. 19
FIG. 5.2. EXAMPLES OF VISIBLE DEFICIENCIES IN OLD INSTALLATIONS. 20
FIG. 5.4. EXAMPLE OF MEASUREMENT WITH A THERMAL IMAGING CAMERA IN AN ELECTRICAL PANEL. 22
FIG. 6.1. A) SINGLE-LINE DIAGRAM OF THE ELECTRICAL PANEL; B) DIAGRAM OF THE ARDUINO THERMAL MONITORING SYSTEM; C) PHOTOGRAPHS TAKEN DURING THE EXPERIMENT. 25
FIG. 6.2. TEMPERATURE VERSUS TIME GRAPH FOR DIFFERENT LOADS. 26
FIG. 6.3. PVC INSULATION DEGRADATION CURVE AS A FUNCTION OF TEMPERATURE, ARRHENIUS MODEL. 27
FIG. 6.4. CONCEPT OF AN EXTENDED MONITORING SYSTEM, IOT + CLOUD. 28
FIG. 7.3. SOURCE AND LOAD CIRCUIT IMPEDANCE. 29
FIG. 7.1. RETURN LOSS AND INSERTION LOSS IN A LOSSLESS CIRCUIT OR TRANSMISSION LINE. 29
FIG. 7.2. MODELLING OF A TWO-PORT MICROWAVE CIRCUIT USING S PARAMETERS. 30
FIG. 7.5. L-TYPE NETWORKS FOR MATCHING THE IMPEDANCE OF A SOURCE OR LOAD TO A TRANSMISSION LINE WITH CHARACTERISTIC IMPEDANCE $Z0$ 30
FIG. 7.7. MATCHING OF A PURELY RESISTIVE LOAD USING A TRANSMISSION LINE OF LENGTH Λ/4. 31
FIG. 7.14**.** MATCHING OF A PURELY RESISTIVE LOAD USING A TRANSMISSION-LINE SECTION OF LENGTH Λ/4. 31
FIG. 7.8. LOSSLESS TRANSMISSION LINE TERMINATED BY AN ARBITRARY IMPEDANCE LOAD, MATCHED BY MEANS OF TWO PURELY REACTIVE ELEMENTS. 32

FIG. 7.10. IMPEDANCE MATCHING BY MEANS OF A REACTIVE MATCHING NETWORK WITH SERIES-PARALLEL TOPOLOGY (JX_1 IN SERIES WITH Z_L AND IN PARALEL WITH JX_2). 32
FIG. 7.26. POSSIBLE CONFIGURATIONS FOR IMPEDANCE MATCHING. 33
FIG. 8.1. SCHEMATIC REPRESENTATION OF A PASSIVE LINEAR QUADRIPOLE. 35
FIG. 8.2. CIRCUIT USED TO DEFINE THE S PARAMETERS. 38
FIG. 8.3. DEFINITION OF THE FOUR TYPES OF CONTROLLED SOURCES. 39
FIG. 8.4, A. DEFINITION OF THE INPUT IMPEDANCE $Z_{II}(S)$. 39
FIG. 8.4, B. DEFINITION OF THE INPUT ADMITTANCE $Y_{II}(S)$. 39
FIG. 8.5. USER INTERFACE OF THE CSAP PROGRAM. 40
FIG. 8.6. USER INTERFACE OF THE TFSYG PROGRAM. 40
FIG. 8.7. TYPE (M) BAND-PASS FILTER. 43
FIG. 8.8. FREQUENCY VARIATIONS OF THE MODULI OF THE S PARAMETERS AND OF THE SIGNAL TRANSMISSION EFFICIENCIES FOR THE FILTER IN FIG. 8.7: A) MODULI EXPRESSED IN DB; B) MODULI EXPRESSED IN %/%; C) ARGUMENTS OF THE S PARAMETERS; D) SIGNAL TRANSMISSION EFFICIENCIES FROM INPUT TO OUTPUT H_{21_S21} AND FROM OUTPUT TO INPUT H_{12_S12}. 44
FIG. 8.9. FREQUENCY VARIATIONS OF THE MODULI OF THE CHARACTERISTIC AND IMAGE IMPEDANCES: A) ABS($Z_{I1\text{-}F}$)-BLUE, ABS($Z_{I2\text{-}F}$)-MAGENTAP, ABS($Z_{C1\text{-}F}$)-GREEN ȘI ABS($Z_{C2\text{-}F}$)-REDP; B) 20.0*LOG10(ABS($Z_{I1\text{-}F}$))-BLUE, 20.0*LOG10(ABS($Z_{I2\text{-}F}$))-MAGENTAP, 20.0*LOG10(ABS($Z_{C1\text{-}F}$))-GREEN ȘI 20.0*LOG10(ABS($Z_{C2\text{-}F}$)). 46
FIG. 8.10. FREQUENCY VARIATIONS OF: A) THE ATTENUATION CONSTANT; B) THE PHASE CONSTANT. 46
FIG. 8.11. TYPE (M) BAND-PASS FILTER. 47
FIG. 8.12. FREQUENCY VARIATIONS OF THE MODULI OF THE S PARAMETERS AND OF THE SIGNAL TRANSMISSION EFFICIENCIES FOR THE FILTER IN FIG. 8.11: A) MODULI EXPRESSED IN DB; B) MODULI EXPRESSED IN %/%; C) ARGUMENTS OF THE S PARAMETERS; D) SIGNAL TRANSMISSION EFFICIENCIES FROM INPUT TO OUTPUT H_{21_S21} AND FROM OUTPUT TO INPUT H_{12_S12}. 49
FIG. 8.13. FREQUENCY VARIATIONS OF THE MODULI OF THE CHARACTERISTIC AND IMAGE IMPEDANCES.: A) ABS($Z_{I1\text{-}F}$)-BLUE, ABS($Z_{I2\text{-}F}$)-MAGENTAP, ABS($Z_{C1\text{-}F}$)-GREEN ȘI ABS($Z_{C2\text{-}F}$)-REDP; B) 20.0*LOG10(ABS($Z_{I1\text{-}F}$))-BLUE, 20.0*LOG10(ABS($Z_{I2\text{-}F}$))-MAGENTAP, 20.0*LOG10(ABS($Z_{C1\text{-}F}$))-GREEN ȘI 20.0*LOG10(ABS($Z_{C2\text{-}F}$)). 50
FIG. 8.14. FREQUENCY CHARACTERISTICS OF THE (M)-TYPE BAND-PASS FILTER IN FIG. 8.11: A) VOLTAGE TRANSFER FACTOR EXPRESSED IN DB; B) VOLTAGE TRANSFER FACTOR EXPRESSED IN V/V. 51
FIG. 8.16. BODE CHARACTERISTICS OF THE BAND-PASS FILTER IN FIG. 8.11: A) BODE DIAGRAM; B) NYQUIST DIAGRAM; C) REPRESENTATION OF POLES AND ZEROS IN THE COMPLEX PLANE; D) POLES AND ZEROS FOR A_{FTB_M}. 51
FIG. 9.1. EQUIVALENT CIRCUIT OF THE INDUCTION MOTOR IN *Π* 53
FIG. 9.2. A) CHARACTERISTIC $\varphi_{LM}(I_{LM}) = \varphi_{L6}(I_{L6})$Ș B) CHARACTERISTIC $R_2(T)$. 54
FIG. 9.3. SPICE SIMULATION OF CURRENT-CONTROLLED NONLINEAR COILS. 54

Chapter 1

Introduction

1.1 Purpose of the Doctoral Thesis

In a global context in which the safety of electrical installations represents an essential component of modern infrastructure, the analysis, assessment and reduction of accident risks in low-voltage systems have become major priorities both for specialists in the field and for the institutions responsible for regulating this sector [4], [6], [8]. In Romania, a significant part of the existing building stock is equipped with outdated, undersized or improperly maintained electrical installations, which leads to a constant increase in incidents caused by electrical faults, such as fires, electric shocks, power supply interruptions or equipment damage [5], [7], [23].

These phenomena have a direct impact on user safety, the durability of buildings and the continuity of public services, especially in sensitive facilities such as hospitals, schools and administrative buildings [3], [5]. In this context, the doctoral thesis entitled **"Contributions to Improving Performance in Reducing the Risk of Accidents in Low-Voltage Electrical Installations"** belongs to a current research direction of national and European strategic interest. Its main objective is to increase the level of safety and reliability of electrical installations through a combination of theoretical analysis, applied studies and innovative technological solutions [1], [7], [23].

1.2 Content of the Doctoral Thesis

The thesis is structured into ten main chapters, reflecting the progressive logic of the research:

Chapter 1 – Introduction:
Low-voltage electrical installations, although apparently simple in design, are complex systems that constantly interact with environmental factors and with the changing requirements of consumers.

Chapter 2 – Current State of Research and Regulations in the Field of Low-Voltage Electrical Installations:
Low-voltage electrical installations represent the vital infrastructure of any modern built environment.

Chapter 3 – Risk Analysis and Determining Factors in Low-Voltage Electrical Installations:
Risk in low-voltage electrical installations is a complex and multidimensional reality, resulting from the interaction between technical, human and organisational factors.

Chapter 4 – Power Supply Schemes and Systems in Medical Infrastructure:
Medical facilities represent one of the most sensitive categories of electrical infrastructure,

because the uninterrupted operation of power supply systems can make the difference between life and death.

Chapter 5 – Criteria and Policies for the Modernisation of Low-Voltage Electrical Installations:
Every electrical installation has a limited service life, influenced by the quality of materials, operating conditions and the level of maintenance.

Chapter 6 – Thermal Monitoring System for Electrical Panels:
Temperature increase in the components of electrical installations is one of the most important indicators of fault and fire risk.

Chapter 7 – Impedance Matching in Signal Transmission Lines:
Impedance matching and signal transmission networks are essential for the efficient transfer of energy between sources and loads in communication systems, audio systems, radio-frequency systems, microelectronics and other technical fields.

Chapter 8 – Generation of Parameters for Quadripoles and Analogue Filters:
In order to characterise linear two-port circuits under harmonic operating conditions, the parameters Z, Y, H, T, F and others are used at low and medium frequencies.

Chapter 9 – Analysis of the Induction Motor in Periodic Sinusoidal Regime, Taking into Account the Magnetisation Characteristic and the Variation of Rotor Resistance with Slip:
The study of the non-sinusoidal periodic regime is important both from the perspective of the disturbing effects produced in electric power transmission and distribution networks and from the perspective of its use in the construction of certain electrical devices.

Chapter 10 – Conclusions and Perspectives:

This chapter synthesises the results obtained during the research, highlights the author's original contributions and proposes future research directions.

Chapter 2

Current State of Research and Regulations in the Field of Low-Voltage Electrical Installations

Low-voltage electrical installations represent an essential component of civil, industrial and medical buildings, as they supply all the equipment required for their normal operation: lighting, air conditioning, technological equipment, IT systems, medical devices, safety installations and monitoring systems [3], [4]. For this reason, the safety of the electrical installation directly influences the safety of users, the continuity of activities and the protection of the building against fires or failures.

In recent years, incidents occurring in public buildings, especially in hospital units, have shown that old, repeatedly modified or improperly maintained electrical installations can become major sources of risk. The publication on reducing risks in hospital buildings presents numerous cases of fires and evacuations in hospitals, including intensive care units, operating theatres, wards and mobile medical units. Examples such as the fires at Giulești Maternity Hospital, Piatra-Neamț County Hospital, the "Matei Balș" Institute, Constanța Infectious Diseases Hospital and Movila COVID Support Hospital highlight the serious consequences that a technical fault may have in a critical medical infrastructure [23]. The same publication emphasises that, in many situations, the analysed fires and accidents were directly or indirectly related to electrical installations, through faults, improvised solutions, overloads, old cables, technically outdated electrical panels or the lack of adequate maintenance [23].



Fig. 2.1. List of incidents occurring in hospital units..

An important motivation for this research is the fact that, according to the information analysed in the case studies and in reports on fires occurring in buildings, a significant part of reported fires is caused by faults in electrical installations or by their improper operation. In the case of hospitals, the risk is

amplified because the power supply supports vital equipment, such as intensive care equipment, oxygen systems, anaesthesia devices, patient monitoring systems, emergency lighting and ventilation systems. An interruption, an overload or a fire in an electrical panel can directly affect the medical act and may require the evacuation of patients.



Fig. 2.2. Examples of electrical panels in hospitals before and after modernisation.

The case studies analyzed revealed several recurring technical deficiencies in existing electrical installations. The most frequent include: mismatch between the protection rating and the cable cross-section, supplying new consumers from existing electrical panels without recalculating the loads, absence of residual current protection, absence of surge protection, damaged connections, old electrical panels, lack of circuit labelling and lack of updated technical documentation [5], [23]. A frequently encountered situation is the installation of high-rated fuses on circuits with small cable cross-sections, which leads to conductor overheating and an increased fire risk [4], [6], [16], [23].

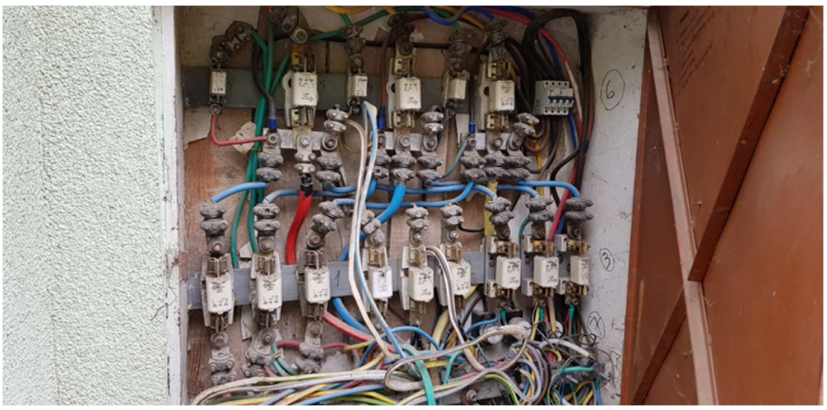


Fig. 2.3. Examples of undersized cables and electrical panels with damaged connections.

Another major issue is the appearance of new consumers with high electrical power, connected to installations designed for much lower requirements. In hospitals, this situation occurs through the introduction of modern medical equipment, such as MRI, CT, X-ray systems, air conditioning systems, intensive care equipment and sterilisation devices. In civil and industrial buildings, similar situations occur through the installation of air conditioning systems, electric machines, IT equipment, CNC machines or photovoltaic panels [23]. If these changes are not accompanied by recalculation of the

installed power, verification of cables, verification of protective devices and updating of the single-line diagram, the installation may operate under overload conditions without the risk being immediately observable.

The safety of electrical installations is regulated by a broad normative framework, which includes technical regulations, European standards and legislative acts. The most important documents are I7/2011, NP015/2022, SR HD 60364, NP061/2002, P118/2015, Law 319/2006, Law 123/2012 and ANRE Order 59/2013 [3], [4], [6]–[11], [16], [17], [24]–[29]. These documents establish requirements regarding design, execution, verification, protection against electric shock, fire safety, supply of critical consumers and authorisation of specialist personnel.

Tabelul 2.1. Main regulations in the field of electrical installations [24]–[29].

Nr. crt.	**Cod / Denumire normativă**	**Domeniu de aplicare**
1	I7/2011	Regulation for the design and execution of electrical installations related to civil and industrial buildings
2	NP015/2022	Regulation for the design and verification of electrical installations in healthcare units
3	SR HD 60364	Standard european privind instalațiile electrice de joasă tensiune
4	NP061/2002	Regulation regarding protection against electric shock
5	P118/2015	Fire safety regulation for buildings
6	Legea 319/2006	Occupational safety and health law
7	Legea 123/2012	Law on electricity and natural gas
8	Ordin ANRE 59/2013	Regulation regarding the authorisation of electricians and electrical installation companies

However, the existence of a broad normative framework does not automatically guarantee the safety of electrical installations. The correct application of regulations is difficult in practice because the legislation is complex, and existing installations have often been modified over time without complete documentation. For this reason, safety must not rely only on the individual interpretation of regulations, but on compliance with the mandatory stages: design, execution, verification, maintenance and updating of technical documentation.

In the case of medical units, this requirement becomes essential. The regulations provide for the classification of medical rooms into safety groups, the use of backup power sources, the supply of critical consumers, the existence of medical IT panels for operating rooms and intensive care units, and the limitation of power interruption times [3], [24]. However, the case studies have shown that many hospital electrical installations no longer meet current requirements, because they have been modified over time, overloaded by new consumers or have not benefited from sufficient technical maintenance [5], [23].

Current research directions aim to complement classical inspections with modern diagnostic and monitoring methods. These include thermographic analysis, real-time monitoring of currents and voltages, harmonic analysis, the use of temperature sensors in electrical panels, the use of

microcontrollers and the development of predictive maintenance systems [1], [7], [19], [20], [21], [22]. These solutions make it possible to identify incipient faults before they produce fires, interruptions or accidents.

Therefore, the current state of research shows that low-voltage electrical installations must be assessed not only through periodic inspections, but through an integrated system of analysis, monitoring and maintenance. Especially in old buildings and hospital units, the safety of the installation depends on the correlation between technical documentation, the real condition on site, current loads, existing protective devices and the continuous monitoring of electrical panels.

Conclusions

The analysis of the current state shows that low-voltage electrical installations, especially old installations or those modified successively, can become significant sources of risk. Incidents occurring in hospitals confirm that electrical faults, overloads, improvised solutions and lack of maintenance can have serious consequences. Although the normative framework is extensive, real safety depends on its correct application, on updating the documentation, on modernising installations and on the continuous monitoring of electrical panels.

Chapter 3

Risk Analysis and Determining Factors in Low-Voltage Electrical Installations

Risk in low-voltage electrical installations is determined by the interaction between technical, human, organisational and environmental factors [1], [4], [7], [27]. As an installation ages, materials lose their initial properties, insulation deteriorates, contacts oxidise, and electrical panels become increasingly difficult to operate and verify. At the same time, the increase in the number of consumers and successive modifications made to the installation may lead to overloads, local overheating and operation under unsafe conditions [5], [7], [11], [23].

In electrical installations, risk may be defined as the product between the probability of occurrence of an unwanted event and the severity of its consequences [1], [7]. Unwanted events may include electric shock, fire, power supply interruption, equipment degradation or economic losses. For this reason, risk assessment must not be limited only to the measurement of electrical parameters, but must also include the analysis of the physical condition of the installation, the history of interventions, the level of maintenance, the operating environment and the competence of the personnel working on the installation [7], [23], [27].

Tabelul 3.1. Classification of types of risks in low-voltage installations.

Risk category	Description	Typical examples
Direct electrical risks	Determined by direct or indirect contact with live parts	Electric shock, burns, ventricular fibrillation
Thermal risks	Generated by overheating of conductors and connections	Fires in electrical panels, melting of insulation

Mechanical risks	Structural deterioration of components	Cable breakage, loose connections, vibrations
Functional risks	Associated with loss of supply or voltage variation	Shutdown of medical equipment, server failures
Organisational risks	Resulting from lack of training, documentation or maintenance plans	Unauthorised interventions, use of improvised solutions
Environmental risks	External factors that accelerate the degradation of installations	Humidity, dust, corrosive gases, extreme temperatures

This classification allows a systematic approach to risks, providing a basis for identifying specific reduction and prevention measures [1], [7], [23].

The case studies analysed within the research highlighted several recurring causes of risk: ageing of installations, overload, undersized conductors, poor maintenance, non-compliant execution, unauthorised interventions, lack of knowledge of regulations and absence of modernisation plans [5], [7], [23]. These causes are common in old buildings, but they become much more dangerous in critical infrastructures such as hospitals, airports, data centres or industrial units, where power supply interruption can produce severe consequences [3], [5], [24], [28].

Figure 3.1 presents an old electrical panel with fuse links, disordered conductors and connections that are difficult to verify, indicating the need for modernisation of the installation.

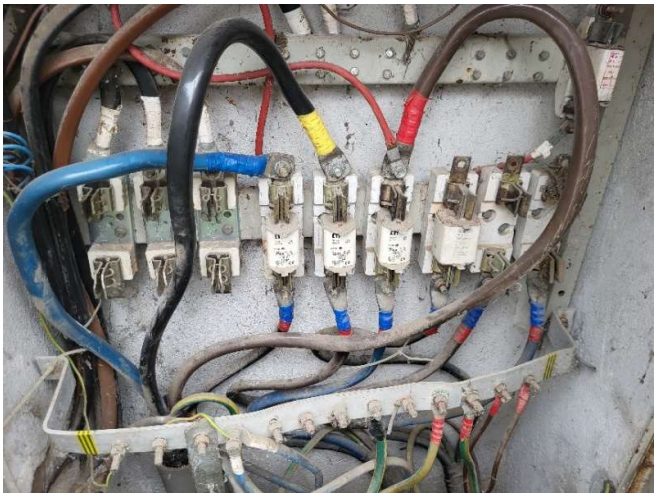


Fig. 3.1. Visual examples of deficiencies: oxidised connections, overheated cables, improvised solutions.

These causes are found in most old buildings in Romania, but they are even more dangerous in critical infrastructures, such as hospitals, airports, factories and data centres, where power supply interruption has severe consequences [3], [5], [24], [28].

For the systematic assessment of risk, the thesis proposes a simple model that can be applied in practice, based on the following relationship:

$$R = P \times S$$

where:

R – risk level;
P – probability of occurrence of the event or fault;
S – severity of the consequence.

By assigning a numerical score to probability and severity, risk can be classified into three levels: low risk, moderate risk and high risk. This approach allows interventions to be prioritised, so that installations or components with a high level of risk are remedied first.

An important element of the chapter is the correlation between electrical risk and thermal risk. Overheating of conductors, terminals and connections is one of the most important indicators of an emerging fault. Temperature increase accelerates insulation ageing and may lead to its melting, the occurrence of electric arcs and fires [1], [7], [23]. In this respect, temperature becomes a predictive indicator of electrical risk.

Tabelul 3.2. Insulation ageing with increasing temperature.

Temperature (°C)	Acceleration factor of insulation ageing
25	1
35	5
45	15
60	100
80	638

The application of this model allows the prioritisation of interventions and the planning of repairs or replacements [1], [7], [23].

Tabelul 3.3. Risk level associated with temperature increase.

Temperature range (°C)	Risk level	Description
0–40	Low	Normal operating conditions
40–70	Medium	Temperature above the normal limit, risk of degradation
70–90	High	Temperature close to the critical limit, high fire risk
>90	Extreme	Critical temperature, imminent fire risk

The proposed methodology for risk assessment includes six stages: data collection, assessment of regulatory compliance, assessment of physical condition, determination of total risk, proposal of remediation measures and periodic reassessment [4], [7], [10], [11], [23]. This methodology allows the transition from a punctual inspection to a continuous and predictive analysis of the electrical installation. It is based on technical documentation, PRAM measurements, visual inspection, thermographic data and real-time monitoring of parameters.

Conclusions

In conclusion, Chapter 3 shows that risk in low-voltage electrical installations is not produced by a single factor, but by the accumulation of several causes: ageing, overload, non-compliant execution, lack of maintenance, unauthorised interventions and unfavourable environmental conditions. The model $\mathbf{R = P \times S}$, together with temperature analysis, provides a practical method for identifying and prioritising risks. It follows that thermal monitoring of electrical panels can become an important tool for fire prevention and for the transition from reactive maintenance to predictive maintenance.

Chapter 4

Power Supply Schemes and Systems in Medical Infrastructures

Medical units represent critical infrastructures, because the continuity of the power supply directly influences patient safety and the performance of medical activities [3], [5], [24]. Operating rooms, intensive care units, imaging laboratories, diagnostic devices, monitoring systems and life-support equipment require a stable, safe and continuous power supply [3], [24]. In this context, the design of electrical installations in hospitals must be treated differently from that of ordinary buildings, because power interruption, the occurrence of an insulation fault or the overheating of an electrical panel may have serious consequences.

Incidents occurring in Romanian hospitals, such as those at Piatra Neamț County Hospital, the "Matei Balș" Institute and Constanța Infectious Diseases Hospital, have highlighted the vulnerability of medical infrastructures to electrical faults, overheating, improvised solutions and the lack of proper maintenance [5], [23], [26]. For this reason, this chapter analyses the main power supply schemes used in hospitals, the regulatory requirements and the measures through which electrical risk can be reduced.

The design of medical electrical installations is regulated by NP015/2022, I7/2011, SR HD 60364-7-710:2012, SR EN 12464-1, Order of the Minister of Health No. 914/2006 and Law 10/1995 [3], [4], [24], [30], [31]. These regulations impose strict conditions regarding power supply continuity, protection against electric shock and fire, selectivity of protective devices, circuit redundancy and separate supply of critical consumers [3], [4], [8], [24]–[26].

Table 4.1. Classification of medical locations according to I7/2011 and SR HD 60364-7-710.

Group	Description	Examples	Safety requirements
Group 0	Spaces where equipment directly connected to the patient is not used	administrative offices, pharmacies	normal power supply, conventional protection
Group 1	Spaces where equipment may be connected to the patient, but without life-critical risk	wards, treatment rooms	residual current protection, backup supply
Group 2	Spaces where equipment is essential for maintaining life	operating rooms, intensive care units	medical IT network, automatic backup sources

This classification determines the level of protection, the type of power supply and the safety equipment requirements that must be applied [3], [24].

To ensure power supply continuity, hospitals must be provided with a main source, a backup source and a safety source [3], [4], [24]. The main source is supplied by the public grid, the backup source is usually provided by an automatically starting generator set, and the safety source is ensured by UPS systems or batteries dedicated to critical equipment [3], [24], [28]. The maximum permitted interruption time differs depending on the importance of the consumer and may vary from 0.5 seconds to 15 seconds [3], [24].

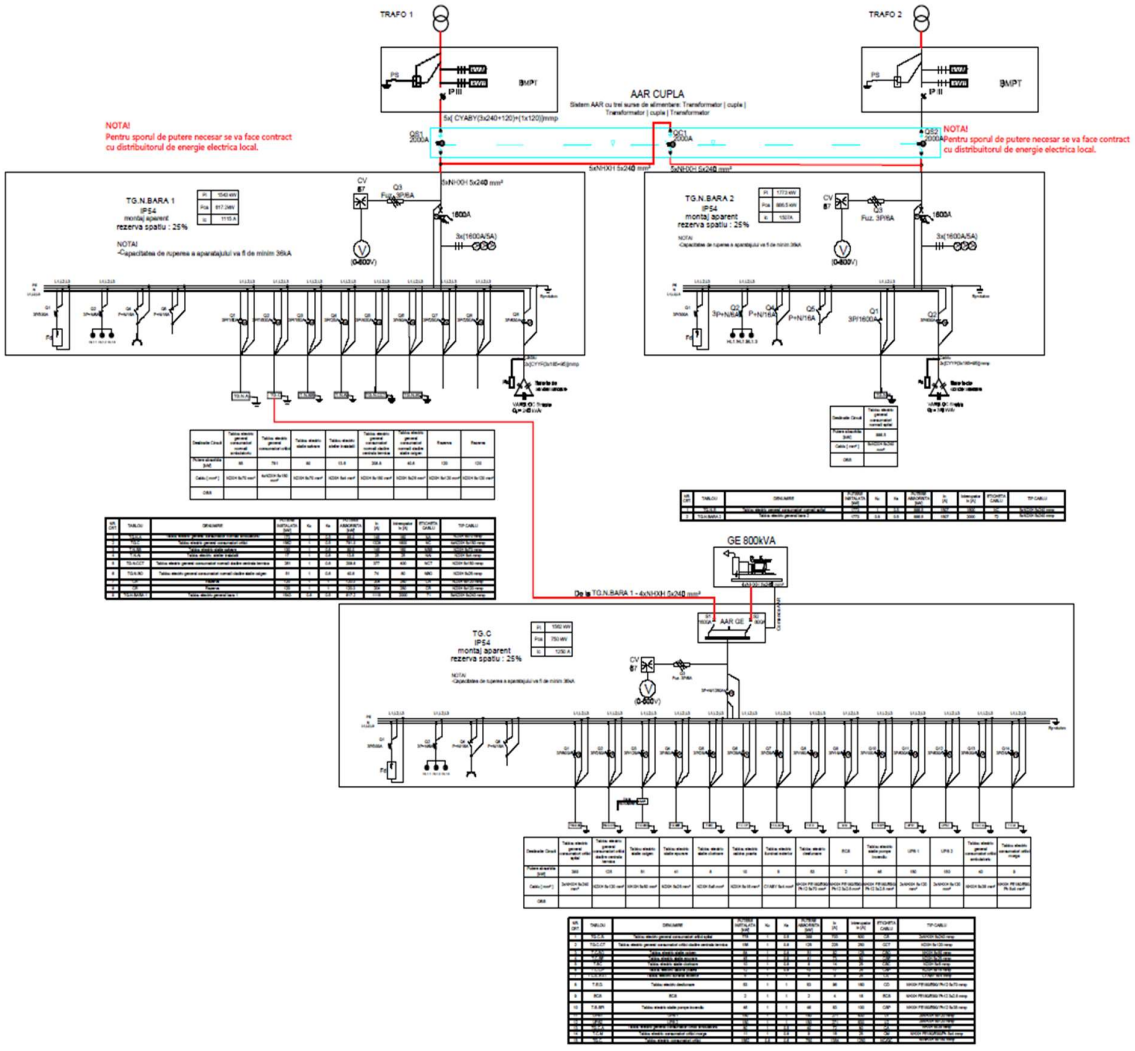


Fig. 4.1. General power supply scheme of a hospital: main source and generator set.

The chapter presents three main types of power supply schemes: the simple radial scheme, the radial scheme with automatic backup and the looped scheme [3], [4], [24]. The simple radial scheme is easy to implement, but it involves a high level of risk because it does not provide redundancy. The scheme with automatic backup allows switching between two sources and is recommended for larger hospitals. The looped scheme provides a higher level of safety, because it allows supply through alternative paths and the isolation of faulty areas without total interruption of the power supply [3], [24].

For Group 2 medical locations, the essential solution is the medical IT network. This allows the installation to continue operating even when the first insulation fault occurs, the fault being signalled visually and acoustically by an insulation monitoring device [3], [24], [25]. The medical IT network reduces leakage currents, ensures galvanic isolation and enables power supply continuity in areas where stopping equipment may endanger the patient's life.

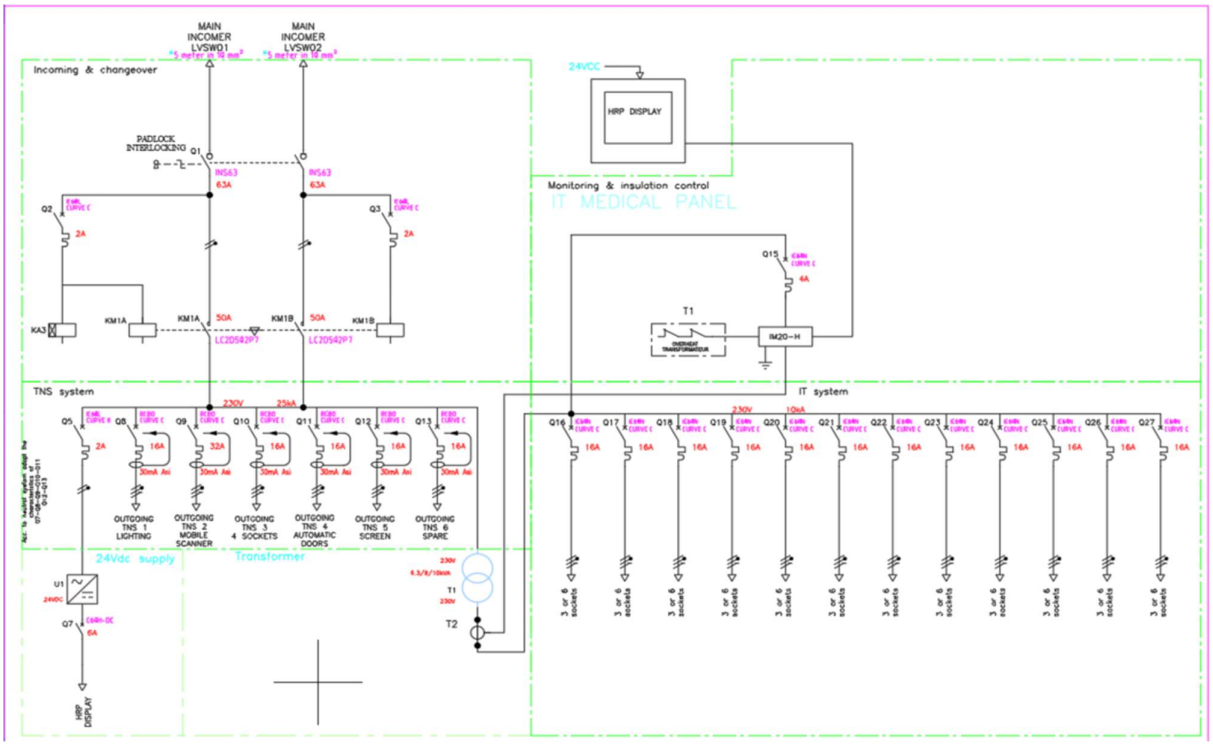


Fig. 4.2. Example of a medical IT scheme for an operating room (Schneider Electric).

To reduce risk, the chapter proposes several measures: design by specialised teams, verification of documentation by independent third parties, periodic maintenance, thermographic inspections, testing of generator sets and UPS systems, monitoring of temperatures and currents in electrical panels, staff training and the use of certified equipment for medical applications [3], [4], [5], [7], [9], [10], [24], [27], [29]. These measures show that the safety of medical electrical installations does not depend only on the initial design, but also on the continuous operation and maintenance of the system.

Table 4.2. Correlation between the type of power supply scheme and the estimated risk level.

Type of Power Supply Scheme	**Probability (P)**	**Severity (S)**	**Risk Level (R)**	**Impact on Safety**
Simple Radial System	High	Constant	MAXIMUM	High risk of total interruption
Dual Supply System	Medium	Constant	MEDIUM	Partial redundancy, switching risk
Looped System / Medical IT	Low	Low*	MINIMUM	IT monitoring, reduced fire/electric shock risk

**Note: In the medical environment, severity (S) remains technically high, but through the medical IT system, the immediate consequences for the patient are neutralised at the first fault [3], [24].*

Partial Conclusions

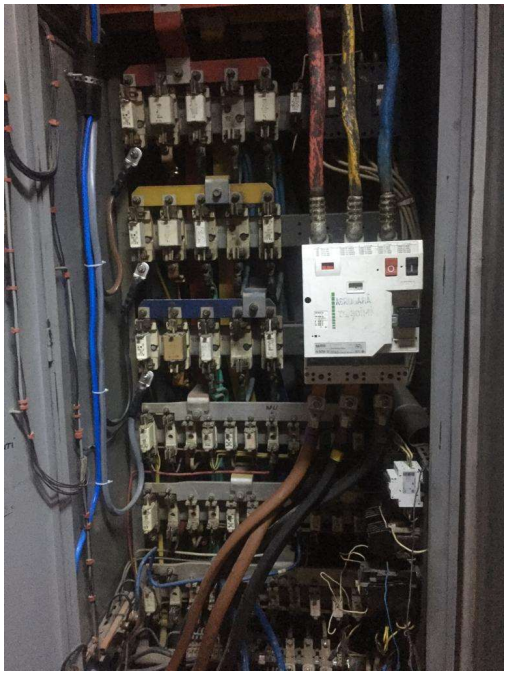
In conclusion, Chapter 4 highlights that hospitals require specially designed power supply schemes, with redundancy, backup sources, medical IT networks and continuous monitoring. The correct choice of the power supply scheme reduces the probability of interruptions, limits the risk of fire or electric shock and contributes to the continuity of medical care. In medical infrastructures, electrical safety must be treated as an essential operating condition, not merely as a technical requirement.

Chapter 5

Criteria and Policies for the Modernisation of Low-Voltage Electrical Installations

Low-voltage electrical installations have a limited service life, influenced by the quality of materials, operating conditions, the level of maintenance and the modifications carried out over time [7], [11], [23], [32]. The degradation of insulation, oxidation of connections, overheating of cables, ageing of electrical panels and increase in electrical loads lead to a decrease in the safety and performance of the installation [1], [7], [23]. In the absence of a modernisation plan, these installations may become sources of risk for fires, failures and major power supply interruptions [1], [2], [23], [26].

In Romania, an important part of the existing electrical installations has exceeded 25–30 years of operation, having been designed for loads much lower than the current ones [5], [23], [32]. In many cases, installations operate close to their capacity limit, and PRAM inspection reports do not always reflect the real condition of the equipment [9], [10], [23]. Cables, protective devices and electrical panels frequently show visible degradation, while the lack of updated technical documentation makes correct verification and safe intervention difficult [5], [11], [23], [31].



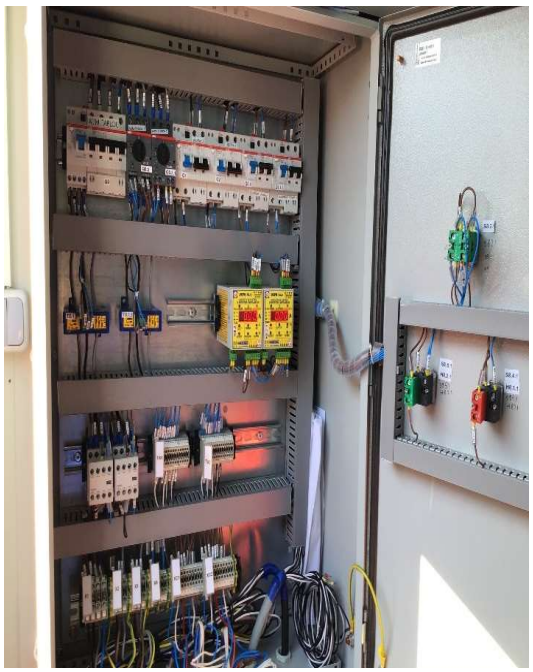


Fig. 5.1. Visual comparison between an old electrical panel and a modern one equipped with residual current protection and sensors.

The service life of electrical components differs depending on the type of equipment and the operating conditions. Copper conductors and cables may have an indicative service life of 25–35 years, electrical panels and automatic protective devices approximately 20–25 years, while connections and terminals require much more frequent checks, because they are exposed to mechanical loosening, oxidation and local overheating [7], [11], [23], [32].

Table 5.1. Indicative service life of electrical installation components.

Component / Equipment	**Average service life (years)**	**Observations**
Copper conductors and cables	25–35	Depending on heating and humidity
Sockets, switches, junction boxes	8–12	Subject to mechanical wear
Electrical panels and automatic protective devices	20–25	Periodic checks of contacts are required
Fuses and circuit breakers	15–20	Preventive replacement after 15 years is recommended
Earthing installations	20–30	Depending on soil corrosion
Connections and terminals	10–15	Require annual tightening and cleaning

These values may vary depending on the operating regime, the number of switching cycles and the operating environment, whether dry, humid, industrial or corrosive [6], [7], [11].

The decision to modernise must be based on three main criteria: the technical criterion, the economic criterion and the risk criterion [7], [11], [23], [32]. The technical criterion considers the age of the installation, equipment wear, repeated faults and non-compliant measurement values. The economic criterion compares maintenance costs with the cost of modernisation. The risk criterion analyses the probability of an accident or fire occurring in relation to the severity of its consequences [1], [2], [23], [26].

In practice, unsafe installations can be identified by visual and technical indicators, based on the design documentation: cables with discoloured or hardened insulation, traces of overheating on terminals, smell of burnt insulation, large temperature differences between phases, oversized fuses, absence of residual current devices, absence of visible earthing and frequent tripping of protective devices [4], [7], [16], [17], [23], [25].

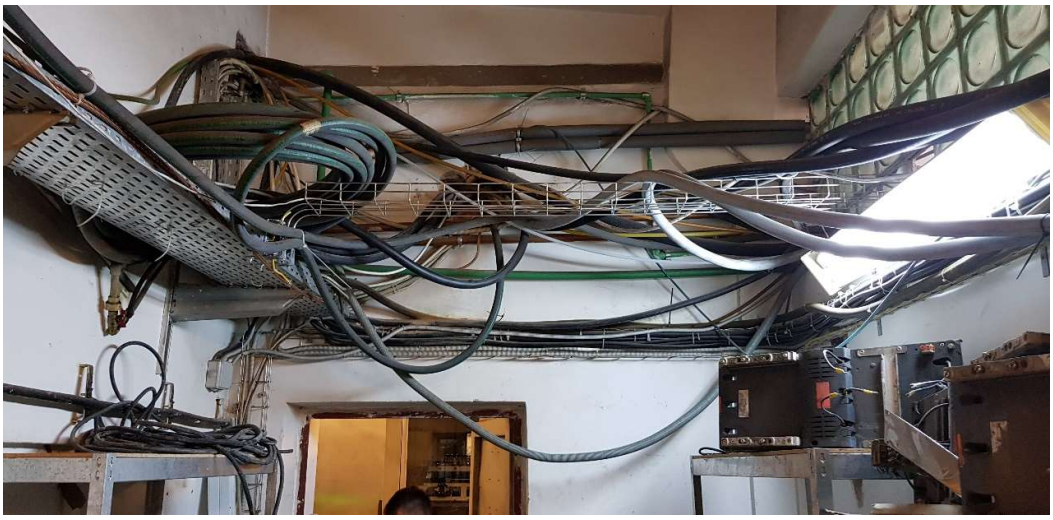


Fig. 5.2. Examples of visible deficiencies in old installations.

To prevent accelerated degradation, the chapter recommends the implementation of a preventive maintenance policy. This should include semi-annual visual inspections, annual PRAM measurements, annual thermographic inspections, cleaning and tightening of connections, testing of automatic protective devices and periodic assessment of the earthing installation [7], [9], [10], [11], [17], [25]. These activities must be complemented by major repair plans every 20–30 years, when the replacement of cables, electrical panels, sockets and protection systems becomes necessary [7], [11], [23].

An essential aspect of the chapter is the clarification of responsibilities in the modernisation process. The designer must develop the technical solution, the contractor must comply with the design and use certified materials, the verifier or consultant must control the quality of the works, the beneficiary must ensure financing and archiving of documentation, and the authorities must verify compliance with legal regulations [4], [11], [27], [29], [31]. The lack of cooperation between these entities is one of the main causes of non-compliant installations [5], [11], [23].

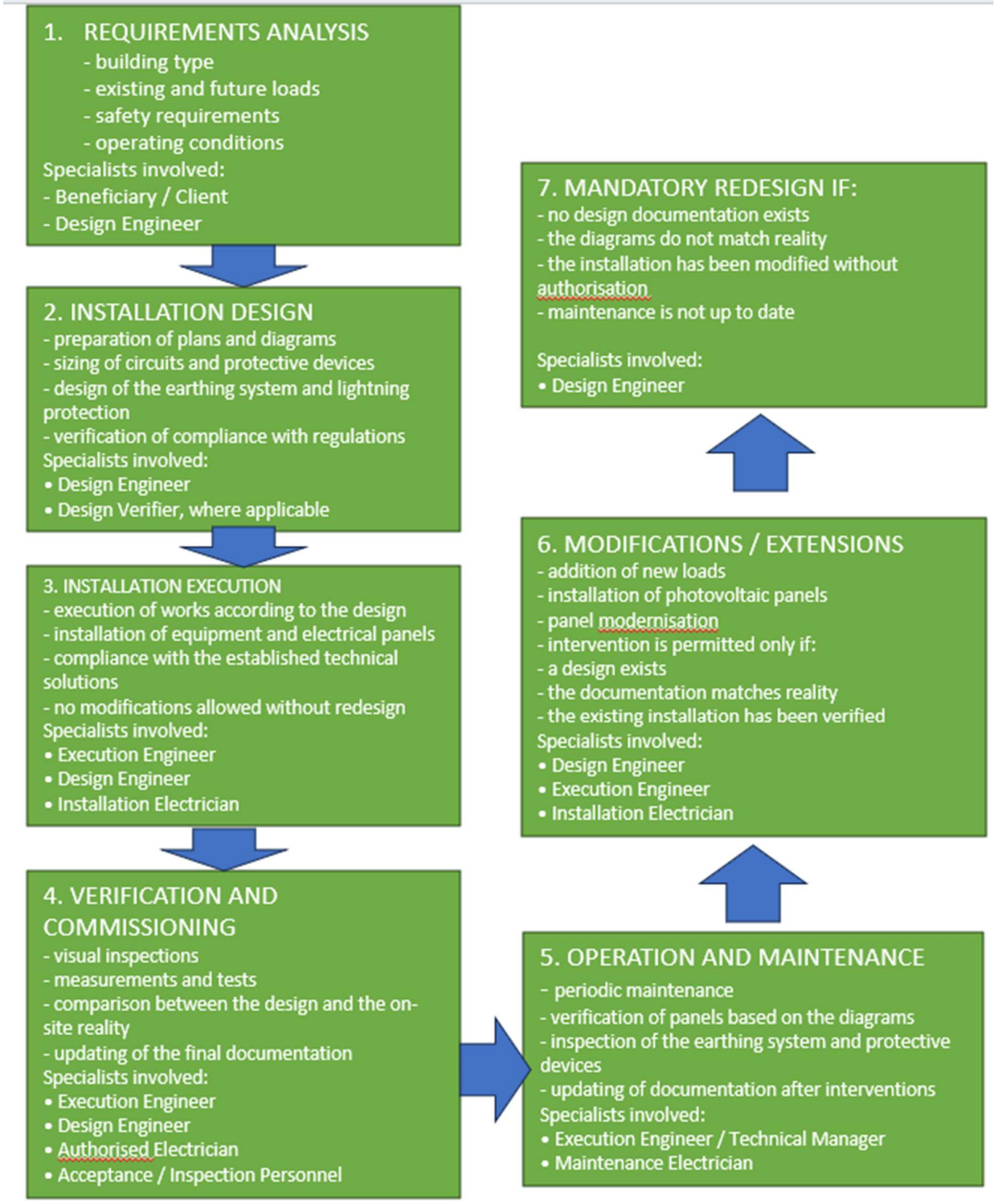


Fig. 5.3. Logical scheme of a safe electrical installation.

The modernisation of installations must be correlated with risk analysis. If the risk level exceeds the accepted threshold, the installation must be declared unsafe and modernised [1], [7], [23]. Thus, the decision must not be based only on the age of the installation, but also on its real behaviour in operation, confirmed by thermal measurements, current and voltage measurements and visual inspections [1], [7], [10].

Figure 5.4 presents an example of a thermographic measurement in an electrical panel, highlighting a hot spot with a maximum temperature of approximately 80.4 °C, indicating possible imperfect contacts or local overloads.

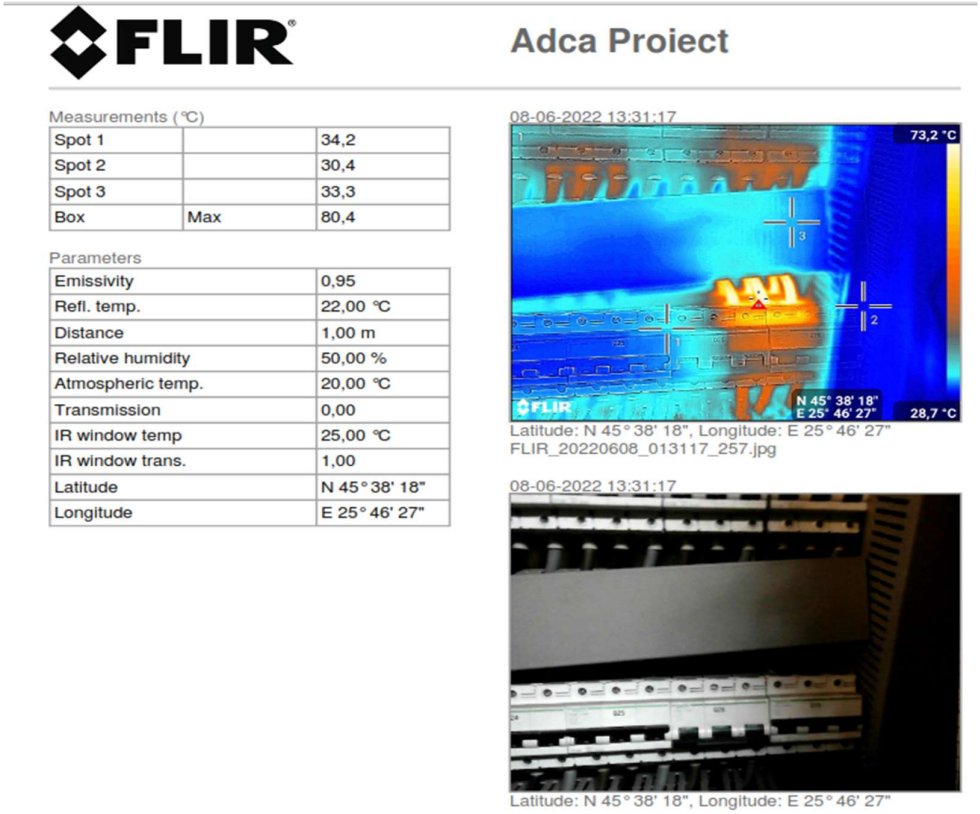


Fig. 5.4. Example of measurement with a thermal imaging camera in an electrical panel.

Conclusions

In conclusion, the modernisation of low-voltage electrical installations is an essential measure for reducing the risk of fires and accidents. Old installations, even if they have compliant inspection reports, may present real risks due to degradation, successive modifications and the increase in loads [7], [10], [23], [32]. The decision to modernise must be based on technical, economic and risk criteria, while the safety of the installation must be supported by preventive maintenance, updated documentation, clear responsibilities and real-time monitoring.

Chapter 6

Thermal Monitoring System for Electrical Panels

Chapter 6 presents an experiment carried out in order to highlight the direct relationship between exceeding the permitted electrical load, the rapid increase in conductor temperature and the occurrence of fire risk. The main purpose of the chapter is not to impose the immediate use of a specific monitoring system in existing electrical panels, but to experimentally demonstrate that an incorrectly sized or overloaded cable can heat up in a very short time to dangerous temperatures [1], [7], [23].

The increase in temperature inside electrical panels is one of the most important indicators of an incipient fault. Imperfect contacts, overloads, oxidation of connections and the incorrect selection of the cable cross-section produce Joule losses, which lead to conductor heating and insulation degradation [1], [7], [10], [23]. In many cases, conventional protective devices may not trip immediately, although the conductor temperature reaches values that affect the insulation and increase the fire risk.

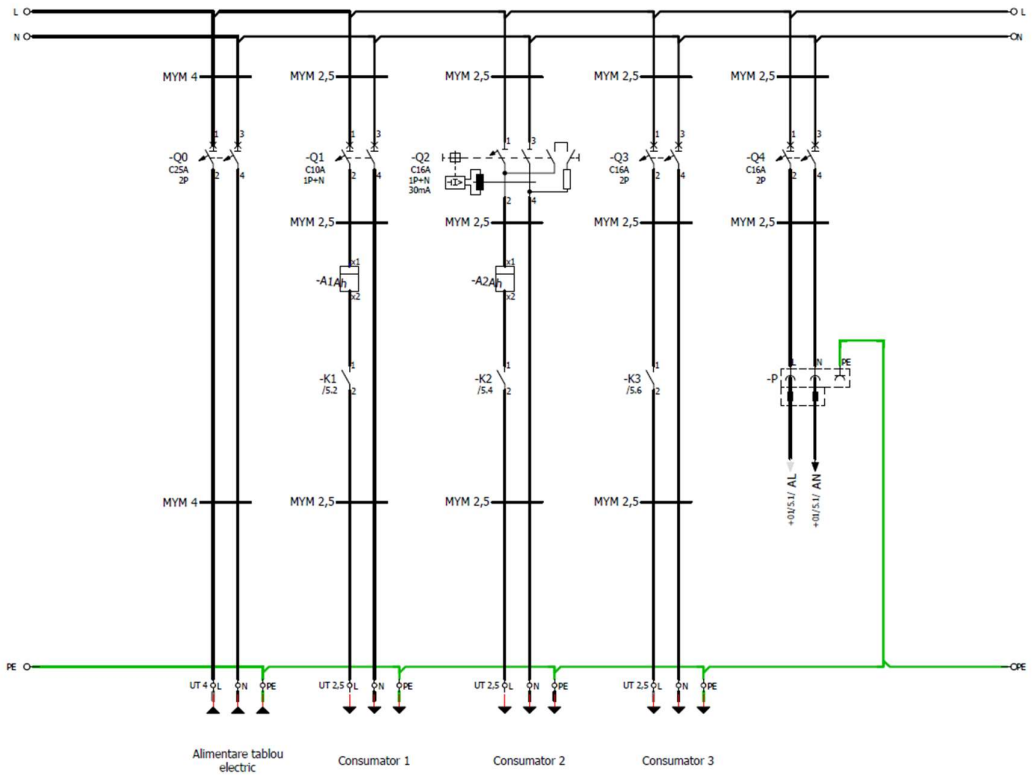
To verify this hypothesis, an experimental setup was developed, consisting of a test electrical panel, temperature sensors, an Arduino microcontroller, an LCD display, relays, optical and acoustic signalling devices and a thermal imaging camera. The system allowed real-time temperature measurement at critical points of the circuit and comparison of the obtained values with the measurements performed using the thermal camera [1], [7], [23].

Table 6.1. Components used in the thermal monitoring experiment.

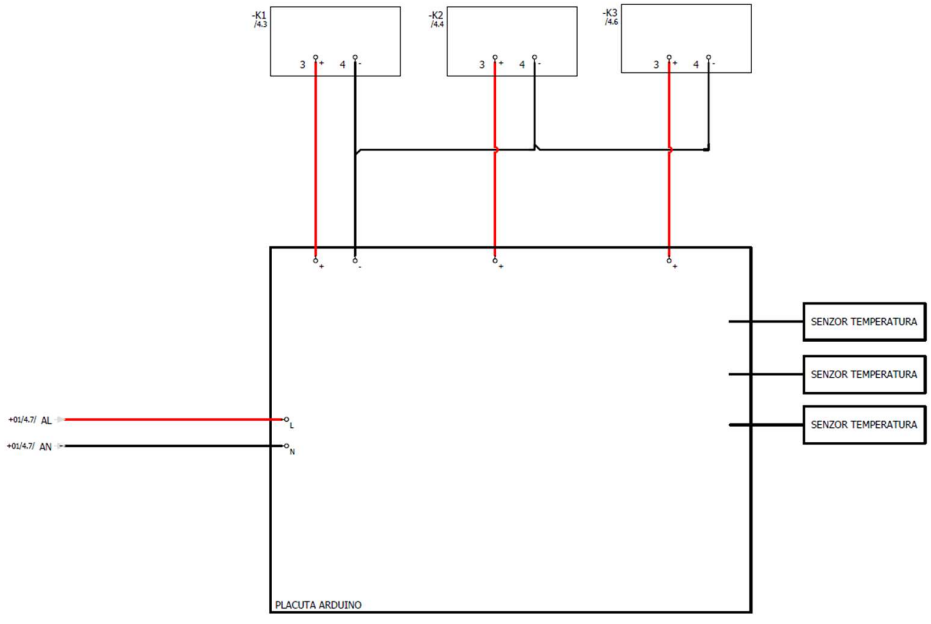
No.	Component	Main specifications	Role
1	Arduino Uno R4	ATmega32U4 microcontroller	data acquisition and control
2	DS18B20 sensors, 6 pcs.	range -55°C to +125°C, accuracy ±0.5°C	temperature measurement on circuits
3	LCD 1602	2x16 character display	local data visualisation
4	SSR relays, Solid State Relay	3 channels, 240 V / 2 A	automatic disconnection at critical threshold
5	Buzzer module + LEDs	-	acoustic and optical signalling
6	5 V and 12 V power supplies	stabilised	supply for microcontroller and sensors
7	Thermal imaging camera, FLIR One Pro	160x120 resolution	experimental verification of values

The temperature sensors were installed in three distinct areas of the panel, two for each phase, A-B, C-D and E-F, so as to cover all main circuits. The SSR relays perform the automatic disconnection of the affected circuit when the temperature exceeds the critical threshold [1],

[7], [23].


L
N
MYM 4
MYM 2,5
-Q0
C25A
2P
-Q1
C10A
1P+N
-Q2
C16A
1P+N
30mA
-Q3
C16A
2P
-Q4
C16A
2P
-A1
-A2
-K1
/5.2
-K2
/5.4
-K3
/5.6
-P
+01/5.1/ AL
+01/5.1/ AN
PE
UT 4 L N PE
UT 2,5 L N PE
Alimentare tablou electric
Consumator 1
Consumator 2
Consumator 3

a)


-K1
/4.3
-K2
/4.4
-K3
/4.6
SENZOR TEMPERATURA
SENZOR TEMPERATURA
SENZOR TEMPERATURA
+01/4.7/ AL
+01/4.7/ AN
PLACUTA ARDUINO

b)



c)

Fig. 6.1. a) Single-line diagram of the electrical panel; b) diagram of the Arduino thermal monitoring system; c) photographs taken during the experiment.

The system was programmed to read the temperatures at short time intervals, compare the values with the preset thresholds and signal when these thresholds were exceeded. The thresholds used in the experiment were: 45°C for warning, 60°C for disconnection and 80°C for critical alarm [1], [7], [23]. These values were used to observe the thermal behaviour of the conductor and to highlight how quickly a dangerous state can be reached.

Table 6.2. emperature thresholds for the monitoring system.

Threshold	**Value (°C)**	**Triggered action**
45°C	45°C	Acoustic warning and yellow LED
60°C	60°C	Circuit disconnection and red LED
80°C	80°C	Critical alarm and system lock

The experimental results showed that the conductor temperature increases very quickly when the current exceeds the permissible value for the cable cross-section. The tests were carried out on 0.75 mm² and 1 mm² conductors, with controlled loads, and the values were monitored simultaneously using the installed sensors and the thermal imaging camera [1], [7], [23]. In the case of the 0.75 mm² cable, it was observed that, at an exceedance of approximately three times the rated current, the temperature exceeded 45°C in only 6 minutes. At an exceedance of 3.6 times, the temperature exceeded 68°C in approximately 7 minutes, and at an exceedance of 3.82 times, the temperature reached over 86°C in approximately 9 minutes [23].

Figure 6.2 shows the evolution of the temperatures measured at points C and D, compared with the variation of electric current over time, highlighting the increase in temperature as the circuit load increases.

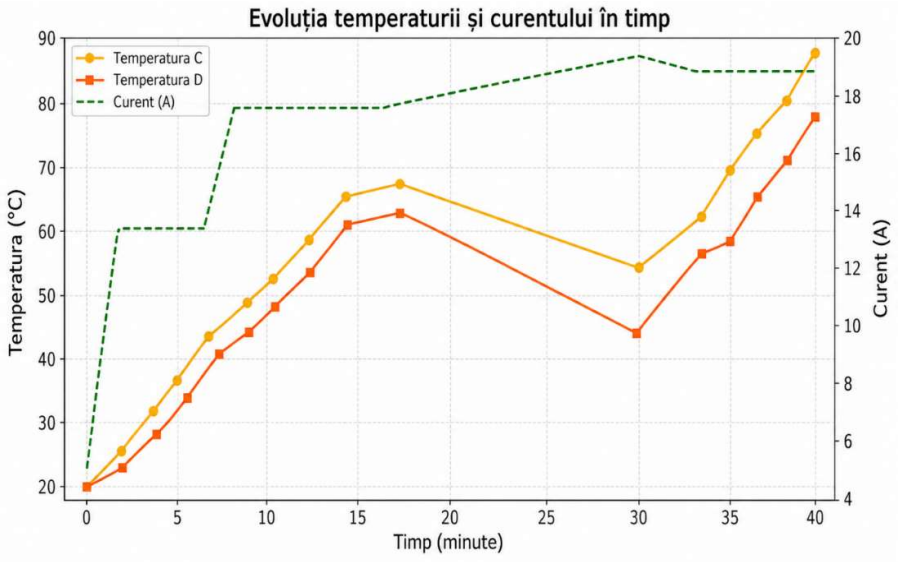


Fig. 6.2. Temperature versus time graph for different loads.

The results confirm that checking only the current or the existence of an automatic protective device is not always sufficient to prevent thermal degradation. In the experiment, there were situations in which the protection did not trip immediately, although the conductor temperature increased to values that were dangerous for the insulation [1], [7], [23]. This observation supports the idea that temperature is a practical and relevant indicator for identifying fire risk.

The correlation between temperature and fire risk is explained by the accelerated degradation of insulation. According to the Arrhenius model, the degradation rate of insulating materials increases exponentially with temperature. At approximately 80°C, the service life of PVC insulation is reduced by approximately 600 times compared with normal operating conditions at 25°C [1], [7], [23]. This finding shows that repeated or prolonged operation at high temperatures can rapidly damage the cable, even if the installation appears to function normally.

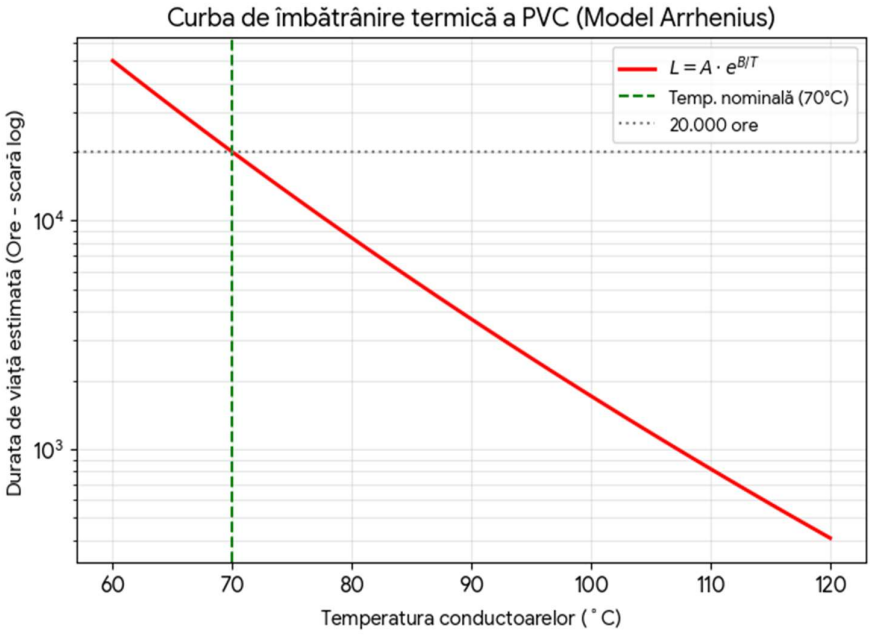


Fig. 6.3. PVC insulation degradation curve as a function of temperature, Arrhenius model.

The chapter also presents the possibility of extending such a concept through digital monitoring systems, with value recording, real-time temperature visualisation and alert transmission when thresholds are exceeded [7], [23]. However, the use of such a system in existing electrical panels must be treated as a direction of research and development. Large-scale practical implementation must be carried out only after homologation, technical verification, certification and approval by the competent bodies, so that the system complies with the safety, electromagnetic compatibility and reliability requirements imposed on electrical installations.

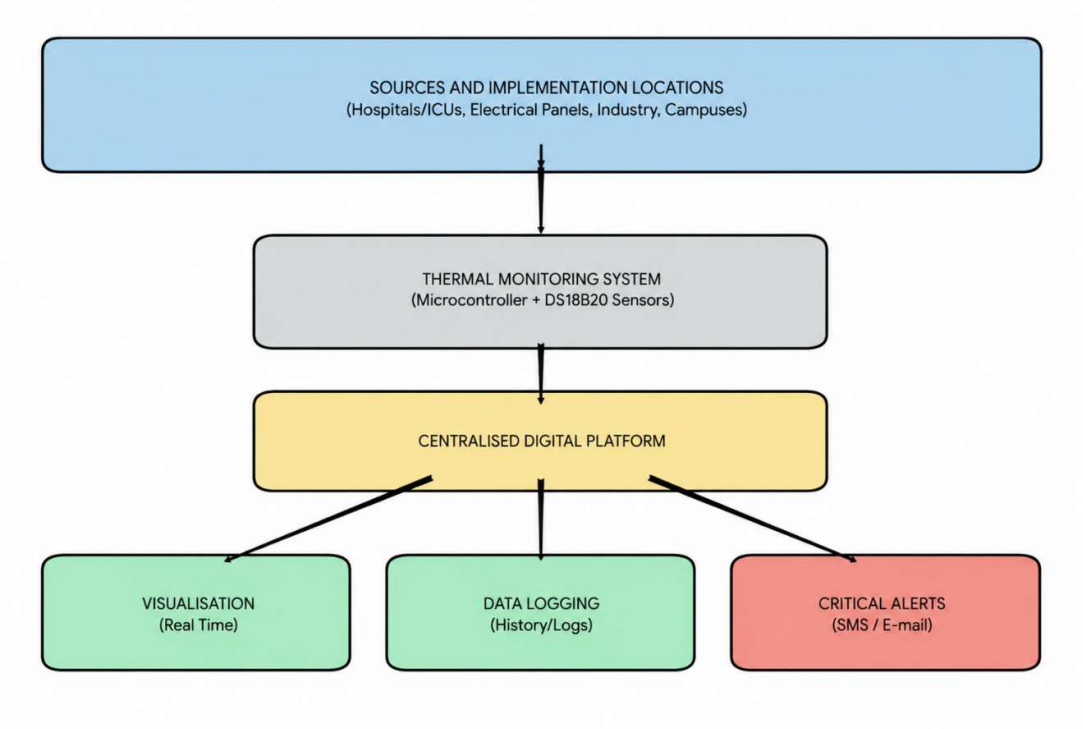


Fig. 6.4. Concept of an extended monitoring system, IoT + cloud.

Conclusions

In conclusion, Chapter 6 experimentally demonstrates that overloading a cable or incorrectly sizing it can lead to rapid temperature increases and accelerated insulation degradation. A cable that appears to be functional may reach dangerous temperatures within a few minutes, which explains why undersized or improperly modified electrical installations represent a major fire risk. The experimental system used confirms the importance of temperature monitoring as a method for identifying incipient faults, but the implementation of similar systems in existing electrical panels must be carried out only after homologation and approval by the competent technical bodies.

Chapter 7

Impedance Matching in Signal Transmission Lines

Chapter 7 presents the theoretical foundations of impedance matching in transmission lines, with emphasis on efficient energy transfer, reduction of signal reflections and limitation of additional losses in electrical and electronic circuits. In the context of the thesis, this chapter complements the experimental and applied part through a theoretical model that explains how the mismatch between source, line and load may lead to improper operation, energy losses, additional stress on components and, indirectly, an increase in technical risk in low-voltage installations [33]–[36].

Impedance matching is the process by which the impedance seen by a source or by a transmission line is adjusted so that the power transfer to the load is as efficient as possible and the reflected energy is minimised. In the general case, maximum power transfer is obtained when the load impedance is the complex conjugate of the source impedance, as expressed by relation (7.1)

$$\underline{Z}_S = \underline{Z}_L^*, \tag{7.1}$$

In relation (7.1), (Z_L) represents the load impedance, (Z_S) represents the source impedance, and the symbol (^*) indicates the complex conjugate. For purely resistive circuits, this condition is reduced to the equality between the source resistance and the load resistance. In the case of transmission lines, in order to reduce reflections, the matching condition is expressed by the equality between the load impedance and the characteristic impedance of the line, as shown in relation (7.2).

$$\underline{Z}_S = \underline{Z}_L. \tag{7.2}$$

This condition is important because, when the load is not matched to the line, part of the transmitted energy does not reach the load, but is reflected back towards the source. Reflections may produce additional losses, distortions, standing waves and frequency-dependent behaviour, especially in radio-frequency circuits and transmission lines [55]–[67].

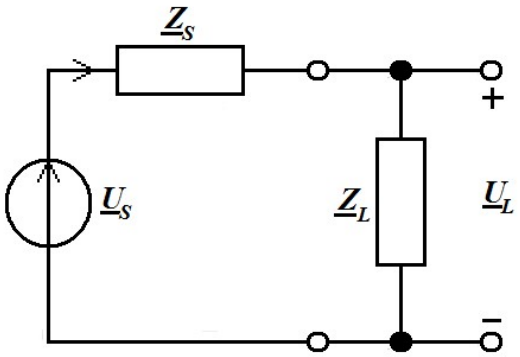


Fig. 7.3. Source and load circuit impedance.

The degree of matching can be assessed through the reflection coefficient, return loss and insertion loss. The reflection coefficient expresses the ratio between the reflected wave and the incident wave and shows the level of mismatch between load and line. For a load connected to a transmission line, the reflection coefficient is defined by relation **(7.15)**.

$$\underline{\Gamma} = \frac{\underline{Z}_L - \underline{Z}_C}{\underline{Z}_L + \underline{Z}_C}. \tag{7.15}$$

If the load impedance is equal to the characteristic impedance of the line, the reflection coefficient becomes zero, which means that there is no reflection and the energy is transmitted to the load under optimal conditions. If the impedances are different, a reflected wave appears, and part of the transmitted energy returns towards the source.

Return loss expresses, in decibels, the level of the reflected wave in relation to the incident wave. A high value of return loss indicates good matching, because the reflected energy is reduced. Insertion loss expresses the decrease in power level between the input and the output of a circuit. Therefore, these parameters allow the efficiency of energy transfer and the quality of matching to be evaluated.



Fig. 7.1. Return loss and insertion loss in a lossless circuit or transmission line.

Another important tool for impedance matching analysis is represented by the scattering parameters, also called **S parameters**, used especially in radio-frequency and microwave circuits. These parameters describe the external behaviour of a circuit through incident and emerging waves, without requiring detailed knowledge of its internal structure. For a two-port circuit, parameters $S_{11}$and S_{22} describe the reflection at the input and output ports, while parameters $S_{21}$and S_{12} describe forward and reverse transmission. This approach is useful because it allows circuits to be characterised through experimental measurements or frequency-domain simulations.

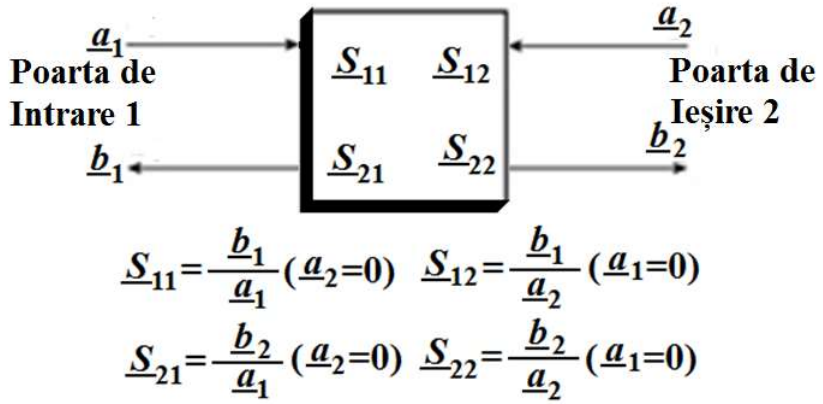


Fig. 7.2. Modelling of a two-port microwave circuit using S parameters.

In this formulation, the quantities a_1 and a_2 represent the incident waves, while b_1 and b_2 represent the emerging or reflected waves. Through this approach, reflection, transmission and isolation of the circuit can be analysed simultaneously.

The chapter presents several methods of impedance matching. The first category is represented by transformers, used for transforming voltage and impedance levels. Another category is represented by L-type networks, formed by two reactive elements, usually an inductor and a capacitor. These networks allow the matching of a source or load to a transmission line by compensating the reactive components and transforming the impedance to the required value.

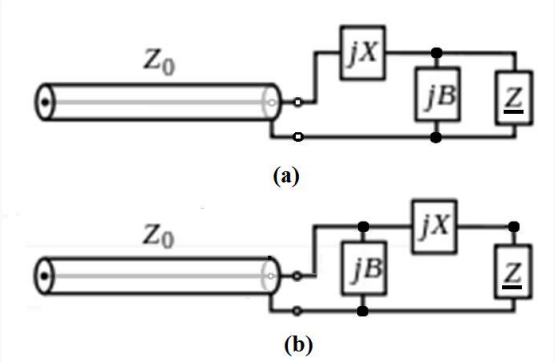


Fig. 7.5. L-type networks for matching the impedance of a source or load to a transmission line with characteristic impedance Z_0

For the case of a purely resistive load, the chapter analyses matching by means of a transmission-line section of length$\lambda/4$. This section acts as an impedance transformer, and the impedance seen at its input is expressed by relation (7.19). To obtain matching, the characteristic impedance of the matching section can be calculated using relation (7.22).

$$\underline{Z}_{in} = Z_c = Z_0. \tag{7.19}$$

$$\underline{Z}_{in} = \frac{Z_0'^2}{\underline{Z}_L}. \tag{7.22}$$

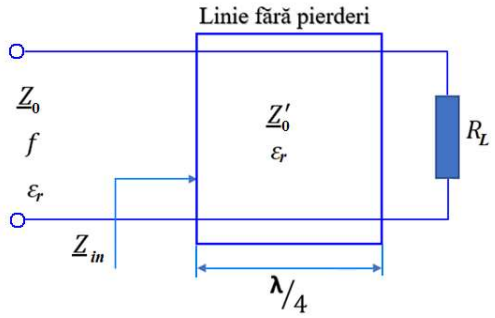


Fig. 7.7. Matching of a purely resistive load using a transmission line of length λ/4.

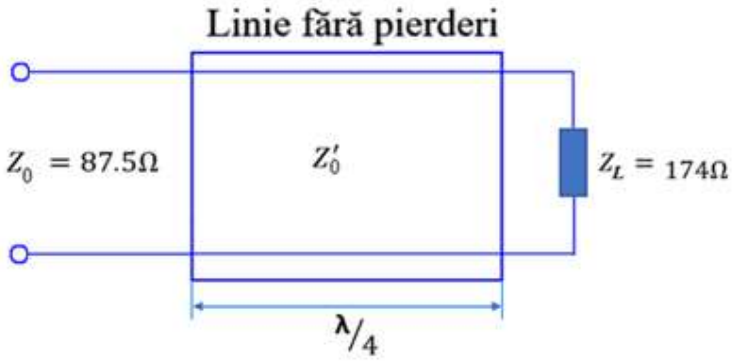


Fig. 7.14**.** Matching of a purely resistive load using a transmission-line section of length λ/4.

For complex loads, matching is more difficult because both the real part and the reactive part of the impedance must be compensated. The chapter presents matching networks consisting of two ideal reactive elements connected in series and in parallel with the load. Depending on the order of the elements, parallel-series or series-parallel configurations can be obtained. These networks allow the complex impedance of the load to be transformed into an equivalent impedance equal to the characteristic impedance of the line..

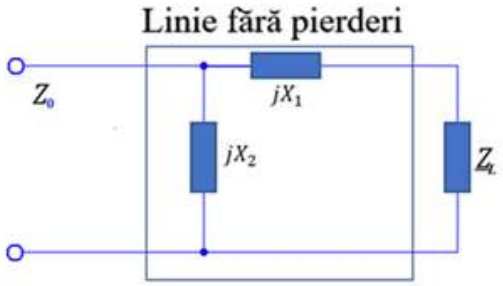


Fig. 7.8. Lossless transmission line terminated by an arbitrary impedance load, matched by means of two purely reactive elements.

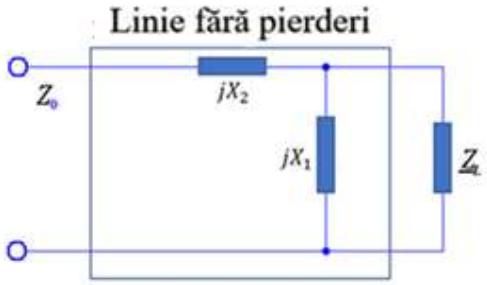


Fig. 7.9. Impedance matching by means of a reactive matching network with parallel-series topology.

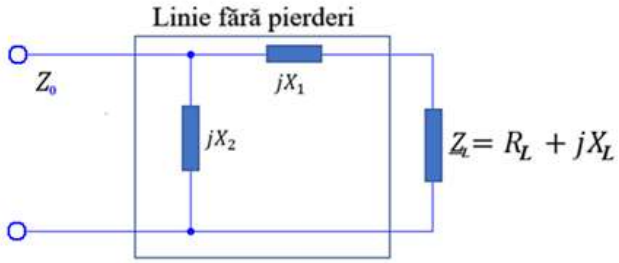


Fig. 7.10. Impedance matching by means of a reactive matching network with series-parallel topology (jX_1 in series with $\underline{Z}_L$ and în paralel with jX_2).

An important graphical tool used in this chapter is the Smith chart. It allows the representation of normalised impedances and admittances, as well as the visualisation of how series or parallel reactive elements change the position of the impedance on the chart. By using the Smith chart, the matching process becomes more intuitive, because it is possible to observe graphically how an impedance moves towards the centre of the chart, which corresponds to the matching point.

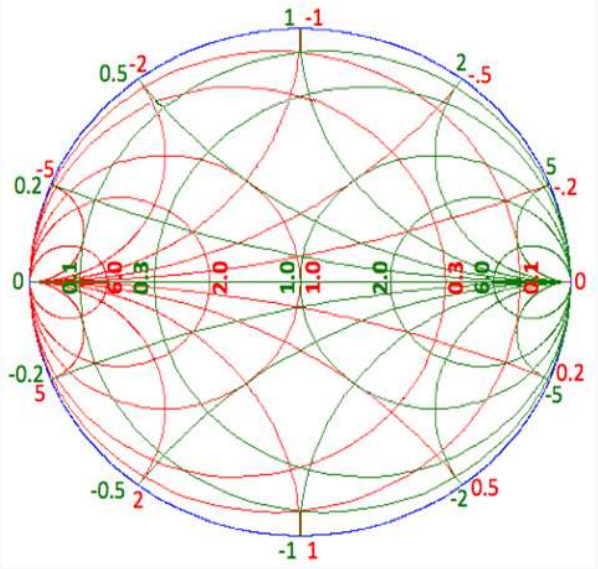


Fig. 7.21. Smith chart with immittances.

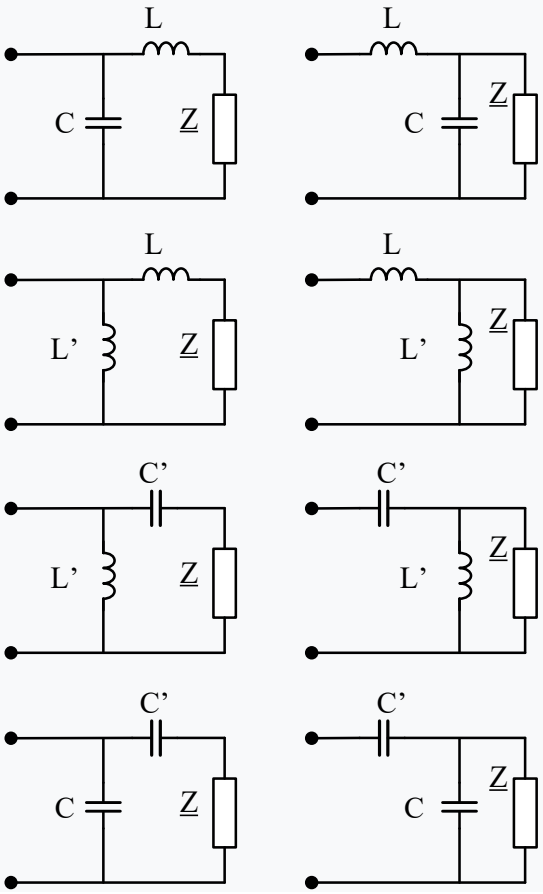


Fig. 7.26. Possible configurations for impedance matching.

In the final part, the chapter presents methods for determining component values for L- and T-type sections. By using the Smith chart or analytical calculation, the values of the inductors and capacitors required for the input impedance to approach the target impedance can be obtained. For example, for a normalising impedance of 50 Ω and an operating frequency of 1 GHz, values in the order of nanohenries for inductances and picofarads for capacitances are calculated. These examples show

the applied character of the presented methods and the possibility of implementing them in computing environments such as MAPLE or MATLAB.

Conclusions

In conclusion, Chapter 7 presents impedance matching as a fundamental method for increasing the efficiency of energy transfer and reducing reflections in transmission lines. Through the matching condition, the reflection coefficient, S parameters, L- and T-type networks, (\lambda/4) lines and the Smith chart, the chapter provides a theoretical framework for analysing losses, reflections and additional stresses in circuits. In relation to the topic of the thesis, this chapter contributes to understanding the mechanisms through which mismatch between source, line and load can lead to energy losses, improper operation and thermal stress on components. Thus, the analysis of impedance matching supports the general objective of the thesis, namely risk reduction and increased reliability of low-voltage electrical installations.

Chapter 8

Generation of Parameters for Quadripoles and Analogue Filters

Chapter 8 presents a theoretical and applied framework for modelling quadripoles and analogue filters, with the purpose of characterising signal propagation, energy transfer and the behaviour of circuits as a function of frequency. Within the thesis, this chapter complements the practical analysis of electrical installations through mathematical and numerical tools that allow the identification of losses, the evaluation of signal transfer and the diagnosis of improper operating regimes.

The quadripole is treated as a passive linear two-port circuit, with one input port and one output port, which can be described by different sets of parameters: fundamental transfer parameters (T), impedance parameters (Z), admittance parameters (Y), hybrid parameters (H), inverse hybrid parameters (F), and scattering parameters (S). Each category of parameters offers a different method of analysing the same circuit, depending on the frequency range, the measurable quantities and the purpose of the study [69]–[94].

The equations associated with a passive linear quadripole, represented in Fig. 8.1, expressed in fundamental transfer parameters and considered under harmonic conditions, are presented by relation (8.1).

$$\begin{bmatrix} \underline{U}_1 \\ \underline{I}_1 \end{bmatrix} = \begin{bmatrix} \underline{A} & \underline{B} \\ \underline{C} & \underline{D} \end{bmatrix} \begin{bmatrix} \underline{U}_2 \\ -\underline{I}_2 \end{bmatrix}. \tag{8.1}$$



Fig. 8.1. Schematic representation of a passive linear quadripole.

The description of the quadripole through fundamental transfer parameters is presented in relation (8.1), while the definition of these parameters is given in relation (8.2). The impedance parameters are introduced through relations (8.3) and (8.4), while the admittance parameters are introduced through relations (8.5) and (8.6). For situations in which the description through impedances or admittances is not convenient, the chapter introduces the hybrid parameters (H), through relations (8.7) and (8.8), respectively the inverse hybrid parameters (F), through relations (8.9) and (8.10).

$$\underline{A} \stackrel{d}{=} \left.\frac{\underline{U}_1}{\underline{U}_2}\right|_{\underline{I}_2=0} = \frac{1}{\underline{A}_{ei}};\quad \underline{B} \stackrel{d}{=} \left.\frac{\underline{U}_1}{-\underline{I}_2}\right|_{\underline{U}_2=0} = \frac{1}{\underline{Y}_{ei}};\quad \underline{C} \stackrel{d}{=} \left.\frac{\underline{I}_1}{\underline{U}_2}\right|_{\underline{I}_2=0} = \frac{1}{\underline{Z}_{ei}};\quad \underline{D} \stackrel{d}{=} \left.\frac{\underline{I}_1}{-\underline{I}_2}\right|_{\underline{U}_2=0} = \frac{1}{\underline{B}_{ei}}\ . \tag{8.2}$$

$$\begin{bmatrix}\underline{U}_1\\ \underline{U}_2\end{bmatrix} = \begin{bmatrix}\underline{Z}_{11} & \underline{Z}_{12}\\ \underline{Z}_{21} & \underline{Z}_{22}\end{bmatrix}\begin{bmatrix}\underline{I}_1\\ \underline{I}_2\end{bmatrix}, \tag{8.3}$$

$$\underline{Z}_{11} \stackrel{d}{=} \left.\frac{\underline{U}_1}{\underline{I}_1}\right|_{\underline{I}_2=0} = \underline{Z}_{ii};\quad \underline{Z}_{12} \stackrel{d}{=} \left.\frac{\underline{U}_1}{\underline{I}_2}\right|_{\underline{I}_1=0} = \underline{Z}_{ie};\quad \underline{Z}_{21} \stackrel{d}{=} \left.\frac{\underline{U}_2}{\underline{I}_1}\right|_{\underline{I}_2=0} = \underline{Z}_{ei};\quad \underline{Z}_{22} \stackrel{d}{=} \left.\frac{\underline{U}_2}{\underline{I}_2}\right|_{\underline{I}_1=0} = \underline{Z}_{ee} \tag{8.4}$$

$$\begin{bmatrix}\underline{I}_1\\ \underline{I}_2\end{bmatrix} = \begin{bmatrix}\underline{Y}_{11} & \underline{Y}_{12}\\ \underline{Y}_{21} & \underline{Y}_{22}\end{bmatrix}\begin{bmatrix}\underline{U}_1\\ \underline{U}_2\end{bmatrix}, \tag{8.5}$$

$$\underline{Y}_{11} \stackrel{d}{=} \left.\frac{\underline{I}_1}{\underline{U}_1}\right|_{\underline{U}_2=0} = \underline{Y}_{ii};\quad \underline{Y}_{12} \stackrel{d}{=} \left.\frac{\underline{I}_1}{\underline{U}_2}\right|_{\underline{U}_1=0} = \underline{Y}_{ie};\quad \underline{Y}_{21} \stackrel{d}{=} \left.\frac{\underline{I}_2}{\underline{U}_1}\right|_{\underline{U}_2=0} = \underline{Y}_{ei};\quad \underline{Y}_{22} \stackrel{d}{=} \left.\frac{\underline{I}_2}{\underline{U}_2}\right|_{\underline{U}_1=0} = \underline{Y}_{ee}. \tag{8.6}$$

$$\begin{bmatrix}\underline{U}_1\\ \underline{I}_2\end{bmatrix} = \begin{bmatrix}\underline{H}_{11} & \underline{H}_{12}\\ \underline{H}_{21} & \underline{H}_{22}\end{bmatrix}\begin{bmatrix}\underline{I}_1\\ \underline{U}_2\end{bmatrix}, \tag{8.7}$$

$$\underline{H}_{11} \stackrel{d}{=} \left.\frac{\underline{U}_1}{\underline{I}_1}\right|_{\underline{U}_2=0} = \underline{Z}_{ii}\big|_{\underline{U}_2=0} = \underline{Z}_{11}\big|_{\underline{U}_2=0}$$

$$\underline{H}_{12} \stackrel{d}{=} \left.\frac{\underline{U}_1}{\underline{U}_2}\right|_{\underline{I}_1=0} = \underline{A}_{ie}\big|_{\underline{I}_1=0}$$

$$\underline{H}_{21} \stackrel{d}{=} \left.\frac{\underline{I}_2}{\underline{I}_1}\right|_{\underline{U}_2=0} = B_{ie}\big|_{\underline{U}_2=0} \tag{8.8}$$

$$\underline{H}_{22} \stackrel{d}{=} \left.\frac{\underline{I}_2}{\underline{U}_2}\right|_{\underline{I}_1=0} = \underline{Y}_{ee}\big|_{\underline{I}_1=0} = \underline{Y}_{22}\big|_{\underline{I}_1=0}$$

$$\begin{bmatrix}\underline{I}_1\\ \underline{U}_2\end{bmatrix} = \begin{bmatrix}\underline{F}_{11} & \underline{F}_{12}\\ \underline{F}_{21} & \underline{F}_{22}\end{bmatrix}\begin{bmatrix}\underline{U}_1\\ \underline{I}_2\end{bmatrix}, \tag{8.9}$$

$$\underline{F}_{11} \stackrel{d}{=} \left.\frac{\underline{I}_1}{\underline{U}_1}\right|_{\underline{I}_2=0} = \underline{Y}_{ii}\big|_{\underline{I}_2=0} = \underline{Y}_{11}\big|_{\underline{I}_2=0}$$

(8.10)

$$\underline{F}_{12} \stackrel{d}{=} \left.\frac{\underline{I}_1}{\underline{I}_2}\right|_{\underline{U}_1=0} = \left.\frac{1}{\underline{B}_{ei}}\right|_{\underline{U}_1=0}$$

$$\underline{H}_{21} \stackrel{d}{=} \left.\frac{\underline{U}_2}{\underline{U}_1}\right|_{\underline{I}_2=0} = A_{ei}|_{\underline{I}_2=0}$$

$$\underline{F}_{22} \stackrel{d}{=} \left.\frac{\underline{U}_2}{\underline{I}_2}\right|_{\underline{U}_1=0} = \underline{Z}_{ee}|_{\underline{U}_1=0} = \underline{Z}_{22}|_{\underline{U}_1=0}$$

The role of these parameters is to show that the same circuit can be described through several equivalent mathematical representations. The important idea is that, once certain parameters of the circuit are determined, the others can be obtained through conversion relations.

The chapter also analyses the reciprocity and symmetry conditions of quadripoles. Relations **(8.11)**–**(8.14)** are used to show when a quadripole is reciprocal and how the parameters change when the input port and the output port are interchanged. For a symmetrical quadripole, the important condition is (A = D), which means that the two ports have an equivalent behaviour from the point of view of transfer.

$$\underline{I}_1|_{\substack{\underline{U}_1=0\\ \underline{U}_2=-\underline{E}}} = \underline{I}_2|_{\substack{\underline{U}_1=\underline{E}\\ \underline{U}_2=0}}. \tag{8.11}$$

$$\underline{AD} - \underline{BC} = 1; \underline{Z}_{12} = \underline{Z}_{12} \text{ si, respectiv } \underline{Y}_{12} = Y_{12}. \tag{8.12}$$

$$\begin{bmatrix}\underline{U}_2\\ \underline{I}_2\end{bmatrix} = \begin{bmatrix}\dfrac{\underline{D}}{\underline{AD}-\underline{BC}} & -\dfrac{\underline{B}}{\underline{AD}-\underline{BC}}\\ \dfrac{\underline{C}}{\underline{AD}-\underline{BC}} & -\dfrac{\underline{A}}{\underline{AD}-\underline{BC}}\end{bmatrix}\begin{bmatrix}\underline{U}_1\\ \underline{I}_1\end{bmatrix}. \tag{8.13}$$

$$\begin{bmatrix}\underline{U}_2\\ \underline{I}_2\end{bmatrix} = \begin{bmatrix}\underline{D} & -\underline{B}\\ \underline{C} & -\underline{A}\end{bmatrix}\begin{bmatrix}\underline{U}_1\\ \underline{I}_1\end{bmatrix}, \tag{8.14}$$

The characteristic impedances and image impedances of the quadripole also play an important role. They are defined by relations (8.15)–(8.19) and allow the evaluation of how the circuit is matched to the source and to the load. In the case of analogue filters, these parameters can be used to determine the pass bands and stop bands, as well as the attenuation and phase constants. The propagation condition for reciprocal and lossless filters is presented by relation (8.22), while the attenuation and phase constants are expressed by relations (8.23) and (8.24).

$$\underline{Z}_{c1} \stackrel{d}{=} \left.\frac{\underline{U}_1}{\underline{I}_1}\right|_{\underline{Z}_s=\underline{Z}_{c1}}; \quad \underline{Z}_{c2} \stackrel{d}{=} \left.\frac{\underline{U}_2}{\underline{I}_2}\right|_{\underline{Z}_i=\underline{Z}_{c2}}, \tag{8.15}$$

$$\underline{Z}_{i1} \stackrel{d}{=} \left.\frac{\underline{U}_1}{\underline{I}_1}\right|_{\underline{Z}_s=\underline{Z}_{i2}}; \quad \underline{Z}_{i2} \stackrel{d}{=} \left.\frac{\underline{U}_2}{\underline{I}_2}\right|_{\underline{Z}_i=\underline{Z}_{i1}}. \tag{8.16}$$

$$\underline{Z}_{c1} = \frac{1}{2\underline{C}}\left[(\underline{A}-\underline{D}) \pm \sqrt{(\underline{A}-\underline{D})^2 + 4\underline{B}\underline{C}}\right], \quad \underline{Z}_{c2} = \frac{1}{2\underline{C}}\left[(\underline{D}-\underline{A}) \pm \sqrt{(\underline{D}-\underline{A})^2 + 4\underline{B}\underline{C}}\right]. \tag{8.17}$$

$$\underline{Z}_{i1} = \pm\sqrt{\frac{\underline{A}\underline{B}}{\underline{C}\underline{D}}}, \quad \underline{Z}_{i2} = \pm\sqrt{\frac{\underline{D}\underline{B}}{\underline{C}\underline{A}}}. \tag{8.18}$$

$$\underline{Z}_{c1} = \underline{Z}_{c2} = \underline{Z}_{i1} = \underline{Z}_{i2} = \pm\sqrt{\frac{\underline{B}}{\underline{C}}}. \tag{8.19}$$

$$0 \le AD \le 1. \tag{8.22}$$

$$a = 0, \quad b = arcctg\frac{1}{\sqrt{\frac{1}{AD}-1}} + k\pi = arccos\sqrt{AD} + k\pi, \tag{8.23}$$

$$a = arg\,c\,tg\frac{1}{\sqrt{1-\frac{1}{AD}}} = \text{argch}\sqrt{AD}, \quad b = \begin{cases} \pm\frac{\pi}{2} & AD \le 0 \\ 0 \text{ sau } 1 & AD \ge 1 \end{cases}. \tag{8.24}$$

In the high-frequency range, the chapter highlights the importance of scattering parameters (S). These are preferred because, unlike parameters (Z), (Y), (T), (H), and (F), they do not require ideal short-circuit or open-circuit conditions at the ports. The (S) parameters describe the relationship between incident and emerging waves and can be determined experimentally using a vector network analyser.

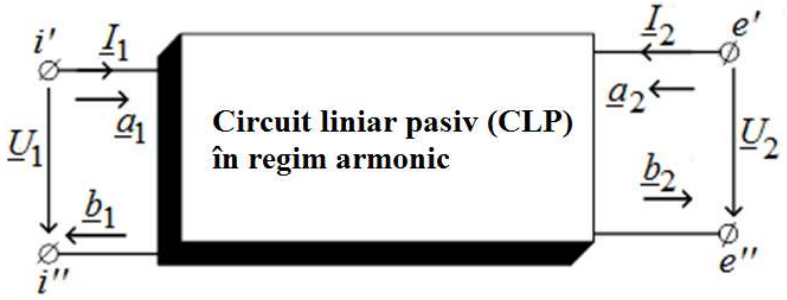


Fig. 8.2. Circuit used to define the S parameters.

The (S) parameters are defined by relations (8.25)–(8.27). These relations show the connection between incident waves, emerging waves and the electrical quantities at the input and output of the quadripole. Relation (8.25) expresses the basic model of the (S) parameters, while relations (8.26) and (8.27) establish the connection with the voltages and currents at the ports. [80-88]:

$$\begin{cases} \underline{b}_1 = \underline{S}_{11}\underline{a}_1 + \underline{S}_{12}\underline{a}_2 \\ \underline{b}_2 = \underline{S}_{21}\underline{a}_1 + \underline{S}_{22}\underline{a}_2' \end{cases} \tag{8.25}$$

$$\underline{a}_1 = \frac{1}{2\sqrt{Z_0}}(\underline{U}_1 + Z_0\underline{I}_1), \underline{b}_1 = \frac{1}{2\sqrt{Z_0}}(\underline{U}_1 - Z_0\underline{I}_1); \quad \underline{a}_2 = \frac{1}{2\sqrt{Z_0}}(\underline{U}_2 + Z_0\underline{I}_2), \underline{b}_2 = \frac{1}{2\sqrt{Z_0}}(\underline{U}_2 - Z_0\underline{I}_2). \tag{8.26}$$

$$\begin{cases} \frac{1}{2\sqrt{Z_0}}\left(\underline{U}_1 - Z_0\underline{I}_1\right) = \underline{S}_{11}\cdot\frac{1}{2\sqrt{Z_0}}\left(\underline{U}_1 + Z_0\underline{I}_1\right) + \underline{S}_{12}\cdot\frac{1}{2\sqrt{Z_0}}\left(\underline{U}_2 + Z_0\underline{I}_2\right) \\ \frac{1}{2\sqrt{Z_0}}\left(\underline{U}_2 - Z_0\underline{I}_2\right) = \underline{S}_{21}\cdot\frac{1}{2\sqrt{Z_0}}\left(\underline{U}_1 + Z_0\underline{I}_1\right) + \underline{S}_{22}\cdot\frac{1}{2\sqrt{Z_0}}\left(\underline{U}_2 + Z_0\underline{I}_2\right). \end{cases} \quad (8.27)$$

The chapter then presents the automatic generation of transfer functions. For linear, time-invariant circuits with lumped parameters, symbolic analysis makes it possible to obtain transfer functions in fully symbolic, partially symbolic or numerical form. Relation **(8.28)** defines the main transfer functions used: transfer impedance, transfer admittance, voltage transfer factor and current transfer factor.

$$Z_{ei} \stackrel{d}{=} \frac{U_e(s)}{J_i(s)},\ Y_{ei} \stackrel{d}{=} \frac{I_e(s)}{E_i(s)},\ A_{ei} \stackrel{d}{=} \frac{U_e(s)}{E_i(s)} \text{ și } B_{ei} \stackrel{d}{=} \frac{I_e(s)}{J_i(s)}. \quad (8.28)$$

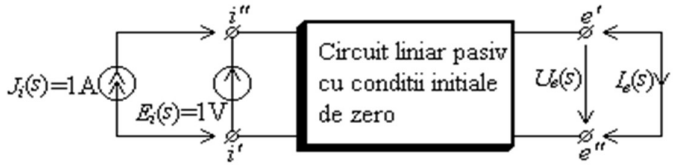


Fig. 8.3. Definition of the four types of controlled sources.

Figure 8.3 is useful because it explains how transfer functions are obtained by applying a unit excitation and observing the response of the circuit.

For determining the input impedance or admittance, the input-output two-port structure shown in Fig. 8.4a and Fig. 8.4b is used. Similarly, the configuration required to calculate the output impedance or admittance can be constructed.

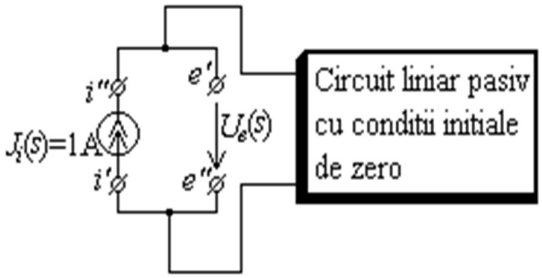


Fig. 8.4, a. Definition of the input impedance $Z_{ii}(s)$.

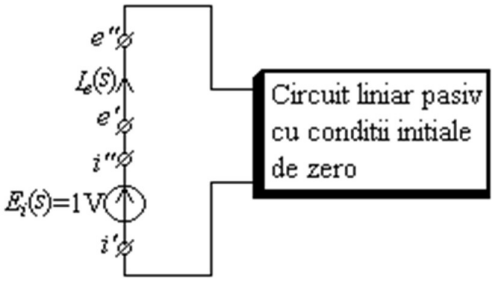


Fig. 8.4, b. Definition of the input admittance $Y_{ii}(s)$.

For the generation of transfer functions and circuit parameters, the CSAP and TFSYG programs are used, developed for the symbolic analysis of analogue circuits. These programs allow the automatic formulation of modified nodal equations, the generation of transfer functions, the calculation of poles and zeros, the determination of the modulus and argument of the transfer function and sensitivity analysis.

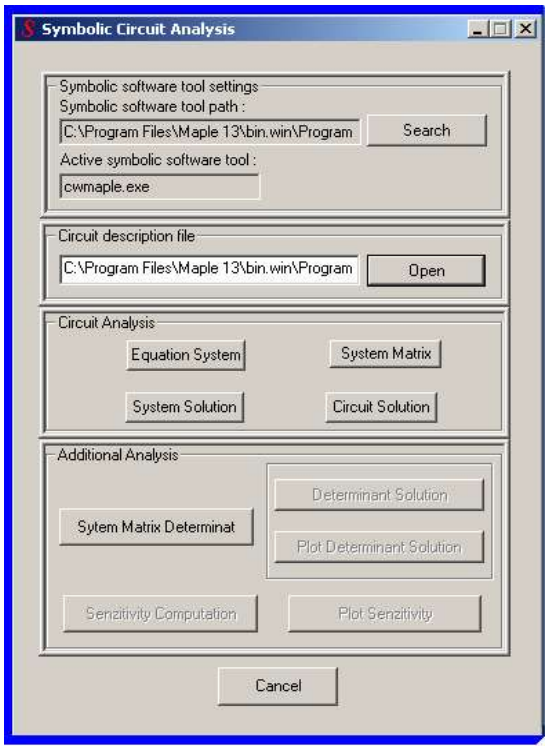


Fig. 8.5. User interface of the CSAP program.

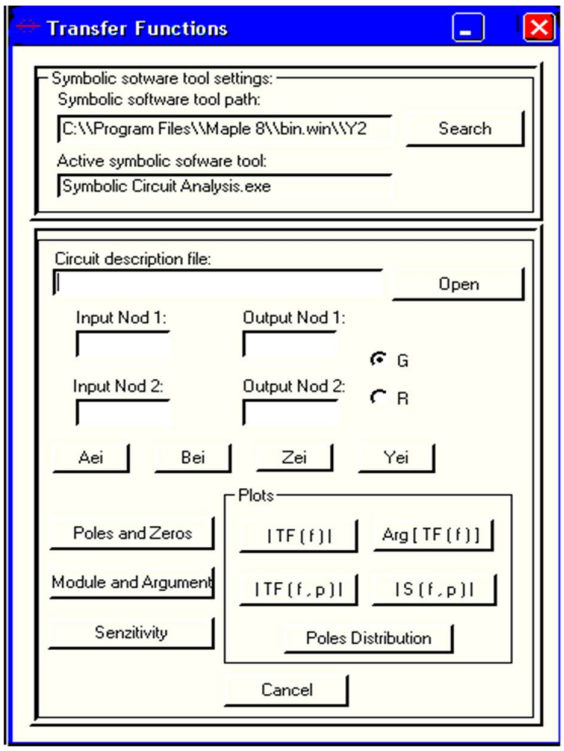


Fig. 8.6. User interface of the TFSYG program.

These two figures demonstrate that the analysis does not remain only at a theoretical level, but is implemented through computational programs.

An important element of the chapter is the conversion between different sets of quadripole parameters. In practice, it is not always necessary to determine all parameters directly. First, the parameters that are more easily obtained through transfer functions are calculated, and then the other parameters are determined through conversion relations. These relations are summarised in Table 8.1, which presents the transformations between parameters (T), (Z), (Y), (H), (F), and (S).

Tabelul 8.1. Relations between the parameters of analogue two-port circuits.

$T_inv := \begin{bmatrix} \frac{D}{-1.BC+DA} & -\frac{1.B}{-1.BC+DA} \\ -\frac{1.C}{-1.BC+DA} & \frac{A}{-1.BC+DA} \end{bmatrix}$	$Z_T := \begin{bmatrix} \frac{A}{C} & -\frac{1.(AD-1.BC)}{C} \\ \frac{1}{C} & -\frac{1.D}{C} \end{bmatrix}$
$Y_T := \begin{bmatrix} \frac{D}{B} & -\frac{1.(-1.BC+DA)}{B} \\ \frac{1}{B} & -\frac{1.A}{B} \end{bmatrix}$	$H_T := \begin{bmatrix} \frac{B}{D} & \frac{-1.BC+DA}{D} \\ \frac{1}{D} & -\frac{1.C}{D} \end{bmatrix}$

$$F_T := \begin{bmatrix} \frac{C_complex}{A} & \frac{1.\left(A\ D_complex - B\ C_complex\right)}{A} \\ \frac{1.}{A} & -\frac{1.\ B}{A} \end{bmatrix}$$

$$S11_T := \frac{A\ Z0 + B - 1.\ C_complex\ Z0^2 - 1.\ Z0\ D_complex}{C_complex\ Z0^2 + Z0\ D_complex + A\ Z0 + B}$$

$$S12_T := \frac{2.\ Z0\ (A\ D_complex - 1.\ B\ C_complex)}{C_complex Z0^2 + Z0\ D_complex + A\ Z0 + B}$$

$$S21_T := \frac{2.\ Z0}{C_complex\ Z0^2 + Z0\ D_complex + A\ Z0 + B}$$

$$S22_T := -\frac{1.\ (C_complex Z0^2 - 1.\ Z0\ D_complex + A\ Z0 - 1.\ B}{C_complex Z0^2 + Z0\ D_complex + A\ Z0 + B}$$

$$A_S := -\frac{0.5000\ (S11\ S22 - 1.\ S11 - 1.\ S21\ S12 + S22 - 1.)}{S21}$$

$$B_S := -\frac{0.5000\ Z0\ (S11\ S22 + S11 - 1.\ S21\ S12 + S22 + 1.)}{S21}$$

$$C_S := \frac{0.5000\ (S11\ S22 - 1.\ S22 - 1.\ S11 + 1. - 1.\ S21\ S12)}{S21\ Z0}$$

$$D_S := \frac{0.5000\ (S11\ S22 - 1.\ S22 + S11 - 1. - 1.\ S21\ S12)}{S21}$$

$$Z11_S := -\frac{1.\ Z0(-1.\ S12S21 + S22S11 + S22 - 1.\ S11 - 1.)}{-1.\ S12S21 + S22S11 - 1.\ S22 - 1.\ S11 + 1.}$$

$$Z12_S := -\frac{2.\ Z0\ S12}{-1.\ S12\ S21 + S22\ S11 - 1.\ S22 - 1.\ S11 +}$$

$$Z21_S := \frac{2.\ Z0\ S21}{-1.\ S12\ S21 + S22\ S11 - 1.\ S22 - 1.\ S11 + 1.}$$

$$Z22_S := \frac{Z0\ (S11 - 1.\ S22 - 1. - 1.\ S12\ S21 + S22\ S11)}{-1.\ S12\ S21 + S22\ S11 - 1.\ S22 - 1.\ S11 + 1.}$$

$$Y11_S := -\frac{1.\ (-1.\ S12\ S21 + S22\ S11 + S11 - 1.\ S22 - 1.)}{Z0\ (-1.\ S12\ S21 + S22\ S11 + S22 + S11 + 1.)}$$

$$Y12_S := -\frac{2.\ S12}{Z0\ (-1.\ S12\ S21 + S22\ S11 + S22 + S11 + 1.)}$$

$$Y21_S := \frac{2.\ S21}{Z0\ (-1.\ S12\ S21 + S22\ S11 + S22 + S11 + 1.)}$$

$$Y22_S := \frac{-1.\ S11 + S22 - 1. - 1.\ S12\ S21 + S22\ S11}{Z0\ (-1.\ S12\ S21 + S22\ S11 + S22 + S11 + 1.)}$$

$$H11_S := -\frac{1.\ Z0\ (S22\ S11 - 1.\ S12\ S21 + S22 + S11 + 1.)}{-1.\ S12\ S21 + S22\ S11 - 1.\ S22 + S11 - 1.}$$

$$H12_S := -\frac{2.\ S12}{-1.\ S12\ S21 + S22\ S11 - 1.\ S22 + S11 - 1.}$$

$$H21_S := -\frac{2.\ S21}{-1.\ S12\ S21 + S22\ S11 - 1.\ S22 + S11 - 1.}$$

$$H22_S := \frac{S22\ S11 + 1. - 1.\ S11 - 1.\ S12\ S21 - 1.\ S22}{(-1.\ S12\ S21 + S22\ S11 - 1.\ S22 + S11 - 1.)\ Z0}$$

$$F11_S := -\frac{1.\ (-1.\ S12\ S21 + S22\ S11 - 1.\ S11 - 1.\ S22 + 1.)}{Z0\ (-1.\ S12\ S21 + S22\ S11 + S22 - 1.\ S11 - 1.)}$$

$$F12_S := -\frac{2.\ S12}{-1.\ S12\ S21 + S22\ S11 + S22 - 1.\ S11 - 1.}$$

$$F21_S := -\frac{2.\ S21}{-1.\ S12\ S21 + S22\ S11 + S22 - 1.\ S11 - 1.}$$

$$F22_S := \frac{Z0\ (S11 + 1. - 1.\ S12\ S21 + S22\ S11 + S22)}{-1.\ S12\ S21 + S22\ S11 + S22 - 1.\ S11 - 1.}$$

$$S11_T := -\frac{1.\ (F11\ F22\ Z0 - F11\ Z0^2 - F12\ F21\ Z0 - F22 + Z0)}{F11\ F22\ Z0 - F11\ Z0^2 - F12\ F21\ Z0 + F22 - Z0}$$

$$S12_T := -\frac{2.\ F12\ Z0}{F11\ F22\ Z0 - F11\ Z0^2 - F12\ F21\ Z0 + F22 - Z0}$$

$$S21_T := -\frac{2.\ F21\ Z0}{F11\ F22\ Z0 - F11\ Z0^2 - F12\ F21\ Z0 + F22 - Z0}$$

$$S22_T := \frac{1.\ (F11\ F22\ Z0 + F11\ Z0^2 - F12\ F21\ Z0 + F22 + Z0)}{F11\ F22\ Z0 - F11\ Z0^2 - F12\ F21\ Z0 + F22 - Z0}$$

$$Z_Y := \begin{bmatrix} \frac{Y22}{Y11Y22 - 1.\ Y21Y12} & -\frac{1.\ Y12}{Y11Y22 - 1.\ Y21Y12} \\ -\frac{1.\ Y21}{Y11Y22 - 1.\ Y21Y12} & \frac{Y11}{Y11Y22 - 1.\ Y21Y12} \end{bmatrix}$$

$$Y_Z := \begin{bmatrix} \frac{Z22}{Z11\ Z22 - 1.\ Z21\ Z12} & -\frac{1.\ Z12}{Z11\ Z22 - 1.\ Z21\ Z12} \\ -\frac{1.\ Z21}{Z11\ Z22 - 1.\ Z21\ Z12} & \frac{Z11}{Z11\ Z22 - 1.\ Z21\ Z12} \end{bmatrix}$$

$T_Y := \begin{bmatrix} -\frac{1.\ Y22}{Y21} & \frac{1}{Y21} \\ -\frac{1.\ (Y11\ Y22 - 1.\ Y12\ Y21)}{Y21} & \frac{Y11}{Y21} \end{bmatrix}$	$T_Z := \begin{bmatrix} \frac{Z11}{Z21} & -\frac{1.\ (Z11\ Z22 - 1.\ Z12\ Z21)}{Z21} \\ \frac{1}{Z21} & -\frac{1.\ Z22}{Z21} \end{bmatrix}$
$T_H := \begin{bmatrix} -\frac{1.\ (H11\,H22 - 1.\,H12\,H21)}{H21} & \frac{H11}{H21} \\ -\frac{1.\,H22}{H21} & \frac{1}{H21} \end{bmatrix}$	$T_F := \begin{bmatrix} \frac{1}{F21} & -\frac{1.\ F22}{F21} \\ \frac{F11}{F21} & -\frac{1.\ (F11\ F22 - 1.\ F12\ F21)}{F21} \end{bmatrix}$
$H_Z := \begin{bmatrix} \frac{Z11\ Z22 - 1.\ Z12\ Z21}{Z22} & \frac{Z12}{Z22} \\ -\frac{1.\ Z21}{Z22} & \frac{1}{Z22} \end{bmatrix}$	$F_Z := \begin{bmatrix} \frac{1}{Z11} & -\frac{1.\ Z12}{Z11} \\ \frac{Z21}{Z11} & \frac{Z11\ Z22 - 1.\ Z21\ Z12}{Z11} \end{bmatrix}$
$S11_Z := -\frac{1.\ (-1.\ Z12\ Z21 - 1.\ Z22\ Z0 + Z22\ Z11 + Z0^2 - 1.\ Z0\ Z1}{Z12\ Z21 - 1.\ Z22\ Z11 - 1.\ Z22\ Z0 + Z0\ Z11 + Z0^2}$ $S12_Z := -\frac{2.\ Z12\ Z0}{Z12\ Z21 - 1.\ Z22\ Z11 - 1.\ Z22\ Z0 + Z0\ Z11 + Z0^2}$ $S21_Z := \frac{2.\ Z0\ Z21}{Z12\ Z21 - 1.\ Z22\ Z11 - 1.\ Z22\ Z0 + Z0\ Z11 + Z0^2}$ $S22_Z := -\frac{1.\ (Z0\ Z11 + Z22\ Z0 + Z0^2 - 1.\ Z12\ Z21 + Z22\ Z11)}{Z12\ Z21 - 1.\ Z22\ Z11 - 1.\ Z22\ Z0 + Z0\ Z11 + Z0^2}$	$S11_Y := -\frac{1.\ (-1.\ Y12\ Z0^2\ Y21 + Y22\ Z0^2\ Y11 - 1.\ Y11\ Z0 - 1.\ Y22\ Z0 + 1.)}{-1.\ Y12\ Z0^2\ Y21 + Y22\ Z0^2\ Y11 + Y22\ Z0 - 1.\ Y11\ Z0 - 1.}$ $S12_Y := \frac{2.\ Y12\ Z0}{-1.\ Y12\ Z0^2\ Y21 + Y22\ Z0^2\ Y11 + Y22\ Z0 - 1.\ Y11\ Z0 - 1.}$ $S21_Y := -\frac{2.\ Y21\ Z0}{-1.\ Y12\ Z0^2\ Y21 + Y22\ Z0^2\ Y11 + Y22\ Z0 - 1.\ Y11\ Z0 - 1.}$ $S22_Y := -\frac{1.\ (Y11\ Z0 + Y22\ Z0 + 1. - 1.\ Y12\ Z0^2\ Y21 + Y22\ Z0^2\ Y11)}{-1.\ Y12\ Z0^2\ Y21 + Y22\ Z0^2\ Y11 + Y22\ Z0 - 1.\ Y11\ Z0 - 1.}$

Table 8.1 is important because it represents the mathematical basis for conversion between the different descriptions of the same circuit.

In the applied part, the chapter presents two examples of (m)-type band-pass filters. The first example is the filter in Fig. 8.7, for which the fundamental parameters (A), (B), (C), and (D) are generated, after which the parameters (Z), (Y), (H), (F), and (S) are determined. The matrix of the fundamental parameters is presented by relation (8.29), while the matrices (Z), (Y), (H), (F), and (S) are presented by relations (8.30)–(8.34).

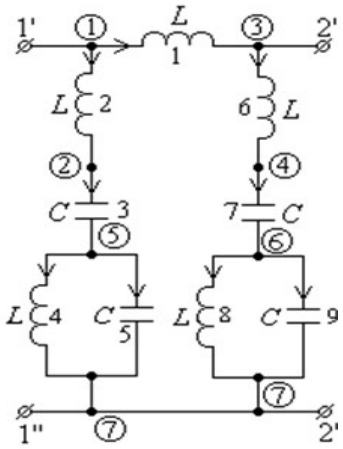


Fig. 8.7. Type (m) band-pass filter.

Since the relation: *A*D - B*C* = 1 is verified, the filter is reciprocal. It is also symmetrical because (A = D).

$$T := \begin{bmatrix} \dfrac{2.\,s^4\,C^2\,L^2 + 4.\,s^2\,C\,L + 1.}{s^4\,C^2\,L^2 + 3.\,s^2\,C\,L + 1.} & s\,L \\ \dfrac{s\,(3.\,s^6\,C^3\,L^3 + 10.\,s^4\,C^2\,L^2 + 9.\,s^2\,C\,L + 2.)\,C}{1. + s^8\,C^4\,L^4 + 6.\,s^6\,C^3\,L^3 + 11.\,s^4\,C^2\,L^2 + 6.\,s^2\,C\,L} & \dfrac{2.\,s^4\,C^2\,L^2 + 4.\,s^2\,C\,L + 1.}{s^4\,C^2\,L^2 + 3.\,s^2\,C\,L + 1.} \end{bmatrix}. \tag{8.29}$$

$$Z := \begin{bmatrix} \dfrac{(s^4\,C^2\,L^2 + 3.\,s^2\,C\,L + 1.)\,(2.\,s^4\,C^2\,L^2 + 4.\,s^2\,C\,L + 1.)}{C\,(3.\,s^6\,C^3\,L^3 + 10.\,s^4\,C^2\,L^2 + 9.\,s^2\,C\,L + 2.)\,s}, \\ -\dfrac{1.\,(1. + s^8\,C^4\,L^4 + 6.\,s^6\,C^3\,L^3 + 11.\,s^4\,C^2\,L^2 + 6.\,s^2\,C\,L)}{s\,(3.\,s^6\,C^3\,L^3 + 10.\,s^4\,C^2\,L^2 + 9.\,s^2\,C\,L + 2.)\,C} \end{bmatrix} \\ \begin{bmatrix} \dfrac{1. + s^8\,C^4\,L^4 + 6.\,s^6\,C^3\,L^3 + 11.\,s^4\,C^2\,L^2 + 6.\,s^2\,C\,L}{s\,(3.\,s^6\,C^3\,L^3 + 10.\,s^4\,C^2\,L^2 + 9.\,s^2\,C\,L + 2.)\,C}, \\ -\dfrac{1.\,(s^4\,C^2\,L^2 + 3.\,s^2\,C\,L + 1.)\,(2.\,s^4\,C^2\,L^2 + 4.\,s^2\,C\,L + 1.)}{C\,(3.\,s^6\,C^3\,L^3 + 10.\,s^4\,C^2\,L^2 + 9.\,s^2\,C\,L + 2.)\,s} \end{bmatrix}. \tag{8.30}$$

$$Y_T := \begin{bmatrix} \dfrac{2.\,s^4\,C^2\,L^2 + 4.\,s^2\,C\,L + 1.}{(s^4\,C^2\,L^2 + 3.\,s^2\,C\,L + 1.)\,s\,L} & -\dfrac{1.}{s\,L} \\ \dfrac{1}{s\,L} & -\dfrac{1.\,(2.\,s^4\,C^2\,L^2 + 4.\,s^2\,C\,L + 1.)}{(s^4\,C^2\,L^2 + 3.\,s^2\,C\,L + 1.)\,s\,L} \end{bmatrix}. \tag{8.31}$$

$$H := \begin{bmatrix} \dfrac{(-1.\,M^2\,C1 + C1\,L1\,L2)\,s^3 + (C1\,L1\,RL2 + C1\,RL1\,L2)\,s^2 + (L2 + C1\,RL1\,RL2)\,s + RL2}{s\,C1\,(RL2 + s\,L2)}, & \dfrac{1.\,s\,M}{RL2 + s\,L2} \\ \dfrac{s\,M}{RL2 + s\,L2}, & -\dfrac{s\,C2\,RL2 + 1. + s^2\,C2\,L2}{RL2 + s\,L2} \end{bmatrix} \tag{8.32}$$

$$F := \begin{bmatrix} \dfrac{C\,(3.\,s^6\,C^3\,L^3 + 10.\,s^4\,C^2\,L^2 + 9.\,s^2\,C\,L + 2.)\,s}{(2.\,s^4\,C^2\,L^2 + 4.\,s^2\,C\,L + 1.)\,(s^4\,C^2\,L^2 + 3.\,s^2\,C\,L + 1.)} & \dfrac{s^4\,C^2\,L^2 + 3.\,s^2\,C\,L + 1.}{2.\,s^4\,C^2\,L^2 + 4.\,s^2\,C\,L + 1.} \\ \dfrac{s^4\,C^2\,L^2 + 3.\,s^2\,C\,L + 1.}{2.\,s^4\,C^2\,L^2 + 4.\,s^2\,C\,L + 1.} & -\dfrac{1.\,s\,L\,(s^4\,C^2\,L^2 + 3.\,s^2\,C\,L + 1.)}{2.\,s^4\,C^2\,L^2 + 4.\,s^2\,C\,L + 1.} \end{bmatrix} \tag{8.33}$$

$$S_T := \tag{8.34}$$

$$[-1.(-1.sL+CZ0^2)(1.+s^8C^4L^4+6.s^6C^3L^3+11.s^4C^2L^2+6.s^2CL)\,/\,(s^9L^5C^4+4.Z0\,s^8C^4L^4$$
$$+3.s^7C^4Z0^2L^3+6.s^7L^4C^3+20.Z0\,s^6C^3L^3+10.s^5C^3Z0^2L^2+11.s^5L^3C^2+30.Z0\,s^4C^2L^2$$
$$+9.s^3C^2Z0^2L+6.s^3L^2C+14.Z0\,s^2CL+2.sCZ0^2+sL+2.Z0),-2.$$
$$(1.+s^8C^4L^4+6.s^6C^3L^3+11.s^4C^2L^2+6.s^2CL)Z0\,/\,(s^9L^5C^4+4.Z0\,s^8C^4L^4+3.s^7C^4Z0^2L^3$$
$$+6.s^7L^4C^3+20.Z0\,s^6C^3L^3+10.s^5C^3Z0^2L^2+11.s^5L^3C^2+30.Z0\,s^4C^2L^2+9.s^3C^2Z0^2L$$
$$+6.s^3L^2C+14.Z0\,s^2CL+2.sCZ0^2+sL+2.Z0)]$$
$$[2.(1.+s^8C^4L^4+6.s^6C^3L^3+11.s^4C^2L^2+6.s^2CL)Z0\,/\,(s^9L^5C^4+4.Z0\,s^8C^4L^4+3.s^7C^4Z0^2L^3$$
$$+6.s^7L^4C^3+20.Z0\,s^6C^3L^3+10.s^5C^3Z0^2L^2+11.s^5L^3C^2+30.Z0\,s^4C^2L^2+9.s^3C^2Z0^2L$$
$$+6.s^3L^2C+14.Z0\,s^2CL+2.sCZ0^2+sL+2.Z0),-1.(-1.sL+CZ0^2)$$

$$(1.+s^8C^4L^4+6.s^6C^3L^3+11.s^4C^2L^2+6.s^2CL)\,/\,(s^9L^5C^4+4.Z0\,s^8C^4L^4+3.s^7C^4Z0^2L^3$$
$$+6.s^7L^4C^3+20.Z0\,s^6C^3L^3+10.s^5C^3Z0^2L^2+11.s^5L^3C^2+30.Z0\,s^4C^2L^2+9.s^3C^2Z0^2L$$
$$+6.s^3L^2C+14.Z0\,s^2CL+2.sCZ0^2+sL+2.Z0)]$$

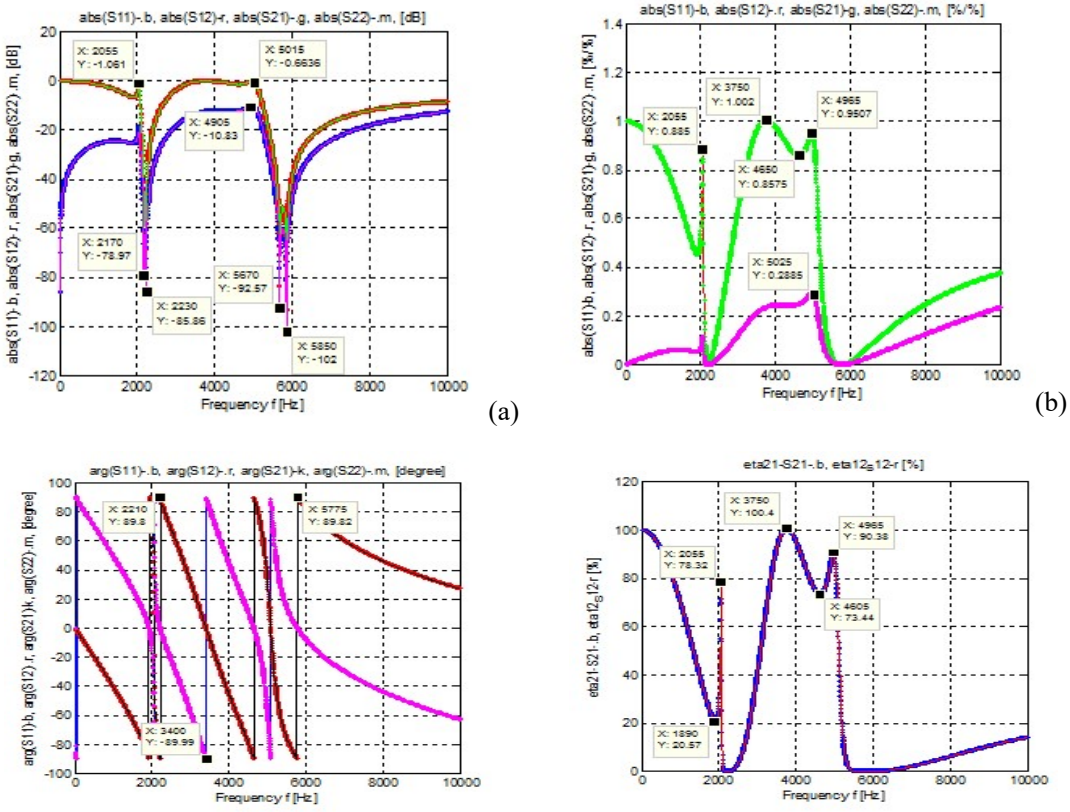


Fig. 8.8. Frequency variations of the moduli of the S parameters and of the signal transmission efficiencies for the filter in Fig. 8.7: a) moduli expressed in dB; b) moduli expressed in %/%; c) arguments of the S parameters; d) signal transmission efficiencies from input to output η_{21_S21} and from output to input η_{12_S12}.

Figure 8.8 shows the results obtained after generating the parameters. It includes the moduli of the (S) parameters, their arguments and the direct and reverse transmission efficiencies. From this figure, it can

be observed that the transmission efficiencies in the two directions have identical variations as a function of frequency, which confirms the symmetrical behaviour of the circuit.

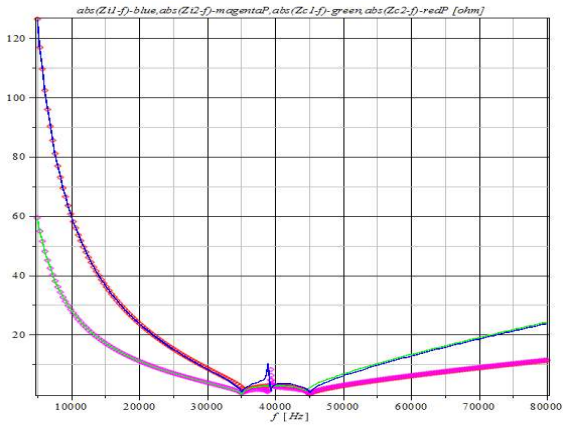
For the filter in Fig. 8.7, the characteristic impedances and image impedances are calculated using relations (8.35)–(8.38). Their variations as a function of frequency are presented in Fig. 8.9. The analysis of the figure shows that (Z_c1 = Z_c2) și (Z_i1 = Z_i2), confirming the symmetrical character of the quadripole.

$$Zc1_f := -60400.\ I\sqrt{-\frac{0.1371\ 10^{-6} f^2\ (-0.7733\ 10^{-20} f^6 + 0.1880\ 10^{-12} f^4 - 0.1234\ 10^{-5} f^2 + 2.)}{1. + 0.3534\ 10^{-27} f^8 - 0.1546\ 10^{-19} f^6 + 0.2068\ 10^{-12} f^4 - 0.8228\ 10^{-6} f^2}}$$
$$(1. + 0.3534\ 10^{-27} f^8 - 0.1546\ 10^{-19} f^6 + 0.2068\ 10^{-12} f^4 - 0.8228\ 10^{-6} f^2) \,/\, (f$$
$$(-0.7733\ 10^{-20} f^6 + 0.1880\ 10^{-12} f^4 - 0.1234\ 10^{-5} f^2 + 2.))) \tag{8.35}$$

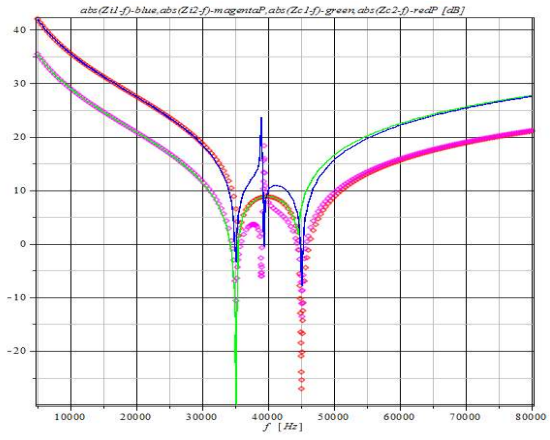
$$Zc2_f := -60400.\ I\sqrt{-\frac{0.1371\ 10^{-6} f^2\ (-0.7733\ 10^{-20} f^6 + 0.1880\ 10^{-12} f^4 - 0.1234\ 10^{-5} f^2 + 2.)}{1. + 0.3534\ 10^{-27} f^8 - 0.1546\ 10^{-19} f^6 + 0.2068\ 10^{-12} f^4 - 0.8228\ 10^{-6} f^2}}$$
$$(1. + 0.3534\ 10^{-27} f^8 - 0.1546\ 10^{-19} f^6 + 0.2068\ 10^{-12} f^4 - 0.8228\ 10^{-6} f^2) \,/\, (f$$
$$(-0.7733\ 10^{-20} f^6 + 0.1880\ 10^{-12} f^4 - 0.1234\ 10^{-5} f^2 + 2.))) \tag{8.36}$$

$$Zi1_f := 22.36\sqrt{\frac{1. + 0.3534\ 10^{-27} f^8 - 0.1546\ 10^{-19} f^6 + 0.2068\ 10^{-12} f^4 - 0.8228\ 10^{-6} f^2}{-0.7733\ 10^{-20} f^6 + 0.1880\ 10^{-12} f^4 - 0.1234\ 10^{-5} f^2 + 2.}} \tag{8.37}$$

$$Zi2_f := 22.36\sqrt{\frac{1. + 0.3534\ 10^{-27} f^8 - 0.1546\ 10^{-19} f^6 + 0.2068\ 10^{-12} f^4 - 0.8228\ 10^{-6} f^2}{-0.7733\ 10^{-20} f^6 + 0.1880\ 10^{-12} f^4 - 0.1234\ 10^{-5} f^2 + 2.}} \tag{8.38}$$



(a)



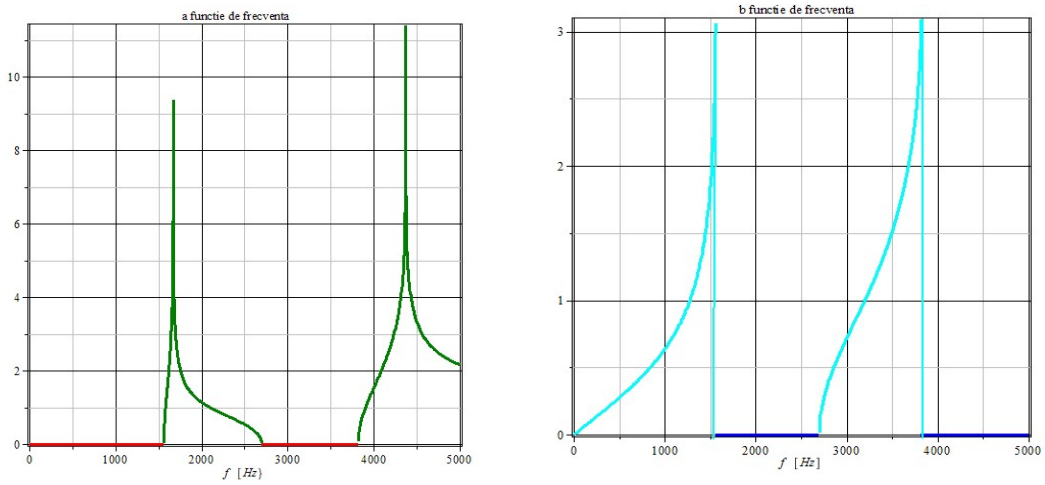
(b)

Fig. 8.9. Frequency variations of the moduli of the characteristic and image impedances: a) abs($\underline{Z}_{i1\text{-}f}$)-blue, abs($\underline{Z}_{i2\text{-}f}$)-magentaP, abs($\underline{Z}_{c1\text{-}f}$)-green și abs($\underline{Z}_{c2\text{-}f}$)-redP; b) 20.0*log10(abs($\underline{Z}_{i1\text{-}f}$))-blue, 20.0*log10(abs($\underline{Z}_{i2\text{-}f}$))-magentaP, 20.0*log10(abs($\underline{Z}_{c1\text{-}f}$))-green și 20.0*log10(abs($\underline{Z}_{c2\text{-}f}$)).

The pass bands and stop bands are determined based on the propagation condition and the expression of parameter (A). The attenuation constant and the phase constant are calculated using relations (8.23) and (8.24) and are represented graphically in Fig. 8.10. This figure confirms that the analysed filter is an (m)-type band-pass filter.

$$a = 0, \quad b = arcctg\frac{1}{\sqrt{\frac{1}{AD}-1}} + k\pi = arccos\sqrt{AD} + k\pi, \tag{8.23}$$

$$a = arg\,c\,tg\frac{1}{\sqrt{1-\frac{1}{AD}}} = \text{argch}\sqrt{AD}, \quad b = \begin{cases} \pm\frac{\pi}{2} & AD \le 0 \\ 0 \text{ sau } 1 & AD \ge 1 \end{cases}. \tag{8.24}$$



(a) (b)

Fig. 8.10. Frequency variations of: a) the attenuation constant; b) the phase constant.

The second example is the (m)-type band-pass filter shown in Fig. 8.11. For this filter, the fundamental parameters are again determined, after which the other sets of parameters are calculated. Relation **(8.39)** presents the matrix (T), while relations **(8.40)**–**(8.44)** present the matrices (Z), (Y), (H), (F), and (S).

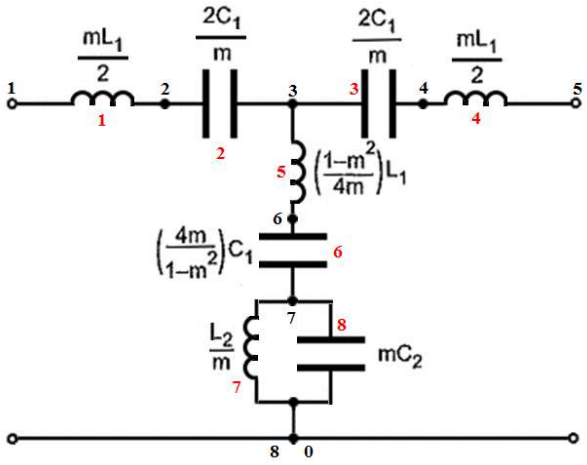


Fig. 8.11. Type (m) band-pass filter.

Since the relation: *A*D - B*C* = 1 is verified, the filter in Fig. 8.11 is reciprocal and symmetrical, because (A = D).

$$T_f := \left[\left[-\frac{1.\left(7.775\ 10^{-17} f^4 - 5.620\ 10^{-8} f^2 + 1.25\right)}{-4.665\ 10^{-17} f^4 + 4.634\ 10^{-8} f^2 - 0.75}, \left(79600.\ \mathrm{I}\left(-3.944\ 10^{-9} f^2 + 1.\right)\left(1. + 6.220\ 10^{-17} f^4 - 5.127\ 10^{-8} f^2\right)\right) \Big/ \left(\left(-4.665\ 10^{-17} f^4 + 4.634\ 10^{-8} f^2 - 0.75\right) f\right)\right], \left[-\frac{0.00001256\ \mathrm{I}\, f\left(-1.578\ 10^{-8} f^2 + 1.\right)}{-4.665\ 10^{-17} f^4 + 4.634\ 10^{-8} f^2 - 0.75}, -\frac{1.\left(7.775\ 10^{-17} f^4 - 5.620\ 10^{-8} f^2 + 1.25\right)}{-4.665\ 10^{-17} f^4 + 4.634\ 10^{-8} f^2 - 0.75}\right]\right] \tag{8.39}$$

$$Z_T_f := \left[\left[-\frac{79600.\ \mathrm{I}\left(7.775\ 10^{-17} f^4 - 5.621\ 10^{-8} f^2 + 1.25\right)}{f\left(-1.578\ 10^{-8} f^2 + 1.\right)}, -\frac{79600.\ \mathrm{I}\left(-4.665\ 10^{-17} f^4 + 4.635\ 10^{-8} f^2 - 0.75\right)}{f\left(-1.578\ 10^{-8} f^2 + 1.\right)}\right], \left[\frac{79600.\ \mathrm{I}\left(-4.665\ 10^{-17} f^4 + 4.635\ 10^{-8} f^2 - 0.75\right)}{f\left(-1.578\ 10^{-8} f^2 + 1.\right)}, -\frac{79600.\ \mathrm{I}\left(7.775\ 10^{-17} f^4 - 5.621\ 10^{-8} f^2 + 1.25\right)}{f\left(-1.578\ 10^{-8} f^2 + 1.\right)}\right]\right] \tag{8.40}$$

$$Y_T_f := \left[\left[\frac{0.00001256\ \mathrm{I}\left(7.775\ 10^{-17} f^4 - 5.621\ 10^{-8} f^2 + 1.25\right) f}{\left(-3.944\ 10^{-9} f^2 + 1.\right)\left(1. + 6.220\ 10^{-17} f^4 - 5.128\ 10^{-8} f^2\right)}, \frac{0.00001256\ \mathrm{I}\, f\left(-4.665\ 10^{-17} f^4 + 4.635\ 10^{-8} f^2 - 0.75\right)}{\left(-3.944\ 10^{-9} f^2 + 1.\right)\left(1. + 6.220\ 10^{-17} f^4 - 5.128\ 10^{-8} f^2\right)}\right], \left[-\frac{0.00001256\ \mathrm{I}\, f\left(-4.665\ 10^{-17} f^4 + 4.635\ 10^{-8} f^2 - 0.75\right)}{\left(-3.944\ 10^{-9} f^2 + 1.\right)\left(1. + 6.220\ 10^{-17} f^4 - 5.128\ 10^{-8} f^2\right)}, -\frac{0.00001256\ \mathrm{I}\left(7.775\ 10^{-17} f^4 - 5.621\ 10^{-8} f^2 + 1.25\right) f}{\left(-3.944\ 10^{-9} f^2 + 1.\right)\left(1. + 6.220\ 10^{-17} f^4 - 5.128\ 10^{-8} f^2\right)}\right]\right] \tag{8.41}$$

$$H_T_f := \left[\left[-\frac{79600.\,\mathrm{I}\left(-3.944\,10^{-9} f^2 + 1.\right)\left(1. + 6.220\,10^{-17} f^4 - 5.128\,10^{-8} f^2\right)}{f\left(7.775\,10^{-17} f^4 - 5.621\,10^{-8} f^2 + 1.25\right)}, -\frac{1.\left(-4.665\,10^{-17} f^4 + 4.635\,10^{-8} f^2 - 0.75\right)}{7.775\,10^{-17} f^4 - 5.621\,10^{-8} f^2 + 1.25} \right], \left[-\frac{1.\left(-4.665\,10^{-17} f^4 + 4.635\,10^{-8} f^2 - 0.75\right)}{7.775\,10^{-17} f^4 - 5.621\,10^{-8} f^2 + 1.25}, \frac{0.000004186\,\mathrm{I} f\left(-1.578\,10^{-8} f^2 + 1.\right)\left(1. - 157.8 f^2\,C\,L\right)}{\left(-4.665\,10^{-17} f^4 + 4.635\,10^{-8} f^2 - 0.75\right)\left(3. - 78.88 f^2\,C\,L\right)} \right]\right] \tag{8.42}$$

$$F_T_f := \left[\left[\frac{0.00001256\,\mathrm{I} f\left(-1.578\,10^{-8} f^2 + 1.\right)}{7.775\,10^{-17} f^4 - 5.621\,10^{-8} f^2 + 1.25}, -\frac{1.\left(-4.665\,10^{-17} f^4 + 4.635\,10^{-8} f^2 - 0.75\right)}{7.775\,10^{-17} f^4 - 5.621\,10^{-8} f^2 + 1.25} \right], \left[-\frac{1.0\left(-4.665\,10^{-17} f^4 + 4.635\,10^{-8} f^2 - 0.75\right)}{7.775\,10^{-17} f^4 - 5.621\,10^{-8} f^2 + 1.25}, \frac{79600.\,\mathrm{I}\left(-3.944\,10^{-9} f^2 + 1.\right)\left(1. + 6.220\,10^{-17} f^4 - 5.128\,10^{-8} f^2\right)}{f\left(7.775\,10^{-17} f^4 - 5.621\,10^{-8} f^2 + 1.25\right)} \right]\right] \tag{8.43}$$

$$S_f := \left[\left[\left(0.5000\left(-2.454\,10^{-25} f^6 - 5.956\,10^{-15} f^4 + 3.392\,10^{-7} f^2 + 1.\right)\right) \Big/ \left(-1.227\,10^{-25} f^6 - 3.530\,10^{-11}\,\mathrm{I} f^3 + 4.885\,10^{-20}\,\mathrm{I} f^5 + 3.242\,10^{-15} f^4 + 0.0007850\,\mathrm{I} f - 2.249\,10^{-7} f^2 + 0.5\right), \left(0.0006280\,\mathrm{I}\left(-4.665\,10^{-17} f^4 + 4.635\,10^{-8} f^2 - 0.75\right) f\right) \Big/ \left(-1.227\,10^{-25} f^6 - 3.530\,10^{-11}\,\mathrm{I} f^3 + 4.885\,10^{-20}\,\mathrm{I} f^5 + 3.242\,10^{-15} f^4 + 0.0007850\,\mathrm{I} f - 2.249\,10^{-7} f^2 + 0.5\right) \right], \left[\left(0.0006280\,\mathrm{I}\left(4.665\,10^{-17} f^4 - 4.635\,10^{-8} f^2 + 0.75\right) f\right) \Big/ \left(-1.227\,10^{-25} f^6 - 3.530\,10^{-11}\,\mathrm{I} f^3 + 4.885\,10^{-20}\,\mathrm{I} f^5 + 3.242\,10^{-15} f^4 + 0.0007850\,\mathrm{I} f - 2.249\,10^{-7} f^2 + 0.5\right), \left(0.5000\left(-2.454\,10^{-25} f^6 - 5.956\,10^{-15} f^4 + 3.392\,10^{-7} f^2 + 1.\right)\right) \Big/ \left(-1.227\,10^{-25} f^6 - 3.530\,10^{-11}\,\mathrm{I} f^3 + 4.885\,10^{-20}\,\mathrm{I} f^5 + 3.242\,10^{-15} f^4 + 0.0007850\,\mathrm{I} f - 2.249\,10^{-7} f^2 + 0.5\right) \right]\right] \tag{8.44}$$

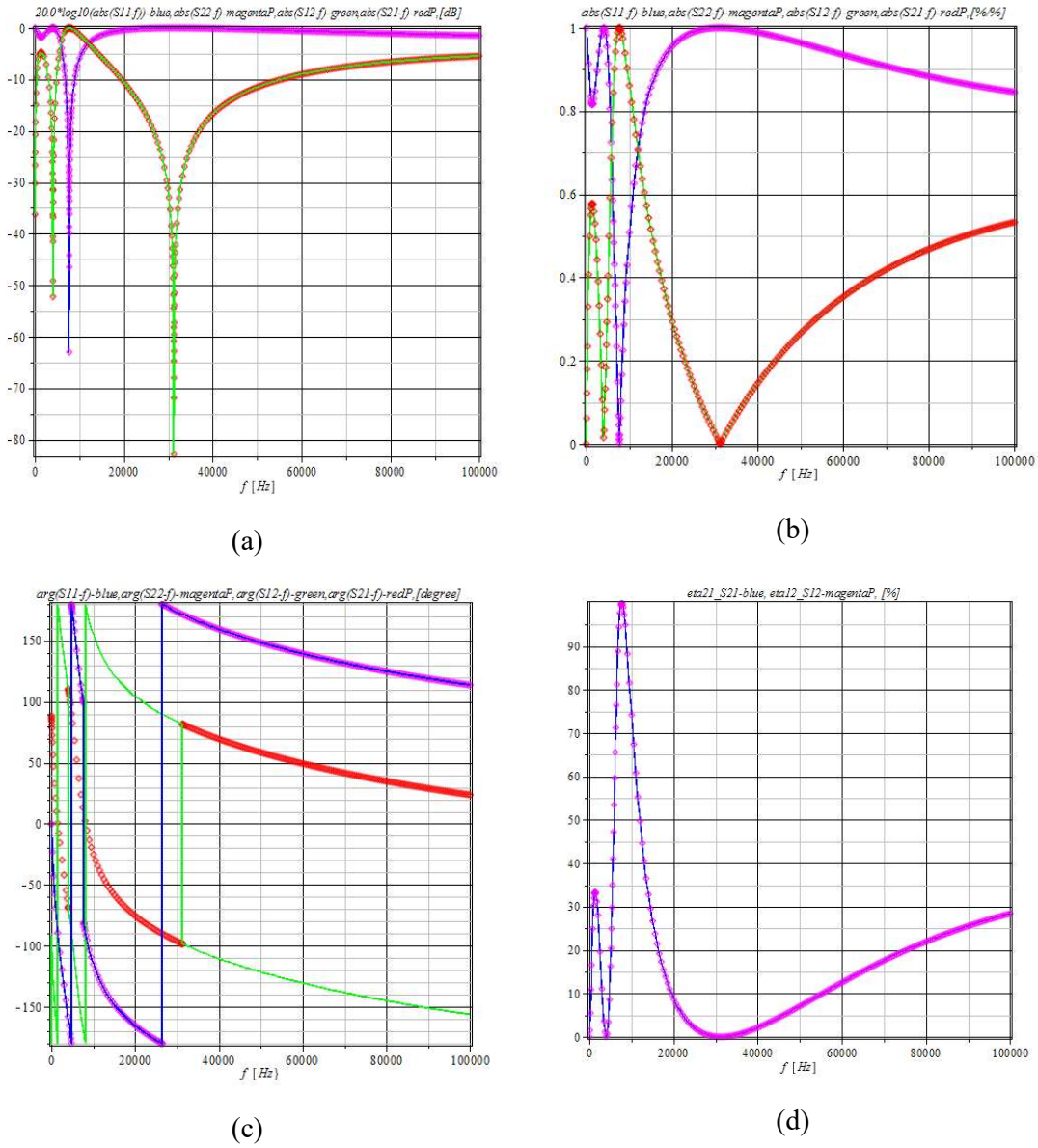
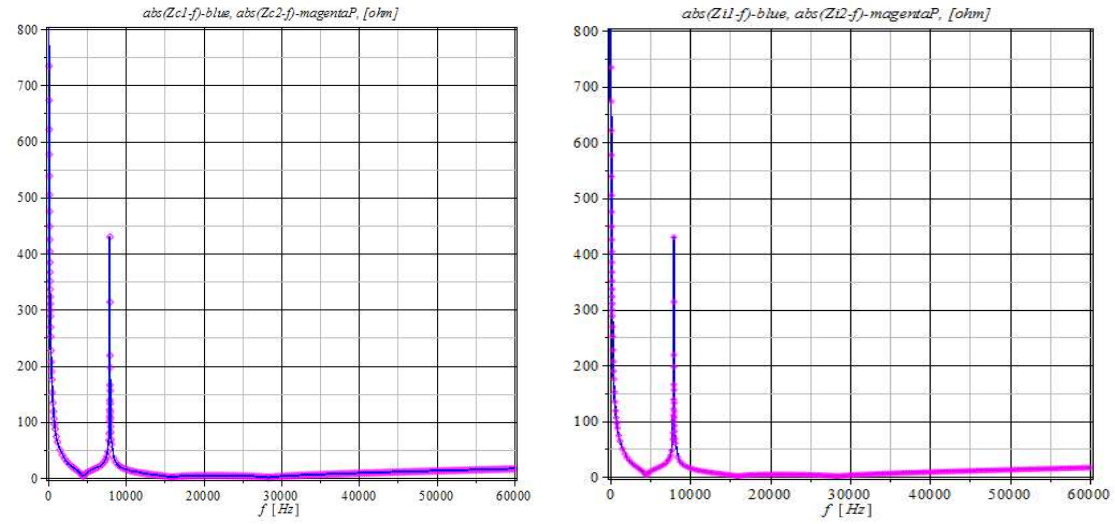


Fig. 8.12. Frequency variations of the moduli of the S parameters and of the signal transmission efficiencies for the filter in Fig. 8.11: a) moduli expressed in dB; b) moduli expressed in %/%; c) arguments of the S parameters; d) signal transmission efficiencies from input to output η_{21_S21} and from output to input η_{12_S12}.

Figure 8.12 is one of the most important figures in the applied part. It shows how the (S) parameters and the transmission efficiencies vary as a function of frequency, allowing the behaviour of the filter to be interpreted.

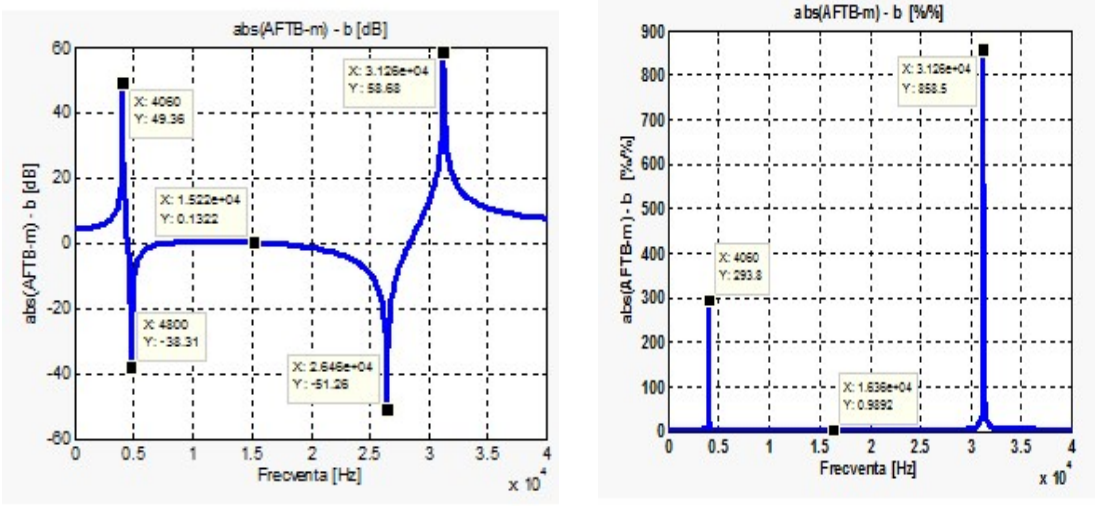
For the filter in Fig. 8.11, the characteristic impedances and image impedances are calculated by relations (8.45)–(8.48), and their variations are presented in Fig. 8.13. Subsequently, the voltage transfer factor is determined by relations (8.49) and (8.50), while the poles and zeros of the transfer function are presented by relations (8.51) and (8.52). These results allow the stability and dynamic behaviour of the filter to be analysed.



(a) (b)

Fig. 8.13. Frequency variations of the moduli of the characteristic and image impedances.: a) abs($\underline{Z}_{i1\text{-}f}$)-blue, abs($\underline{Z}_{i2\text{-}f}$)-magentaP, abs($\underline{Z}_{c1\text{-}f}$)-green și abs($\underline{Z}_{c2\text{-}f}$)-redP; b) 20.0*log10(abs($\underline{Z}_{i1\text{-}f}$))-blue, 20.0*log10(abs($\underline{Z}_{i2\text{-}f}$))-magentaP, 20.0*log10(abs($\underline{Z}_{c1\text{-}f}$))-green și 20.0*log10(abs($\underline{Z}_{c2\text{-}f}$)).

Figure 8.14 presents the frequency characteristics of the (m)-type band-pass filter in Fig. 8.11, namely the frequency variation of the modulus of the voltage transfer factor (A_{FTB_m}) expressed in dB in Fig. 8.14a and in V/V in Fig. 8.14b.



$$Q_{AFTB_m1} = \frac{f_2 - f_1}{f_0} = \frac{3.126e04 - 4080.0}{1.522e04} = 1.786$$

$$Q_{AFTB_m2} = \frac{f_{min\,2} - f_{min\,1}}{f_0} = \frac{2{,}646e04 - 4300.0}{1.522e04} = 1.456$$

(a) (b)

Fig. 8.14. Frequency characteristics of the (m)-type band-pass filter in Fig. 8.11: a) voltage transfer factor expressed in dB; b) voltage transfer factor expressed in V/V.

Figure 8.14 is very suitable for the summary because it shows the frequency response of the filter, both in dB and in V/V. It creates a direct connection between the mathematical calculations and the visible behaviour of the filter.

The pass bands and stop bands of the filter are determined using relations (8.53) and (8.54). The results show the frequency ranges in which the filter allows signal propagation and the ranges in which the signal is attenuated. The variations of the attenuation constant and phase constant are presented in Fig. 8.15, while the Bode characteristics, Nyquist diagram and the pole-zero representations are presented in Fig. 8.16.

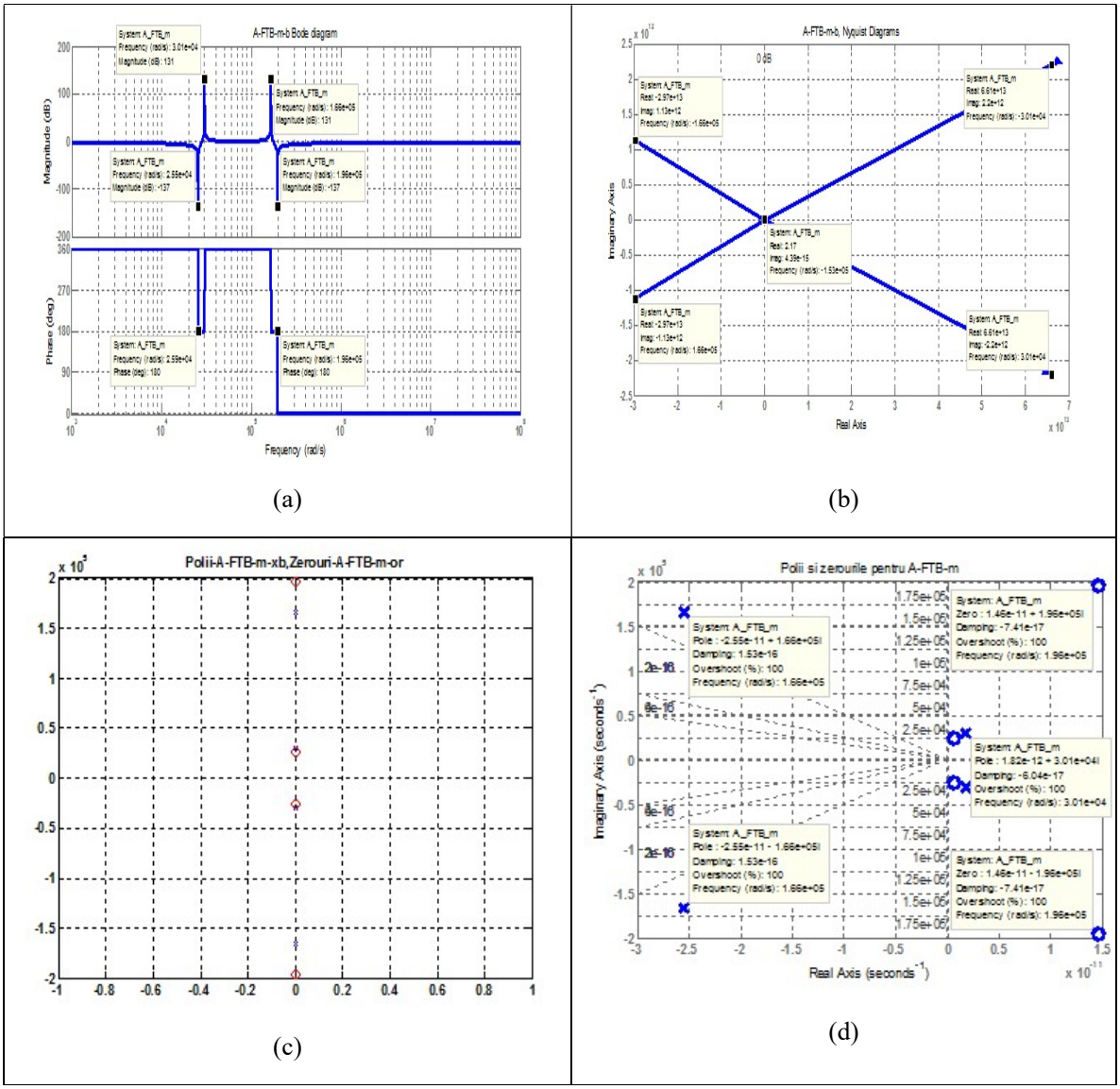


Fig. 8.16. Bode characteristics of the band-pass filter in Fig. 8.11: a) Bode diagram; b) Nyquist diagram; c) representation of poles and zeros in the complex plane; d) poles and zeros for A_{FTB_m}.

Figure 8.16 is very useful because it summarises the behaviour of the filter through several graphical representations: Bode response, Nyquist diagram and the position of poles and zeros.

Conclusions

In conclusion, Chapter 8 shows that quadripole parameters and transfer functions are important tools for the analysis, design and diagnosis of electrical circuits. The automatic generation of parameters (T), (Z), (Y), (H), (F), and (S), together with the conversion relations between them, allows the rapid evaluation of circuit behaviour under harmonic or operational conditions. Through the examples of (m)-type band-pass filters, the chapter demonstrates that symbolic and numerical methods can be used to identify pass bands and stop bands, losses, signal transmission, poles and zeros and circuit stability.

In relation to the topic of the thesis, this chapter contributes to the development of a modern approach to the analysis of low-voltage electrical installations. Through circuit modelling and the determination of characteristic parameters, improper operating regimes, additional losses, imbalances or frequency-dependent behaviours can be identified, which may favour overloads, local overheating and reduced installation reliability. Thus, Chapter 8 supports the idea that the safety of electrical installations must be evaluated not only through practical inspections, but also through computational, simulation and computer-aided design tools.

Chapter 9

Analysis of the Induction Motor in Periodic Sinusoidal Regime, Taking into Account the Magnetisation Characteristic and the Variation of Rotor Resistance with Slip

Chapter 9 analyses the induction motor as an important consumer in low-voltage electrical installations. Asynchronous motors are widely used in industrial applications, technical buildings, pumping systems, ventilation, air conditioning and electric drives, and their operating regimes may significantly influence the electrical network. Especially during starting, load variations or nonlinear operating regimes, these motors may produce high currents, additional heating, harmonics, a decrease in power factor and energy losses [95]–[112].

The integration of this study into the thesis is justified by the fact that the safety of electrical installations does not depend only on the condition of cables, electrical panels and protective devices, but also on the behaviour of the supplied consumers. An induction motor operating under improper conditions may additionally stress the supply circuits, produce imbalances and contribute to overloads or local overheating. From this perspective, motor modelling helps to understand how important consumers may influence the technical risk of a low-voltage electrical installation.

The chapter starts from the idea that the non-sinusoidal periodic regime, also called the distorted regime, has disturbing effects on electrical networks. In such regimes, the power factor decreases, reactive power compensation becomes difficult, additional losses occur and

resonance phenomena, overvoltages or overcurrents may appear. These effects are important for low-voltage installations, because they may contribute to equipment degradation and to the increase of thermal stresses.

The analysis of the induction motor is carried out using two main categories of methods: time-domain methods and frequency-domain methods. The first category includes the "shooting" method, used for determining the steady-state regime, while the second category includes the harmonic balance method. In this chapter, the analysis is performed through state equations, modified nodal equations and simulations using programs such as MATLAB, ACAP and SPICE [95]–[112].

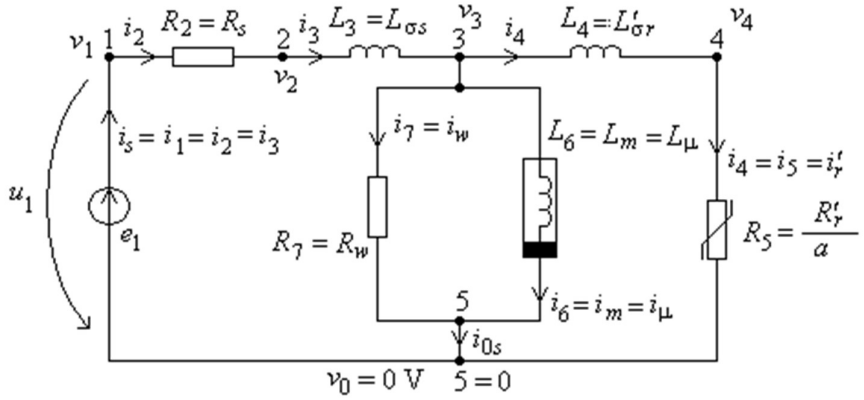


Fig. 9.1. Equivalent circuit of the induction motor in *Π*

Figure 9.1 represents the electrical model on which the analysis is based. The diagram shows the motor as an equivalent circuit consisting of resistances, inductances, the magnetisation branch and the rotor resistance referred to the stator. This figure is essential for understanding the modelling of the motor as an electrical circuit.

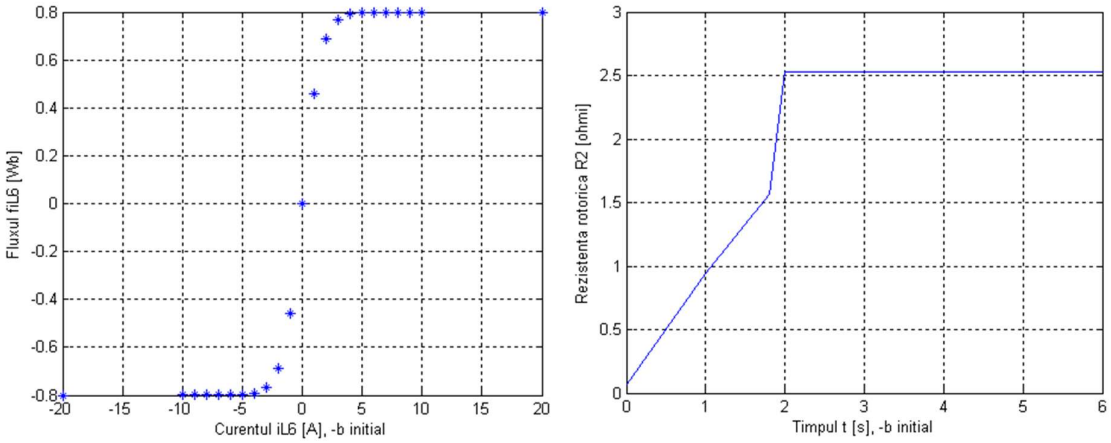
The analysed model takes into account two important aspects: the nonlinear magnetisation characteristic and the variation of the referred rotor resistance as a function of slip. The magnetisation coil is treated as a nonlinear current-controlled coil, and the rotor resistance is considered variable, depending on the operating regime. These elements make the model more realistic than a simplified linear model.

The state equations of the motor are presented in relation (9.1). This relation describes the evolution of currents and voltages in the equivalent circuit of the motor, taking into account the nonlinear character of the magnetisation branch. Within this relation, the differential inductance of the magnetisation coil appears, which depends on the current. This dependence is important because, when the magnetic core enters saturation, the inductance no longer remains constant.

$$\frac{d}{dt}\begin{bmatrix} i_3 \\ i_4 \\ i_6 \end{bmatrix} = \begin{bmatrix} -\frac{R_2+R_7}{L_3} & \frac{R_7}{L_2} & \frac{R_7}{L_2} \\ \frac{R_7}{L_4} & -\frac{R_7+R_{p5}}{L_4} & -\frac{R_7}{L_4} \\ \frac{R_7}{L_{di6}(i_6)} & -\frac{R_7}{L_{di6}(i_6)} & -\frac{R_7}{L_{di6}(i_6)} \end{bmatrix} \cdot \begin{bmatrix} i_3 \\ i_4 \\ i_6 \end{bmatrix} + \begin{bmatrix} \frac{1}{L_3} \\ 0 \\ 0 \end{bmatrix} \cdot [e_1], \tag{9.1}$$

For the numerical solution of the model, the chapter uses modified nodal equations and the implicit Euler algorithm. These are presented by relations **(9.2)** and **(9.3)**. The nonlinear magnetisation characteristic is approximated by straight-line segments, according to relation **(9.4)**. This approximation

allows magnetic saturation to be introduced into the numerical analysis and makes it possible to integrate the equations in MATLAB or to compare the results obtained using ACAP and SPICE.



(a) (b)

Fig. 9.2. a) Characteristic $\varphi_{Lm}(i_{Lm}) = \varphi_{L6}(i_{L6})$ş b) Characteristic $R_2(t)$.

In Fig. 9.2a, the flux-current magnetisation characteristic is presented, showing the nonlinearity of the magnetic core. In Fig. 9.2b, the variation of the rotor resistance over time or as a function of slip is presented. These two graphs visually explain why the motor cannot always be treated as a linear consumer.

For the SPICE simulation of the nonlinear current-controlled coil, the chapter presents a dedicated equivalent scheme. This scheme allows the nonlinear behaviour of the magnetisation coil to be represented by controlled sources and auxiliary elements, so that the saturation phenomenon can be analysed numerically.

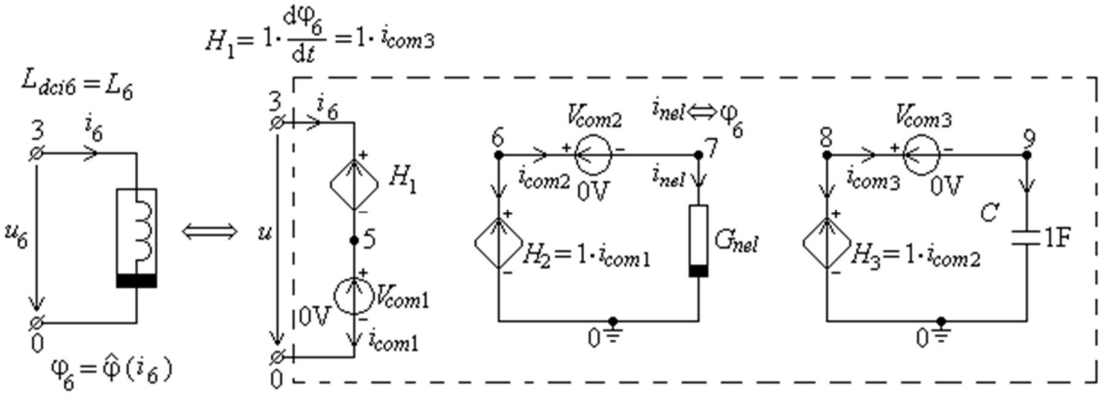
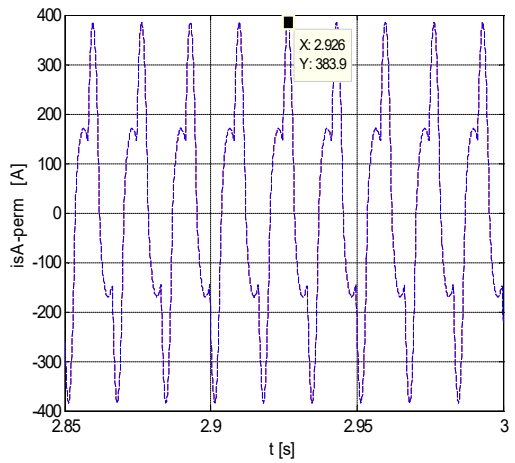


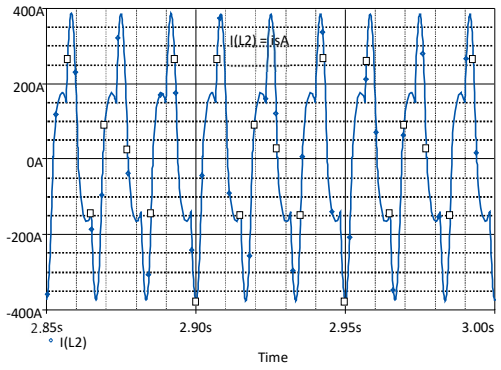
Fig. 9.3. SPICE simulation of current-controlled nonlinear coils.

The simulation results are presented in Table 9.1, which compares the results obtained using the ACAP and SPICE programs. Time waveforms and frequency spectra are analysed for stator currents, rotor currents, magnetisation current, voltages across inductances, copper losses, iron losses, mechanical power and electromagnetic torque.

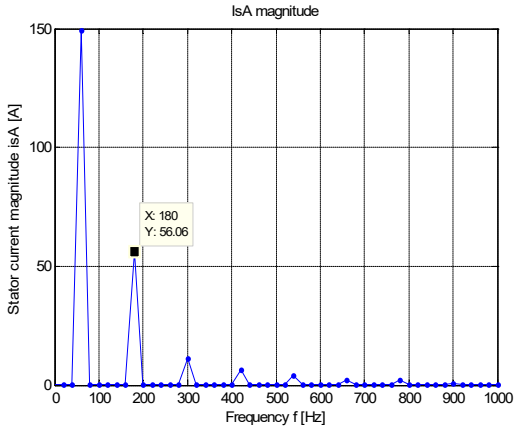
Table 9.1. Obtained results.



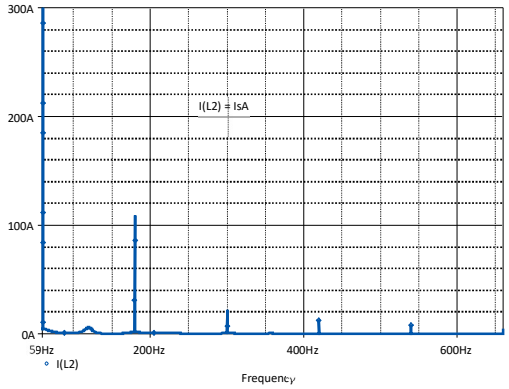
$i_{sA} - t$ – programul ACAP.



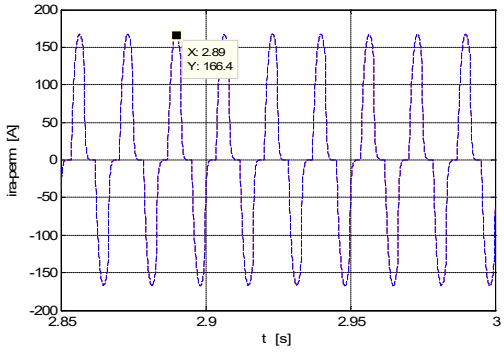
$i_{sA} - t$ – programul SPICE.



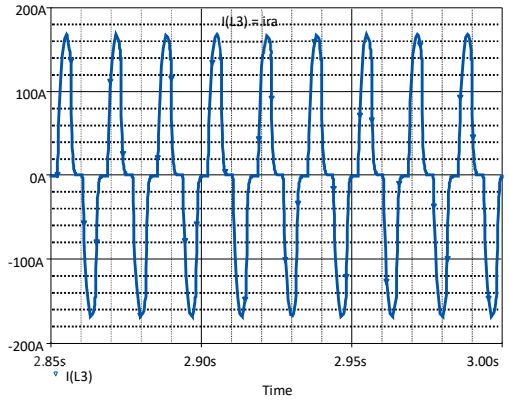
$I_{sA} - f$ –programul ACAP.



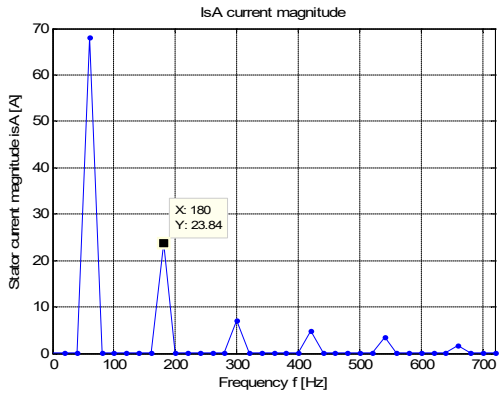
$I_{sA} - f$ –programul SPICE.



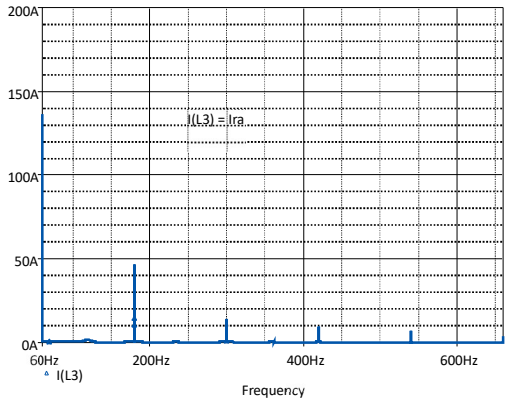
$i_{ra} - t$ – programul ACAP.



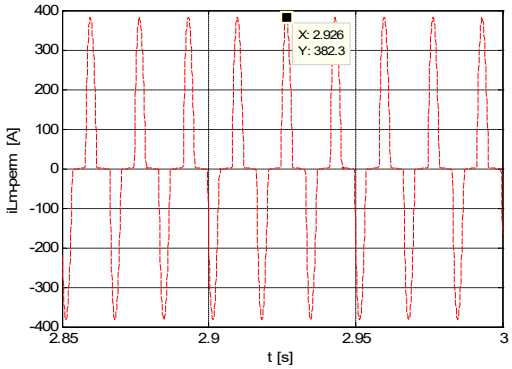
$i_{ra} - t$ – programul SPICE.



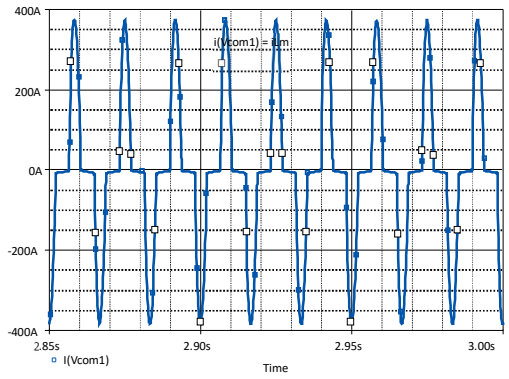
$I_{ra} - f$ – programul ACAP.



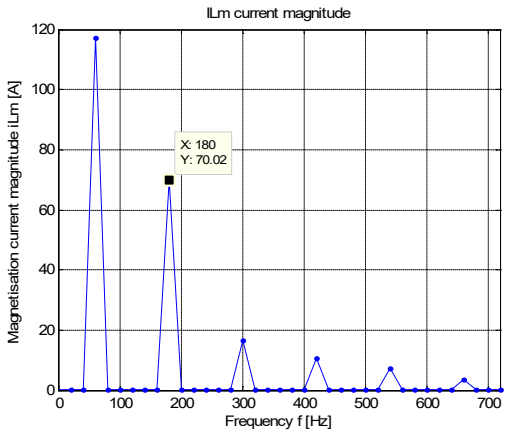
$I_{ra} - f$ – programul SPICE.



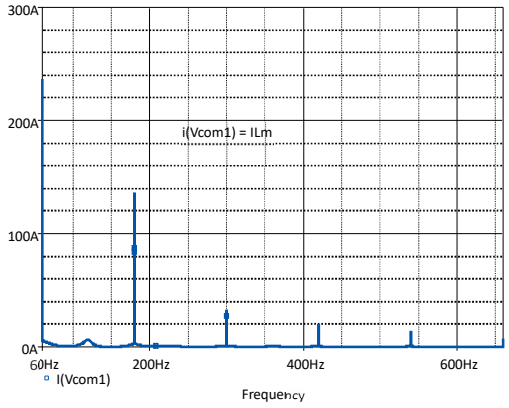
$i_{Lm} - t$ – programul ACAP.



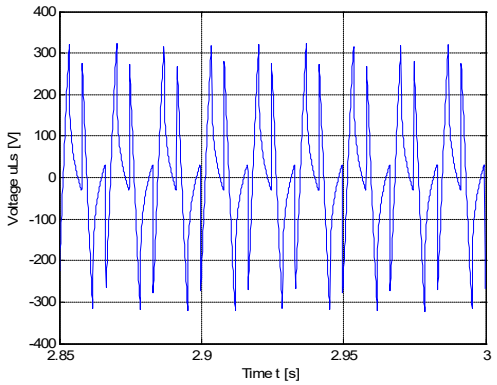
$i_{Lm} - t$ – programul SPICE.



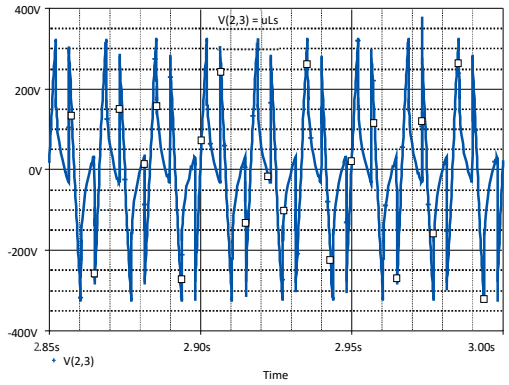
$I_{Lm} - f$ – programul ACAP.



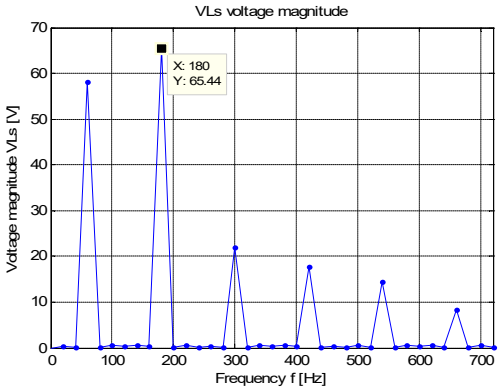
$I_{Lm} - f$ – programul SPICE.



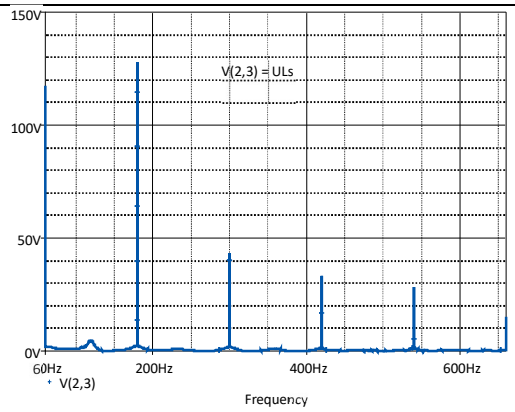
$u_{Ls} - t$ – programul ACAP.



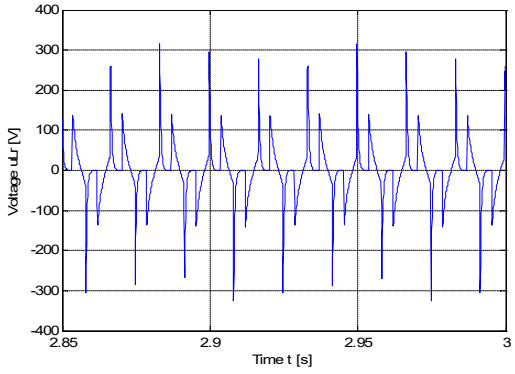
$u_{Ls} - t$ – programul SPICE.



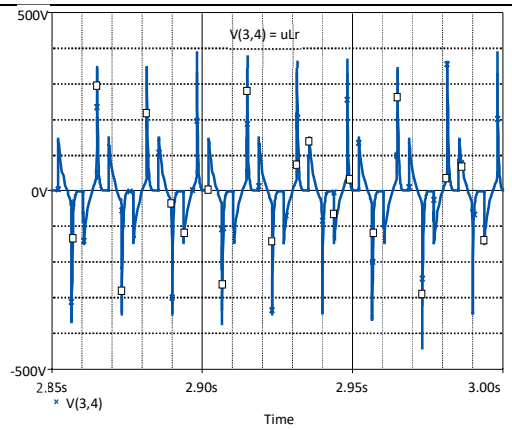
$U_{Ls} - f$ – programul ACAP.



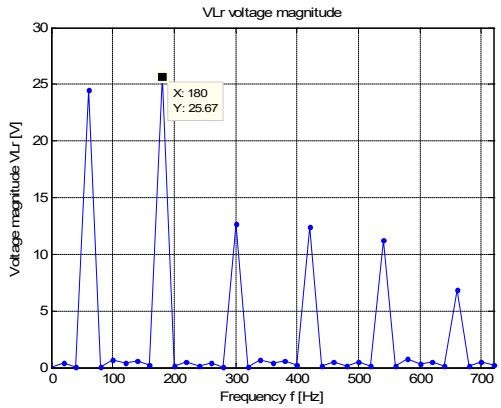
$U_{Ls} - f$ – programul SPICE.



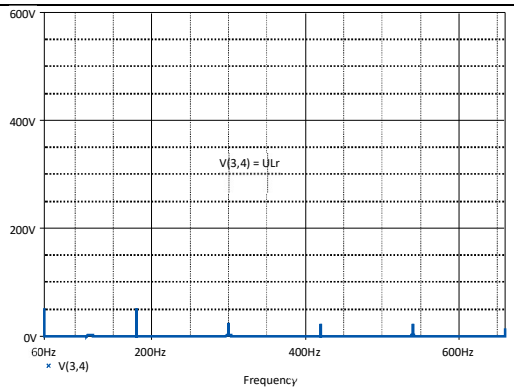
$u_{Lr} - t$ – programul ACAP.



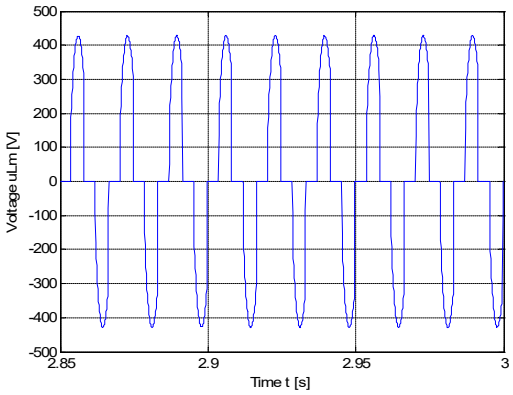
$u_{Lr} - t$ – programul SPICE.



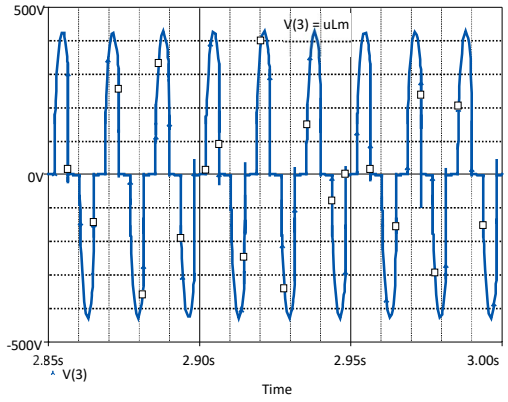
$U_{Lr} - f$ – programul ACAP.



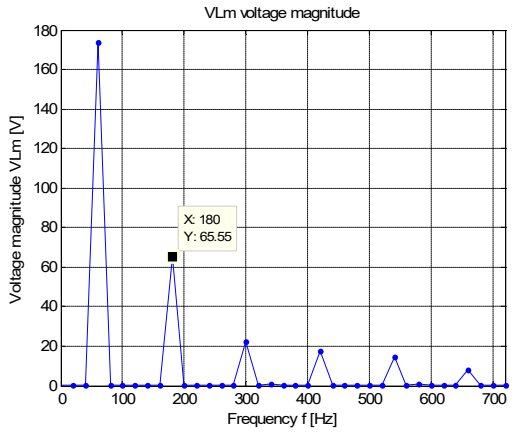
$U_{Lr} - f$ – programul SPICE.



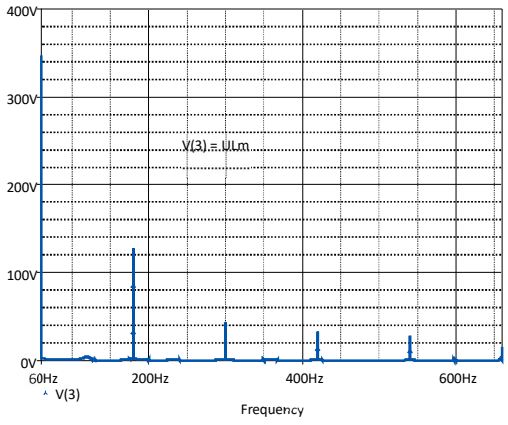
$u_{Lm} - t$ – programul ACAP.



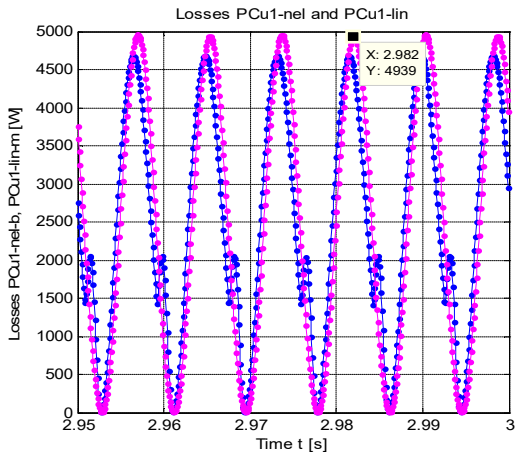
$u_{Lm} - t$ – programul SPICE.



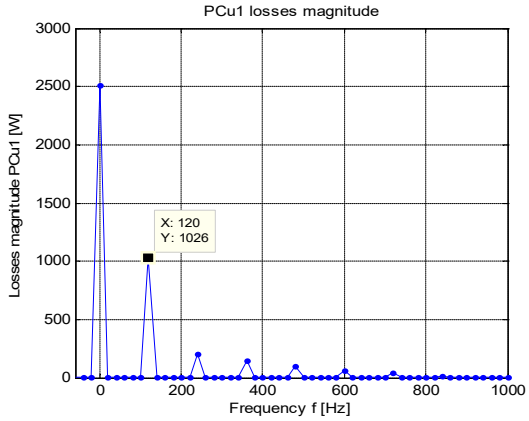
$U_{Lm} - f$ – programul ACAP.



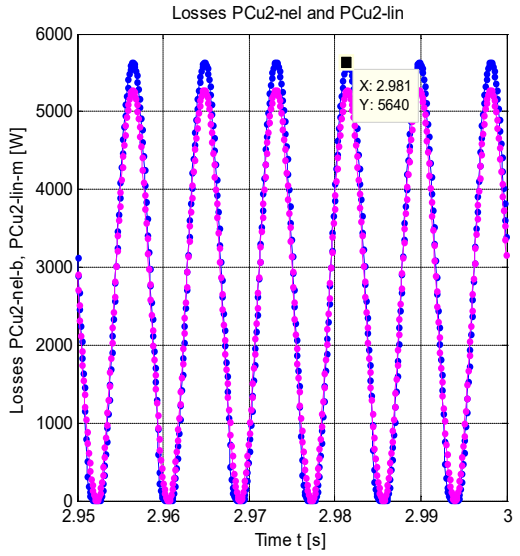
$U_{Lm} - f$ – programul ACAP.



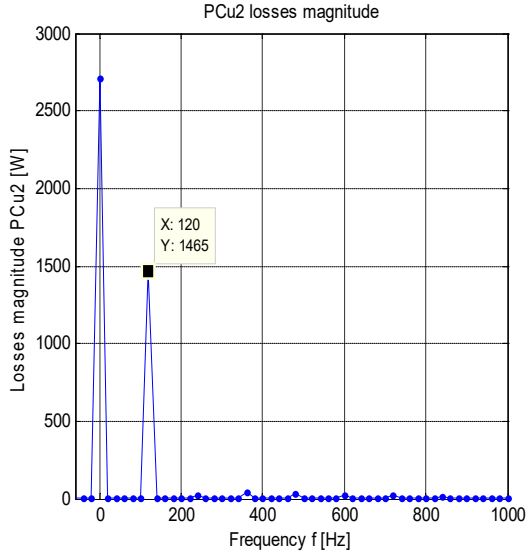
$P_{Cu1} - t$ – programul ACAP.



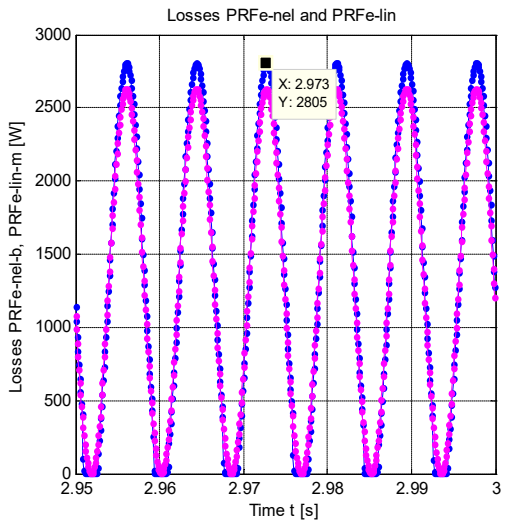
$P_{Cu1} - f$ – programul ACAP.



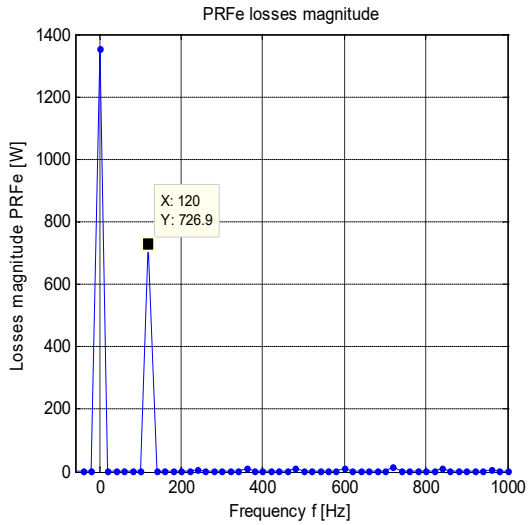
$P_{Cu2} - t$ – programul ACAP.



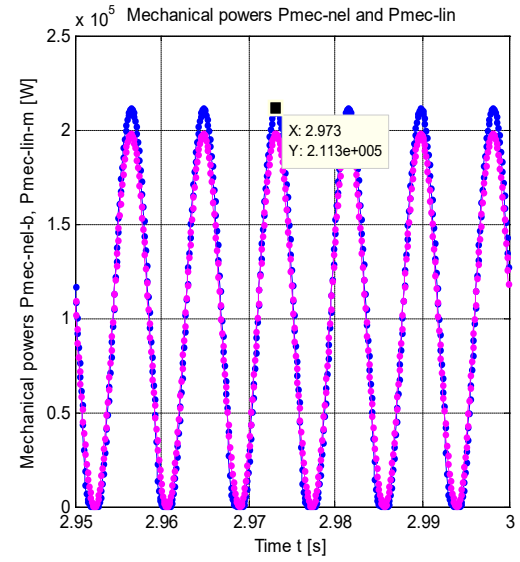
$P_{Cu2} - f$ – programul ACAP.



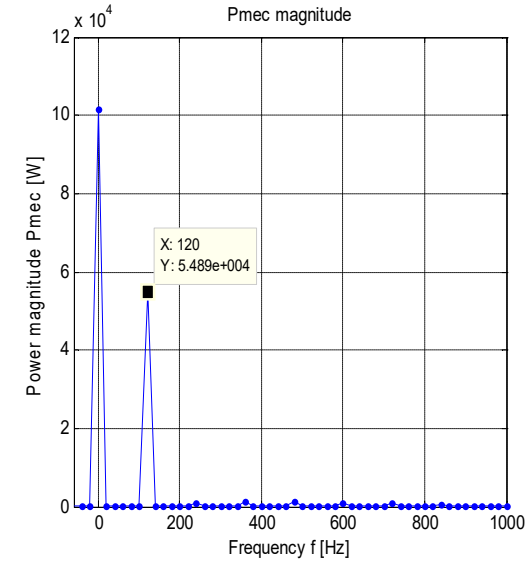
$P_{RFe} - t$ – programul ACAP.



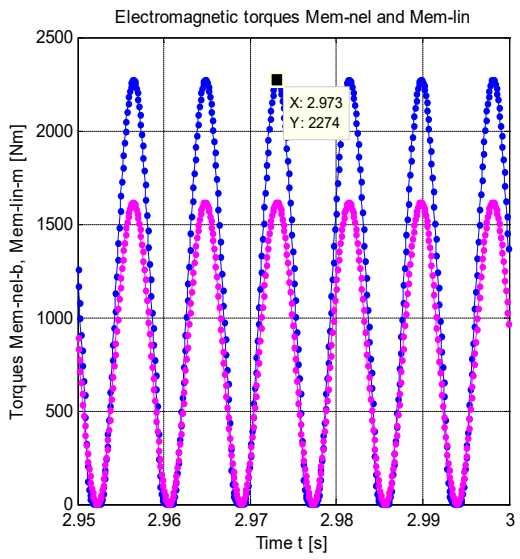
$P_{RFe} - f$ – programul ACAP.



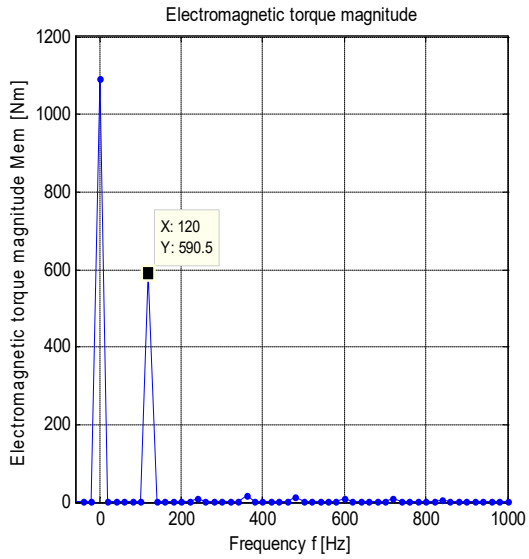
$P_{mec} - t$ – programul ACAP.



$P_{mec} - t$f– programul ACAP.



$M_{em} - t$ - Programul ACAP.



$M_{em} - f$ - Programul ACAP

From the obtained results, it can be observed that, when magnetic saturation is taken into account, the waveforms of currents and voltages are no longer perfectly sinusoidal. Higher-order harmonics appear in the frequency spectra, producing additional losses and affecting motor efficiency. These harmonics may contribute to additional heating of conductors, windings and supply equipment, which is important for risk analysis in low-voltage installations.

The analysis of the results confirms that magnetic saturation causes a high harmonic content in both currents and voltages. The presence of these harmonics leads to an increase in copper and core losses, a decrease in efficiency and a reduction of the power factor. From a practical point of view, these effects may lead to greater stress on the electrical supply installation, heating of conductors and equipment, and the need for correct sizing of protective devices.

The chapter also highlights that simulations performed with ACAP, CSAP, MATLAB and SPICE allow the behaviour of the motor in linear and nonlinear regimes to be compared. The originality of the approach lies in the possibility of treating certain parameters of the equivalent circuit as symbols or as variable quantities, which allows the motor to be analysed under different operating regimes. This flexibility is important for assessing motor performance and identifying operating regimes that may produce additional stresses in the electrical installation.

Conclusions

In conclusion, Chapter 9 shows that the induction motor must be analysed not only as a simple electrical consumer, but as a system with variable parameters and nonlinear behaviour. The magnetisation characteristic, core saturation, variation of rotor resistance and slip influence the absorbed currents, harmonics, losses, efficiency, power factor and thermal stresses. In relation to the topic of the thesis, this chapter contributes to understanding how important consumers may produce overloads, imbalances, additional losses and local overheating. Thus, induction motor modelling becomes a useful tool for sizing protective devices, preventing faults and reducing risk in low-voltage electrical installations.

Chapter 10

General Conclusions and Future Research Directions

The safety of low-voltage electrical installations cannot be ensured only through the existence of regulations, periodic inspections or measurement reports. The main conclusion of the thesis is that the verification of an electrical installation must always be carried out on the basis of the technical design, the real diagrams and the updated documentation. In the absence of the design documentation, the verification cannot be complete and correct, because it cannot be established with certainty whether the existing installation corresponds to the designed solution, whether the protective devices are correctly sized, whether the circuits are correctly identified and whether the modifications carried out over time are compliant.

An electrical installation without updated design documentation becomes difficult to control, difficult to verify and risky to operate. Maintenance cannot be carried out correctly when the real single-line diagram, the circuit routes, the conductor cross-sections, the associated protective devices and the supplied consumers are not known. Under these conditions, the verification becomes only partial, while the safety of the installation remains only apparent.

The research also highlights that technological development, automation, digitalisation, intelligent systems and new consumers have evolved very rapidly, while, in many situations, the basic knowledge related to electrical installations has not been sufficiently consolidated or correctly applied. Modern technologies have been adopted quickly, without the basic electrical infrastructure always being properly verified, modernised and maintained.

With the emergence of new technologies, the optimal operation and maintenance of electrical installations have sometimes been minimised or neglected. However, any modern technology, regardless of how advanced it is, relies on a safe, correctly designed and properly operated electrical installation. If this foundation is not safe, then the modern systems supplied by it also become vulnerable.

The thesis shows that the electrical installation represents the foundation on which new technologies are developed. For this reason, it must be treated as an essential infrastructure, requiring correct design, compliant execution, verification based on real documentation, periodic maintenance and continuous monitoring of critical parameters.

In conclusion, reducing the risk of accidents in low-voltage electrical installations requires compliance with a fundamental principle:

An electrical installation cannot be correctly verified, maintained or modernised without technical design documentation, updated diagrams and complete documentation.

The safety of electrical installations must be the result of a continuous process of design, execution, verification, maintenance and monitoring, not merely the result of punctual inspections or individual interpretations of regulations.

10.1. List of Published Works

This list includes the works published during the doctoral programme, on topics related to the subject of the doctoral thesis, in which the doctoral candidate is author or co-author:

1. Dragoș Niculae, Mihai Iordache, Marilena Stănculescu, Lavinia Bobaru, **Adrian Georgescu,** Victor Bucată, "Computer Aided Design of Two-Element Matching Network Using ZY Smith Chart", Proc. of the 16th International Conference on Applied and Theoretical Electricity, ICATE 2024, Publisher: IEEE Xplore, Date of Conference: October 24-26, 979-8-3503-8810-7/24/2024, Date Added to IEEE *Xplore*: 28 June 2021,DOI**:** 10.1109/ICATE62934.2024.10748638,pag. 1 – 6. https://ieeexplore.ieee.org/document/10748637/

2. **Adrian Georgescu**, Mihai Iordache, Constantin Dragoș, "When Does It Become Necessary to Replace the Electrical Instalation in an Old Building to Reduce Risk of Accidents?", Proceedin of 10th International Conference on Materials Sciene and Technologies _ ROMAT 2024, Bucharest, Romania, November 14th – 15th, 2024, www.sim.upb.ro, https://materialfest.upb.ro/editia-2024/

3.**Adrian-Florian Georgescu,** Dragos, Niculae, Mihai Iordache, Marilena Stănculescu, Ana-Maria Bumbeneci, Lavinia Bobaru, Georgiana Zainea and Mihai Rotaru, "Automatic Procedure and the Use of the Smith Chart in Impedance Matching in Analog Circuits", Electronics 2025, 14, 2746 https://doi.org/10.3390/electronics14142746, Published: 8 July 2025, **WOS:001539842500001,** pp. 1 – 17.

https://www.webofscience.com/wos/woscc/full-record/WOS:001539842500001

4. Mihai Iordache, Marilena Stanculescu, Lavinia Bobaru, Dragoş Niculae, Sorin Deleanu, **Adrian Georgescu**, Mihai Rotaru, Anton Anastasie Moscu, "Using the SSEMGP – SEMI - STATE Equation Matrix Generation Program for Transfer Function Generation in Analog Circuits with Single Input – Single Output and Multiple Inputs - Multiple Outputs", Published in: 2025 International Conference on Electromechanical and Energy Systems (SIELMEN), Date of Conference**:**16-18 October 2025, Date Added to IEEE *Xplore*: 03 December 2025, ISBN Information: DOI: 10.1109/SIELMEN67352.2025.11260820, Accession Number: **WOS: 001669739200039**, Publisher: IEEE, pp. 1 -30. https://0d10tkmr4-y-https-www-webofscience-com.z.e-nformation.ro/wos/woscc/full-record/WOS:001669739200039

5. **Adrian Georgescu**, Mihai Iordache, Dragoș Niculae, Lavinia Bobaru, Georgiana Rezmeriță, Mihai Rotaru, Ana-Maria Tudor. "Generation of Two–Port Circuit and Filter Parameters". Proceeding of the 14th International Symposium Advanced Topics in Electrical Engineering – ATEE'25. Anul publicării: 2025, Paginile: 373-377, Editura: Politehnica Press / IEEE, ISBN: 979-8-3315-2646-7. DOI:

https://doi.org/10.1109/ATEE66006.2025.11299872 IEEE Xplore.

6. Mihai Rotaru, **Adrian Georgescu**, Dragoș Niculae, Georgiana Zainea, Mihai Iordache and Steliana Pușcașu, "Conversions Among Z, Y, H, F, T, and S Parameters, Which are Highly Beneficial for the Analysis of Two-Port Circuits and Filters*"*, Energies 2026, 15(2), 1344, https://doi.org/10.3390/electronics 15020255, Accession Number: **WOS:001670332900001**, pp. 1 – 23.

https://www.webofscience.com/wos/woscc/full-record/WOS:001670332900001

7. Mihai Rotaru, **Adrian-Florian Georgescu**, Mihai Iordache**,** Dragoș Niculae, Steliana Pușcașu, Georgiana Zainea, "Analysis of the Asyncronous Motor in Steady-State Regime When Taking into Consideration the Magnetization Characteristic and the Variation of the Rotor Resistance with Slip", Electric Machines, Materials, and Drives Present and Trends. APME/SME'25, Ediţia XXI, 28 noiembrie 2025, UNSTP Bucharest. Vol. 21 No. 1 (2025): APME DOI: https://doi.org/10.36801/yqxg8c71,https://journal.iem.pub.ro/apme/en/article/view/1763.

8. Prof. emerit dr. arh. Cristina Olga GOCIMAN, Facultatea de Arhitectura UAUIM; Prof. univ. dr. ing. **Mihai IORDACHE**, Universitatea Politehnica din Bucureşti; Drd. ing. **Adrian Florian GEORGESCU** Universitatea Politehnica din Bucureşti; Dr. arh. Stefania TRIFAN, UAUIM; Dr. arh. urb. Cristian Iosif MOSCU, UAUIM. "Case Studies on Risk Reduction in Hospital Buildings", INNOMINCU 2022 Conference: Research Days at UAUIM, The Health of Cities. Healthy Architecture. Interior Design of Healthy Spaces. https://www.uauim.ro/evenimente/conferinta-innomincu-2022/

10.2. Scientific and Applied Impact

The research presented in this thesis has a twofold impact, both theoretical and applied.

From a scientific perspective, the thesis extends numerical circuit analysis methods towards the field of electrical installations, offering an interdisciplinary framework that connects electronics, energy systems and safety.

From an applied perspective, the results may be implemented in modernisation programmes, predictive maintenance strategies and professional training activities for electricians and engineers.

The implementation of the proposed system may contribute to:

- reducing the number of fires caused by faulty electrical installations;
- increasing the reliability of low-voltage networks;
- improving energy management;
- creating a national database of monitored electrical installations.

References

[1] *Chen, X.,* et al. (2021). BN-RA: A Hybrid Model for Risk Analysis of Overload-Induced Early Cable Fires. Applied Sciences, 11(18), 8922.

[2] *U.S. Fire Administration* (2014). Residential Building Electrical Fires (2009–2011).

[3] *SR HD 60364-7-710* - Instalaţii electrice de joasă tensiune. Partea 7-710: Prescripţii pentru instalaţii sau amplasamente speciale. Amplasamente pentru utilizări medicale;

[4] *NORMATIV privind* proiectarea, executia si exploatarea instalatiilor electrice aferente cladirilor - Indicativ I 7 – 2011
[5] *Prof. emerit dr. arh. Cristina Olga GOCIMAN,* Facultatea de Arhitectura UAUIM; *Prof. univ. dr. ing. Mihai IORDACHE,* Universitatea Politehnica din București; *Drd. ing. Adrian Florian GEORGESCU* Universitatea Politehnica din București; *Dr. arh. Stefania TRIFAN*, UAUIM; *Dr. arh. urb. Cristian Iosif MOSCU,* UAUIM, Studii de caz cu privire la reducerea riscurilor la clădirile unităților spitalicești;
[6] NORMATIV NTE 007_08_00 – Pentru proiectarea si executarea retelelor de cabluri electrice;
[7] *Ionuț-Cătălin Munteanu, Emil Cazacu, Lucian Petrescu*, Predictive-adaptive maintenance applied for optimizing the performance of industrial electrical systems and equipment;
[8] *STAS 12604/4-89* - PROTECŢIA ÎMPOTRIVA ELECTROCUTĂRILOR;
[9] *PE 016 – E/2001* Normativ pentru lucrarile de Expoatare-Mentenanta in Retele Electrice de distributie.
[10] *PE 116-94,* NORMATIV DE ÎNCERCĂRI ŞI MĂSURĂTORI LA ECHIPAMENTE ŞI INSTALAłII ELECTRICE;
[11] *NORMATIV C 56-02*, PENTRU VERIFICAREA CALITATII SI RECEPTIA LUCRARILOR DE INSTALATII AFERENTE CONSTRUCTIILOR;
[12] *NFPA 780* – Standard for the installation of Lightning Protection Systems 2020
[13] *RC62*-Recommendations-for-fire-safety-with-PV-panel-installations
[14] *IEC 62446-2-2020* – Photovoltaic system – requirements for testing, documentation and mentenance.
[15] Requirements of persons doing electrical wiring – Canada Rules; Residential_wiring_guide (1) _240414_101620 – Canada, Homeowner electrical wiring guide Including the 2015 Canadian Electrical Code amendments
[16] *NTE 006/06/00* - Normativ privind metodologia de calcul al curenților de scurtcircuit în reţelele electrice cu tensiunea sub 1 kV, aprobat prin Ordin ANRE nr. 7/2006
[17] *1RE-Ip30-2004* - Îndreptar de proiectare și execuție a instalațiilor de legare la pământ, avizat în CTS SC Electrica SA cu PV 299/2004
[18] *M. Iordache, N. Ludu,* "Calculul regimurilor tranzitorii din convertizorul static de frecvenţă de 500 Hz, asistat de calculatorul numeric", E.E.A. - Electrotehnica 5
[19] *Dragoş Marin Niculae, Marilena Stanculescu, Sorin Deleanu, Mihai Iordache and Lavinia Bobaru*,"Wireless Power Transfer Systems Optimization Using Multiple Magnetic Couplings", Electronics 2021, 10 (20), https://doi.org/10.3390/electronics10202463, 2463, www.mdpi.com/journal/electronics- 2463, 11 Oct 2021, 16 pags. Impac Factor: 2.397, CITESCORE: 2.7 SCOPUS, ELECTRONICS Volume: 10 Issue: 20 Article Number: 2463 DOI: 10.3390/electronics10202463 Published: OCT 2021 Accession Number: WOS:000715322800001.
[20] *Ioana-Gabriela Sirbu, Lucian Mandache, Marilena Stanculescu, Mihai Iordache, and Lavinia Bobaru,* "Generation Algorithms for Thévenin and Norton Equivalent Circuits", Energies 2025, 18, 1344. https://doi.org/10.3390/en18061344, Accession Number: WOS:000715322800001.
[21] *Sorin Deleanu, Mihai Iordache, Dragos Niculae, Bogdan Venescu, Mihaela Cristina Turcu, Neculai Galan*, "The Overvoltage Distribution across TransformeWindings in presence of Long Feeders", Publisher: IEEE, IEEE Xplore, 2018 International Conference on Applied and Theoretical Electricity (ICATE), 4-6 Oct. 2018, DOI: 10.1109/ICATE.2018.8551469, 978-1-5386-3806-4/18/$31.00 ©2018 IEEE, Accession Number: WOS:000487278600080, Page(s): 1 - 6.
[22] *Dragoş Niculae, Mihai Iordache, Marilena Stănculescu, Lavinia Bobaru, Adrian Georgescu, Victor Bucată*, "Computer Aided Design of Two-Element Matching Network Using ZY Smith Chart", Proc. of the 16th International Conference on Applied and Theoretical Electricity, ICATE 2024, Publisher: IEEE Xplore, Date of Conference: October 24-26, 979-8-3503-8810-7/24/2024, Date Added to IEEE Xplore: 28 June 2021, DOI: 10.1109/ICATE62934.2024.10748638, pag. 1 – 6.
[23] *Adrian Georgescu, Mihai Iordache, Constantin Dragoș*, "When Does It Become Necessary to Replace the Electrical Instalation in an Old Building to Reduce Risk of Accidents?", Proceedin of 10th International Conference on Materials Sciene and Technologies _ ROMAT 2024, Bucharest, Romania, November 14th – 15th, 2024, www.sim.upb.ro, pp. 12 – 20;
[24] NP 015/2022 – Normativ pentru proiectarea și executarea instalațiilor electrice aferente clădirilor spitalicesti;
[25] NP061/2002 - Normativ privind protecția împotriva electrocutărilor;
[26] P118/2015 - Normativ de siguranță la incendiu a construcțiilor;
[27] Legea 319/2006 - Legea securității și sănătății în muncă;
[28] Legea 123/2012 - Legea energiei electrice și a gazelor naturale;
[29] Ordin ANRE 59/2013 - Regulament privind autorizarea electricienilor și firmelor de execuție;
[30] Ordinul Ministrului Sănătății nr. 914/2006;

[31] Legea 10/1995 privind calitatea în construcții.
[32] Hotărârea Guvernului nr. 2139/2004 pentru aprobarea Catalogului privind clasificarea și duratele normale de funcționare a mijloacelor fixe, publicată în Monitorul Oficial nr. 46 din 13 ianuarie 2005.
[33] D. M. Pozar, Microwave Engineering, Wiley 2012.
[34] S. Liao, Microwave devices and circuits, Prentice Hall 1996.
[35] G. Lojewski, Dispozitive si circuite de microunde, Ed. Tehnica 2005.
[36] N. Voicu, Sisteme de microunde. Elemente de teorie, constructie, Matrixrom 2004,
[37] G. Lojewski, Microunde, .dispozitive si circuite, Teora 1999.
[38] G. Lojewski, N. Militaru, Circuite de microunde. Culegere probleme, Matrixrom 2014.
[39] Gheorghe GAVRILOAIA Circuite pasive de microunde, Editura Academiei Tehnice Milit 2010.
[40] Daniel Alexandru Vişan, Ioan Liţă, Mariana Jurian, Ion Bogdan Cioc, "Dispozitive semiconductoare pentru microunde", Ed. Matrix Rom, Bucuresti, 2015.
[41] Microwaves 101: https://www.microwaves101.com/
[42] AT3000 Kit – manual de utilizare.
[43] Electromagnetic Harvesters: Free Lunch or Theft: http://www.industrytap.com/electromagnetic-harvesters-free-lunch-or-theft/1805.
[44] Real-Life Physics, vol.3:
[45] http://www.scienceclarified.com/everyday/Real-Life-Physics-Vol-3-Biology-Vol-1/
[46] Microwaves – Wikipedia: https://en.wikipedia.org/wiki/Microwave.
[47] Tiberiu Mociran, Aplicatiile microundelor, http://cursuri.flexform.ro.
[48] Magnetic monopole – Wikipedia: https://en.wikipedia.org/wiki/Magnetic_monopole.
[49] Triple vector product – Wikipedia: https://en.wikipedia.org/wiki/Triple_product#Vector_triple_product.
[50] Polarization – Wikipedia: https://en.wikipedia.org/wiki/Polarization_(waves).
[51] Polarization of light: https://www.youtube.com/watch?v=8YkfEft4p-w
[52] The polarization of the sky: https://www.polarization.com/sky/sky.html.
[53] Wave and Anthenna Polarization: http://www.antenna-theory.com/basics/polarization.php.
[54] G. A. Iordăchescu, "Microunde: teorie și aplicații", Editura Universității din Pitești, ISB 978-606-560-595-4, 2018.
[55] Adrian-Florian Georgescu, Dragos, Niculae , Mihai Iordache , Marilena Stănculescu , Ana-Maria Bumbeneci, Lavinia Bobaru , Georgiana Zainea and Mihai Rotaru, "Automatic Procedure and the Use of the Smith Chart in Impedance Matching in Analog Circuits", Electronics 2025, 14, 2746 https://doi.org/10.3390/electronics14142746, Published: 8 July 2025, WOS:001453861100001, pp. 1 – 17.
[56] https://www.microwaves101.com/calculators/872-vswr-calculatorhttp://rfcalculator.mobi/vswr-forward-reverse-power.html
[57] https://www.everythingrf.com/rf-calculators/vswr-calculator
[58] https://www.pasternack.com/t-calculator-vswr.aspx
[59] https://www.antenna-theory.com/definitions/vswr-calculator.php
[60] http://www.flexautomotive.net/flexcalc/VSWR2/VSWR.aspx
[61] https://www.allaboutcircuits.com/tools/vswr-return-loss-calculator/
[62] http://www.csgnetwork.com/vswrlosscalc.html
[63] https://www.ahsystems.com/EMC-formulas-equations/VSWR.php
[64] http://cgi.www.telestrian.co.uk/cgi-bin/www.telestrian.co.uk/vswr.pl[34]
[65] https://www.changpuak.ch/electronics/calc_14.php
[66] https://chemandy.com/calculators/return-loss-and-mismatch-calculator.htm
[67] https://www.atmmicrowave.com/calculator/vswr-calculator/
[68] http://www.emtalk.com/vswr.php
[69] L.O. Chua, C.A. Desoer, E.S. Kuh, "Linear and nonlinear circuits", McGraw-Hill Book Company, New York, 1987.
[70] A.F. Schwarz, "Computer-aided design of microelectronic circuits and systems. Fundamentals, Methods and Tools", Academic Press, New York, 1987.
[71] C.I. Mocanu, "Teoria circuitelor electrice", Editură Didactică şi Pedagogică, Bucureşti, 1979.
[72] M. Preda, P. Cristea, "Bazele electrotehnicii", vol. I şi vol. II. Circuite electrice, Editura Didactică şi Pedagogică, Bucureşti, 1980.
[73] C .I. Mocanu, "Teoria campului electromagnetic", Editura Didactică şi Pedagogică, Bucureşti, 1981.W. J. McCalla, "Fundamentals of Computer-Aided Circuit Simulation", Kluwer Academic Publishers, Boston/Dordecht/Lancaster, 1988.
[74] S. Franco, "Electric Circuits Fundamentals", Saunders College Publishing, New York, 1995.
[75] S.J. Orfanidis*, Electromagnetic Waves and Antennas*, 2008, http://www.ece.rutgers.edu/ orfanidi/ewa/.

[76] D. A. Frickey, "Conversions between S, Z, Y, H, ABCD, and T parameters which are valid for complex source and load impedances," IEEE Trans. on Microwave Theory and Techniques, No. 42, 1994, pp. 205–211.
[77] R. B. Marks and D. F. Williams, "Comments on conversions between S, Z, Y, H, ABCD, and T parameters which are valid for complex source and load impedances," IEEE Trans. on Microwave Theory and Techniques, No. 43, 1995, pp. 914–915.
[78] Mihai Iordache**,** Lucia Dumitriu, *Generation of the Transfer Functions for MIMO Systems*, Chapter 4; in book *Design of Analog Circuits through Symbolic Analysis,* Mourad Fakhfakh, Esteban Tlelo-Cuautle and Francisco V Fernandez (Eds), Bentham Science Publishers, 2012, pp. 83-114, pp. 228-262 respectively (e-book), **DOI:** 10.2174/97816080509561120101, **eISBN:** 9781-60805-095-6, **ISBN:** 978-1-60805-425-1, 2012, Accession Number: **WOS:000425767300006.**
[79] M. Iordache, *Symbolic, Numeric – Symbolic and Numeric Simulation of Analog Circuits – User Guides*, MATRIX ROM, Bucharest, 2015, ISBN 978 – 606 – 25 – 0126 - 6, 621.3.049.77
[80] M. Iordache, Lucia Dumitriu, *Computer-Aided Simulation of Analoque Circuits – Algorithms and Computational Techniques*, Editura POLITEHNICA Press, Vol. I and Vol. II, Bucharest 2014, ISBN 978–606-515-567-1, ISBN 978-606-515-585-5.
[81] http://www.keysight.com/en/pc-1297113/advanced-design-system-ads?cc=US&lc=eng
[82] Agilent Technologies, AGILENT TECHNOLOGIES, Large-Signal S-Parameter Simulation, Sept, 2004.
[83] ANSOFT Q3D EXTRACTOR, User Guide, www.ANSOFT.com.
[84] https://www.feko.info/support.
[85] Marilena Stanculescu, Lavinia Bobaru, Dragoș Niculae, Sorin Deleanu, Victor Bucată, Mihai Iordache - Coordonator, "*Wireless Electromagnetic Energy Transfer Systems*", MATRIX ROM, Bucharest, 2021, ISBN 978 – 606 – 25 – 0623 - 0, 621.3.
[86] M. Iordache, H. S. Popescu, I. Vlad and M. F. Staniloiu, "ACAP - Analog Circuit Analysis Program," 2021 12th International Symposium on Advanced Topics in Electrical Engineering (ATEE), Bucharest, Romania, 2021, pp. 1-6, doi: 10.1109/ATEE52255.2021.9425307.
[87] M. Stanculescu, S. Deleanu, D. Sanatescu, A. Ionescu, A. Moscu and L. Bobaru, "CSAP and TFSG – Circuit Symbolic Analysis Programs and Transfer Function SYmbolic Generation" 2019 International Conference on Electromechanical and Energy Systems (SIELMEN), Craiova, Romania, 2019, pp. 1-6, doi: 10.1109/SIELMEN.2019.8905907.
[88] M. Iordache, Lucia Dumitriu, D. Delion, "Automatic Formulation of Symbolic State Equations for Analog Circuits with Degeneracies", Proceedings of 6th International Workshop on Symbolic Methods and Applications in Circuit Design, SMACD 2000, October 12-13, 2000, pp. 65-72.
[89] M. M. Hassoun and Pen-Min Lin, "A hierarchical network approach to symbolic analysis of large-scale networks," in IEEE Transactions on Circuits and Systems I: Fundamental Theory and Applications, vol. 42, no. 4, pp. 201-211, April 1995, doi: 10.1109/81.382473.
[90] Comparisons between Maple, Mathematica and Macsyma, by alleyne@hera.ics.uci.edu (Brian D. Alleyne) Univ. of Calif., Irvine, Info. & Computer Sci. Dept. 16 Feb 93 07:25:10 GMT.
[91] G. Gielen, P. Wambacq, W. M. Sansen, "Symbolic Analysis Methods and Applications for Analog Circuits: A Tutorial Overview", Proceedings of the IEEE, Vol. 82, No.2, Feb. 1994, pp. 287-303.
[92] P. M. Lin, Symbolic Network Analysis, Elsevier, 1991.
[93] A. Vladimirescu, SPICE, Editura tehnică, Bucureşti, 1999.
[94] Mihai Iordache - Coordonator, Marilena Stanculescu, Răzvan Asanache, Lavinia Bobaru, Sorin Deleanu, Dragoș Niculae, Georgiana Rezmeriță, "A*nalog Circuit Analysis Using S-Parameters and Smith Chart*", ISBN 978 – 606 – 25 – 0771 - 8, 621.3, Publishing House MATRIX ROM, Bucharest, 2022.
[95] L. O. Chua, and P. M. Lin, Computer-Aided Analysis of Electronic Circuits: Algorithms and Computational Techniques, Englewood cliffs, NJ: Prentice-Hall, 1975.
[96] A. E. Schwarz, Computer-aided design of microelectronic circuits and systems, Academic Press, London, 1987.
[97] M. Iordache, Lucia Dumitriu, Computer-Aided Simulation of Analog Circuits – Algorithms and Computational Techniques, POLITEHNICA Press Publishing House , Bucharest,
[98] Mihai Iordache, Sorin Deleanu, Ciprian Curteanu, Neculai Galan, Anastasie Anton Moscu, „SYSEG - SYmbolic State Equation Generation", Proc. of the 11-th International Conference on Electromechanical and Power Systems, SIELEM 2017, October 11-14, 2017, Chişinău Rep. MOLDOVA, Accession Number: WOS:000426906000036, Publisher: IEEE, pp. 1-7.
[99] Marilena Stănculescu, Alexandra Ionescu, Diana Sanatescu, Sorin DELEANU, Lavinia Bobaru, Anastasie Anton Moscu, "CSAP – Transfer Function SYmbolic Generation and TFSYG – Transfer Function SYmbolic Generation", Proc. of the 12th International Conference on Electromechanical and Power Systems, SIELEM 2019, October 10-11, 2019, Chişinău Rep. MOLDOVA, IEEE Xplore, DOI: 10.1109/SIELMEN.2019.8123295 , Publisher: IEEE, pp. 1-7.

[100] Mihai Iordache, Horatiu Samir Popescu, Ionela Vlad, Marius Florin Staniloiu, "ACAP – Analog Circuit Analysis Program", Proceeding of the 12th International Symposium Advanced Topics in Electrical Engineering – ATEE'21, March 25-27, 2021, Bucharest, Romania, Editura Politehnica Press, pp. 373 - 377, IEEE Xplore, 978-1-6654-1878-2/20/$31.00 ©2017, DOI: 10.1109/ATEE.2021.9425098, Accession Number: **WOS:000676164800143**, Publisher:IEEE.

[101] C. Mihăilescu, Fl. Rezmeriță, Ileana Calomfirescu, M. Iordache, N. Galan, Performance Analysis of Three Phase-Squirred Cage Induction Motor with Deep Rotor Bars in Transient Behavior, Electrical and Electronic Engineering, p-ISSN:2162-9455 e-ISSN: 2162-8459, vol. 2, No. 2, 2012, pp. 11-17, WOS:000421805200018, DOI: 10.5923/j.eee.2012020202, pp. 235 - 248.

[102] Rodica Voiculescu, Iordache Mihai, „Analog Circuit Simulation by State Variable Method", U.P.B. Scientific Bulletin Series C – Electrical Engineering, Vol 71. Iss. 3. 2015, ISSN 2286-3540, WOS:000421805200018, pp. 213-224.

[103] Bogdan Florin VENESCU, Adrian Florinel BUCSA, Mihai IORDACHE, „ANALYSIS OF THE PERMANENT SINUSOIDAL REGIME OF THE ASYNCHRONOUS MOTOR OF THE PRIMARY CIRCUIT PUMPS FROM A NUCLEAR POWER PLANT", U.P.B. Scientific Bulletin Series C – Electrical Engineering, Vol. 83, Iss. 2, 2021, ISSN 2286-3540, Accession Number: WOS:000692193500017, pp. 221 – 230.

[104] A.-K. Repo, P. Rasilo, a. A. Arkkio, Dynamic electromagnetic torque model and parameter estimation for a deep-bar induction machine, IET Electr. Power Appl., vol. 2, No. 3, pp. 183 -192, 2008.

[105] Levi E., Main flux saturation modelling in double-cage and deep-bar induction machines, IEEE Trans. Energy Conversion, vol. 11, No. 2, pp.305 – 311, 1996.

[106] K.S. Huang, Q.H. Wu, D.R. Turner, Effective Identification of Induction Motor Parameters Based on Fewer Measurements. IEEE Trans. Energy Converssion, vol. 17, No. 1, pp.305 – 311, pp. 55 – 59, 2002.

[107] *J. Pedra, L Sainz*, Parameter estimation of squirrel-cage induction motors without torque measurements, IEE Proc. Electr. Power Appl., **vol. 153**, no.2, pp. 87 -94, 2006.

[108] *Rik W.A.A. De Doncker*, Field-Oriented Controllers with Rotor Deep Bar Compensation Circuits, IEEE Trans. Industry Applications, **vol. 28**, nr. 5 , pp. 1062 – 1070, 1992.

[109] *Jul-Ki Seok, Seung-Ki Sul*, Pseudorotor-Flux-Oriented Control of an Induction Machine for Deep-Bar-E ffect Compensation, IEEE Trans. Industry Applications, vol. 34, nr. 3 , pp. 429 – 434 , 1998.

[110] *Alexander C. Smith, Russell C. Healez, Stephen Williamson*, A Transient Induction Motor Model Including Saturation and Deep Bar Effect, IEEE Trans. Energy Converssion, **vol. 11**, No. 1, pp.8 -15, 1996.

[111] *L. Ljung,* "System identification: Theory for the user, 2nd edition", Prentice Hall, USA, 1999. [7]. *J. Pedra, F. Corcoles* "Estimation of Induction Motor Double-Cage Model Parameters from Manufacturer Data", IEEE Transactions on Energy Conversion, June 2004.

[112] *T.Phumiphak, C. Chatuthai*, „Estimation of induction motor parameters based on a field test coupled with genetic algorithm", in Proc. Int. Conf. Power System Technology 2002, pp. 1199-1203.